NRL Memorandum Report 5055

SSM/I Project Summary Report

J. P. HOLLINGER AND R. C. LO

Space Sensing Applications Branch
Aerospace Systems Division

April 20, 1983

NAVAL RESEARCH LABORATORY
Washington, D.C.

Approved for public release; distribution unlimited.

SECURITY CLASSIFICATION OF THIS PAGE (When Data Entered)

REPORT DOCUMENTATION PAGE		READ INSTRUCTIONS BEFORE COMPLETING FORM
1. REPORT NUMBER NRL Memorandum Report 5055	2. GOVT ACCESSION NO. AD-A128803	3. RECIPIENT'S CATALOG NUMBER
4. TITLE (and Subtitle) SSM/I PROJECT SUMMARY REPORT		5. TYPE OF REPORT & PERIOD COVERED Interim report on a continuing NRL problem. 6. PERFORMING ORG. REPORT NUMBER
7. AUTHOR(s) J. P. Hollinger and R. C. Lo		8. CONTRACT OR GRANT NUMBER(s)
9. PERFORMING ORGANIZATION NAME AND ADDRESS Naval Research Laboratory Washington, DC 20375		10. PROGRAM ELEMENT, PROJECT, TASK AREA & WORK UNIT NUMBERS 35160N; SPW0524-CC; 79-1543-00
11. CONTROLLING OFFICE NAME AND ADDRESS Navy Space Systems Activity P. O. Box 92960 Los Angeles, CA 90009		12. REPORT DATE April 20, 1983 13. NUMBER OF PAGES 110
14. MONITORING AGENCY NAME & ADDRESS(if different from Controlling Office)		15. SECURITY CLASS. (of this report) UNCLASSIFIED 15a. DECLASSIFICATION/DOWNGRADING SCHEDULE
16. DISTRIBUTION STATEMENT (of this Report) Approved for public release; distribution unlimited.		
17. DISTRIBUTION STATEMENT (of the abstract entered in Block 20, if different from Report)		
18. SUPPLEMENTARY NOTES		
19. KEY WORDS (Continue on reverse side if necessary and identify by block number) Parameters, Retrieval, Geophysical SSM/I, Microwave, Passive Algorithm		

20. ABSTRACT (Continue on reverse side if necessary and identify by block number)
The Special Sensor Microwave/Imager (SSM/I) is a passive microwave radiometric system designed to provide retrievals of the environmental parameters sea surface wind, precipitation, atmospheric moisture content, soil moisture and sea ice conditions. It is a joint Navy/Air Force project developed by the Hughes Aircraft Company under the direction of the Navy Space System Activity (NSSA) and the Air Force Space Division to be flown on the Defense Meteorological Satellite Program (DMSP). The Space Sensing
(Continues)

DD FORM 1 JAN 73 1473 EDITION OF 1 NOV 65 IS OBSOLETE
S/N 0102-014-6601

SECURITY CLASSIFICATION OF THIS PAGE (When Data Entered)

20. ABSTRACT (Continued)

Applications Branch of the Naval Research Laboratory has served as a technical consultant to NSSA beginning in fiscal year 1982.

A summary description of the SSM/I instrument; and descriptions of the geophysical models, the interaction model, the retrieval technique and climatology used for the SSM/I environmental retrieval algorithm are presented. This information may serve as an introduction to the SSM/I for those individuals who have an interest in the SSM/I and its geophysical data products.

The studies, conducted at the request of the NSSA to evaluate and investigate specific details of the instrument and algorithms are attached as Appendix A through E.

CONTENTS

Acknowledgements

The authors wish to thank Messrs. A. T. Edgerton and J. L. Pierce of the Hughes Aircraft Company for providing a set of photographs of the SSM/I and for various detailed discussions concerning the instrument. Appreciation is also due Dr. Kenneth R. Hardy for providing information concerning the algorithms developed at the Environmental Research & Technology, Inc. for the SSM/I. This work would not have been possible without the support of CMDRS F. Wooldridge and T. M. Piwowar of the Navy Space Systems Activity.

SSM/I PROJECT SUMMARY REPORT

I. INTRODUCTION

The Microwave Environmental Sensor System, referred to as the Mission Sensor Microwave/Imager (SSM/I), is a joint Navy/Air Force Project. It is a passive microwave radiometric system developed by the Hughes Aircraft Company under the direction of the Navy Space Systems Activity (NSSA) and the Air Force Space Division to be flown on the Defense Meteorological Satellite Program (DMSP) operational spacecraft as an all weather oceanographic and meteorological sensor. The Space Sensing Applications Branch of the Naval Research Laboratory (NRL) has served as technical consultant to the NSSA beginning in fiscal year 1982.

In this capacity NRL has performed a number of studies and analyses requested by NSSA, prepared a draft SSM/I calibration/validation plan and conducted the SSM/I Calibration/Validation Workshop on 10 and 11 August 1982. This report is intended to describe and document these efforts. In addition, a description of the instrument and the geophysical retrieval algorithms is included so that this report might also serve as an introduction to the SSM/I for those individuals who have an interest in the SSM/I or its geophysical data products.

A summary description of the SSM/I instrument is presented in Section II. Section III contains a description of the environmental retrieval algorithm designed by Environmental Research and Technology, Inc. (ERT) under subcontract to Hughes Aircraft Company. Five letter reports, describing studies which were conducted at the request of NSSA, are attached as Appendix A through E.

II. DESCRIPTION OF THE SSM/I

The SSM/I is a seven channel, four frequency, linearly polarized, passive microwave radiometric system. The instrument measures atmospheric/ocean surface brightness temperatures at 19.3, 22.2, 37.0, and 85.5 GHz. These data will be processed by the Naval Oceanography Command and the Air Force Air Weather Service to obtain near real time global precipitation maps, sea ice morphology, marine surface wind speed, columnar integrated liquid water, and soil moisture percentage. In addition, Navy and Air Force DMSP tactical sites will be capable of receiving this same data directly from the satellite to satisfy their unique customer mission requirements.

The DMSP Block 5D-2 satellite and the SSM/I are depicted in Figure II.1. The instrument consists of an offset parabolic reflector of dimensions 24 x 26 inches, fed by a corrugated, broad-band, seven-port horn antenna. The

Manuscript approved January 27, 1983.

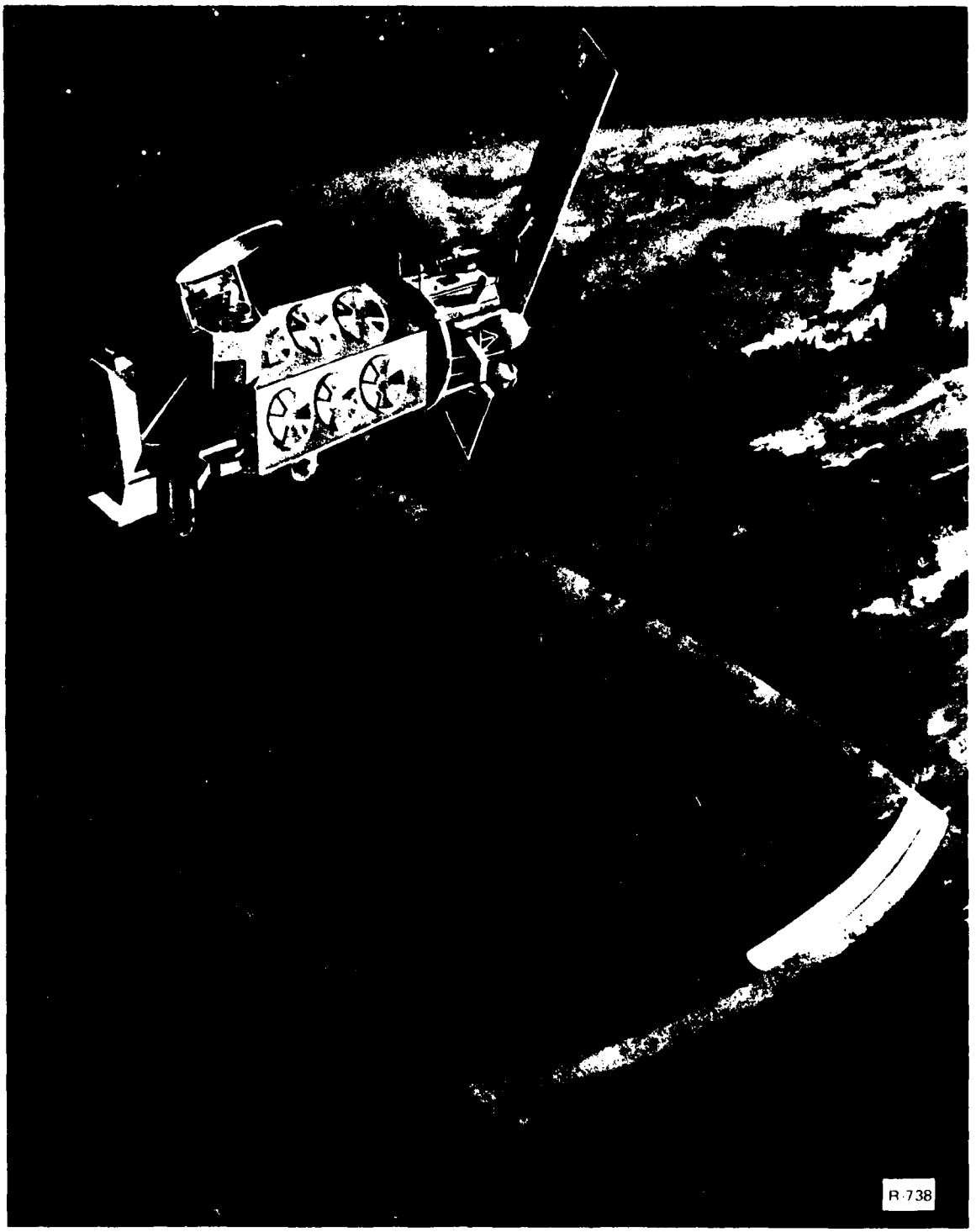

Figure II.1 The DMSP Block 5D-2 Satellite

reflector and feed are mounted on a drum which contains the radiometers, digital data subsystem, mechanical scanning subsystem, and power subsystem. The reflector-feed-drum assembly is rotated about the axis of the drum by a coaxially mounted bearing and power transfer assembly (BAPTA). All data, commands, timing and telemetry signals, and power pass through the BAPTA on slip ring connectors to the rotating assembly.

A small mirror and a hot reference absorber are mounted on the BAPTA and do not rotate with the drum assembly. They are positioned off axis such that they pass between the feed horn and the parabolic reflector, occulting the feed once each scan. The mirror reflects cold sky radiation into the feed thus serving, along with the hot reference absorber, as calibration references for the SSM/I. This scheme provides an overall absolute calibration which includes the feed horn. Corrections for spillover and antenna pattern effects from the parabolic reflector are incorporated in the data processing algorithms.

The prototype of the SSM/I is shown in the stowed position in Figure II.2 and deployed in Figure II.3. The feed horn antenna may be seen in Figure II.2 and the sky reference reflector in Figure II.3. The hot absorber reference is under the thermal blanket in both figures. Photographs of the feed horn antenna, sky reference reflector, and hot absorber reference are given in Figures II.4, II.5, and II.6, repectively.

The radiometers are total power, balanced mixer, superheterodyne type receivers. The exact operating frequencies and radiometric performance characteristics are given in Figure II.7. The weight, size, power, and orbit specifications are given in Figure II.8.

Details of the scan geometry are shown in Figure II.9. The SSM/I rotates at a uniform rate making one revolution in 1.90 seconds during which time the satellite advances 12.5 km. The antenna beams are at an angle of 45° to the BAPTA rotational axis, which is normal to the earth's surface. Thus as the antenna rotates the beams define the surface of a cone and, from the orbital altitude of 833 km, make an angle of incidence of 53.1° at the earth's surface. The scene is viewed over a scan angle of 102.4° centered on the ground track aft of the satellite resulting in a scene swath width of 1394 km. The radiometer outputs are sampled differently on alternate scans. During the scene portion of the scans labeled scan A in Figure II.9, the five lower frequency channels are each sampled over 64 equal 1.6° intervals and the two 85.5 GHz channels are each sampled over 128 equal 0.8° intervals or approximately each 11 km along the scan. During the alternate type B scans, only the two 85.5 GHz channels are sampled at 128 equal intervals. Sampling, to 12 bit precision, is accomplished by the integrate, hold and dump method with an integration period of 7.95 milliseconds for the five lower frequency channels and 3.89 milliseconds for the two 85.5 GHz channels. Alternate 0.8° intervals are centered on the midpoints of the 1.6° intervals so that samples of all seven channels are collocated with additional 85.5 GHz samples equally spaced between them. Thus the five lower channels are sampled on an approximate 25 km grid along the scan and along the track. The two 85.5 GHz channels are sampled at one half this spacing both cross and along track.

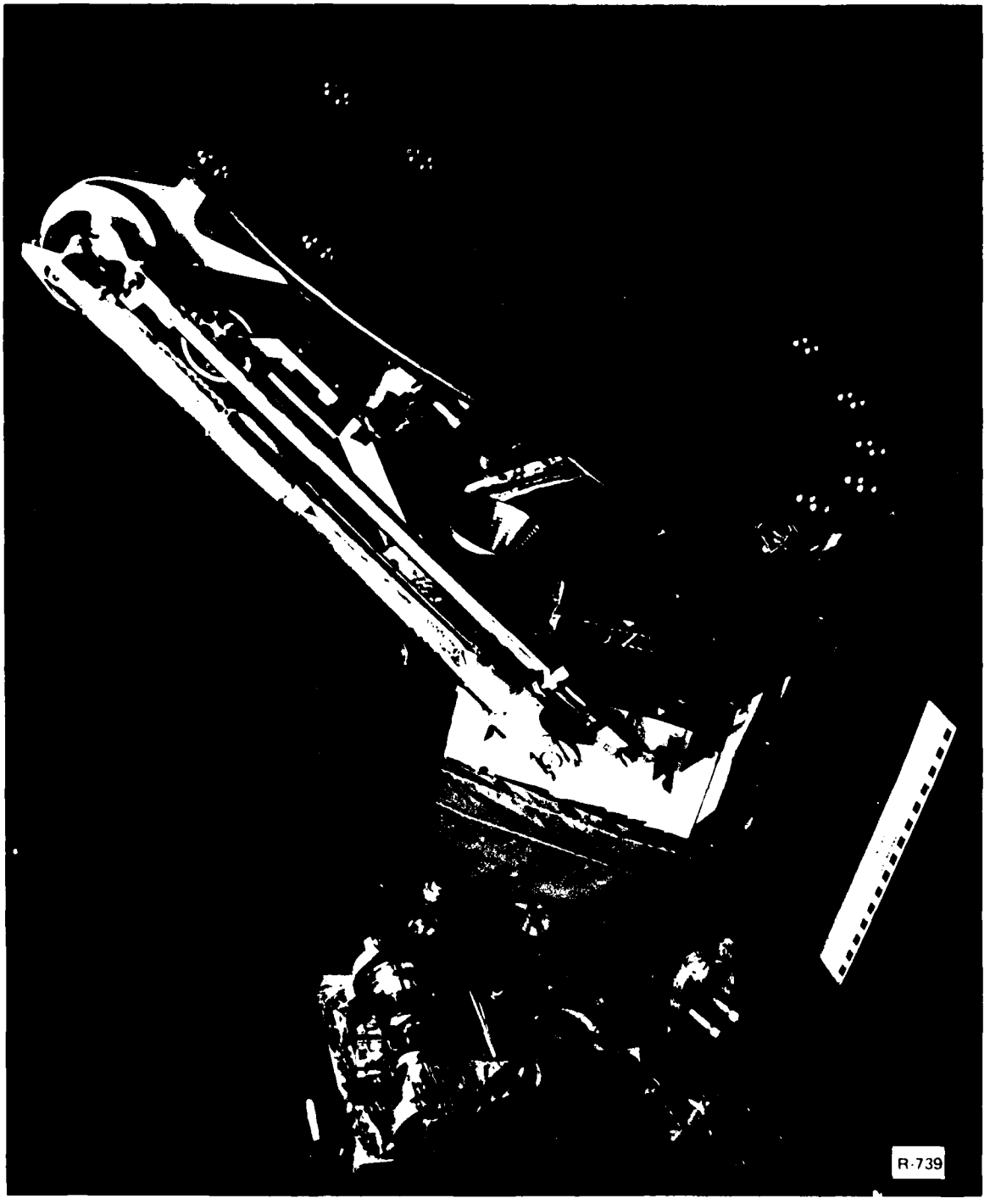

Figure II.2 The prototype of the SSM/I in the stowed position

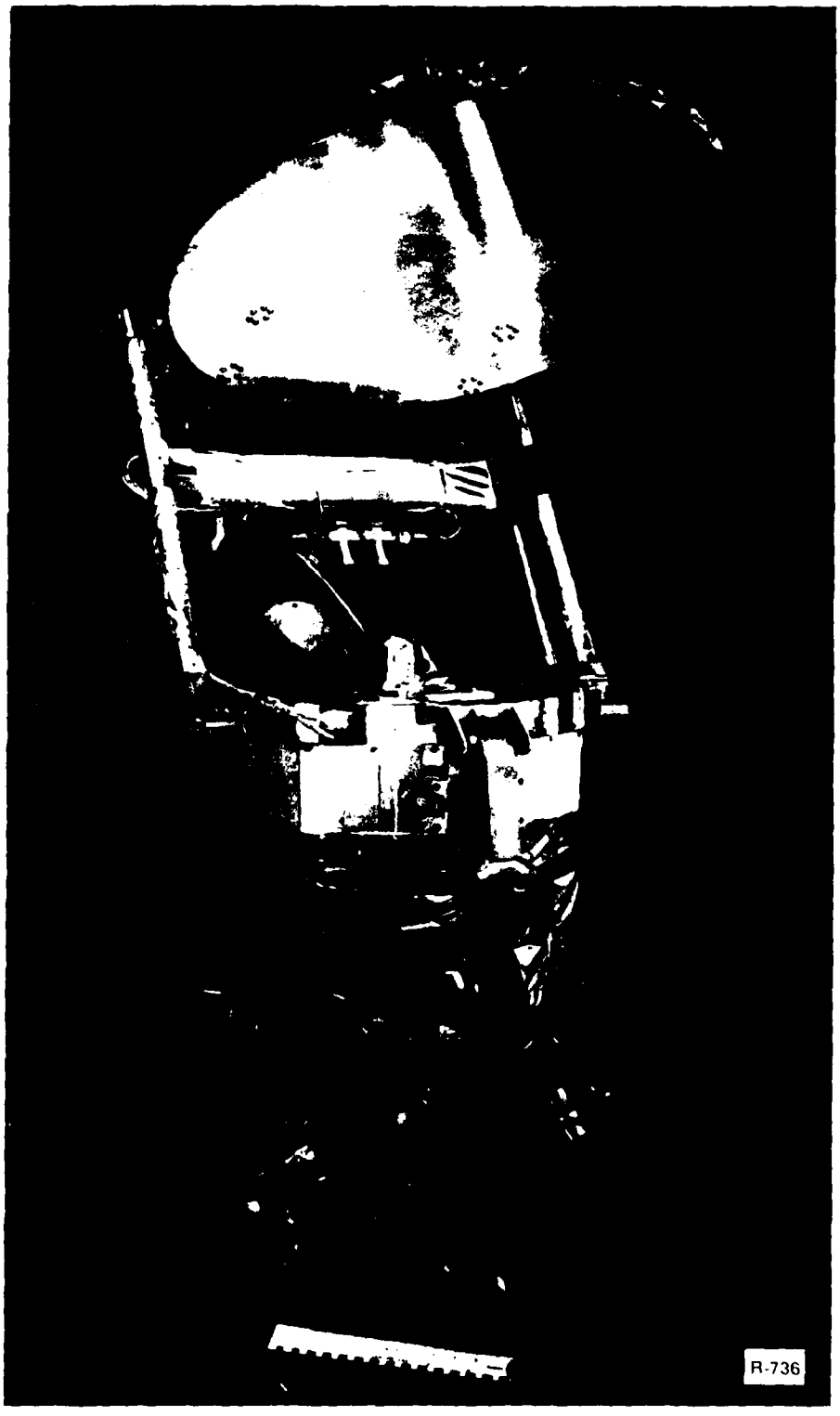

Figure II.3 The prototype of the SSM/I in the deployed position

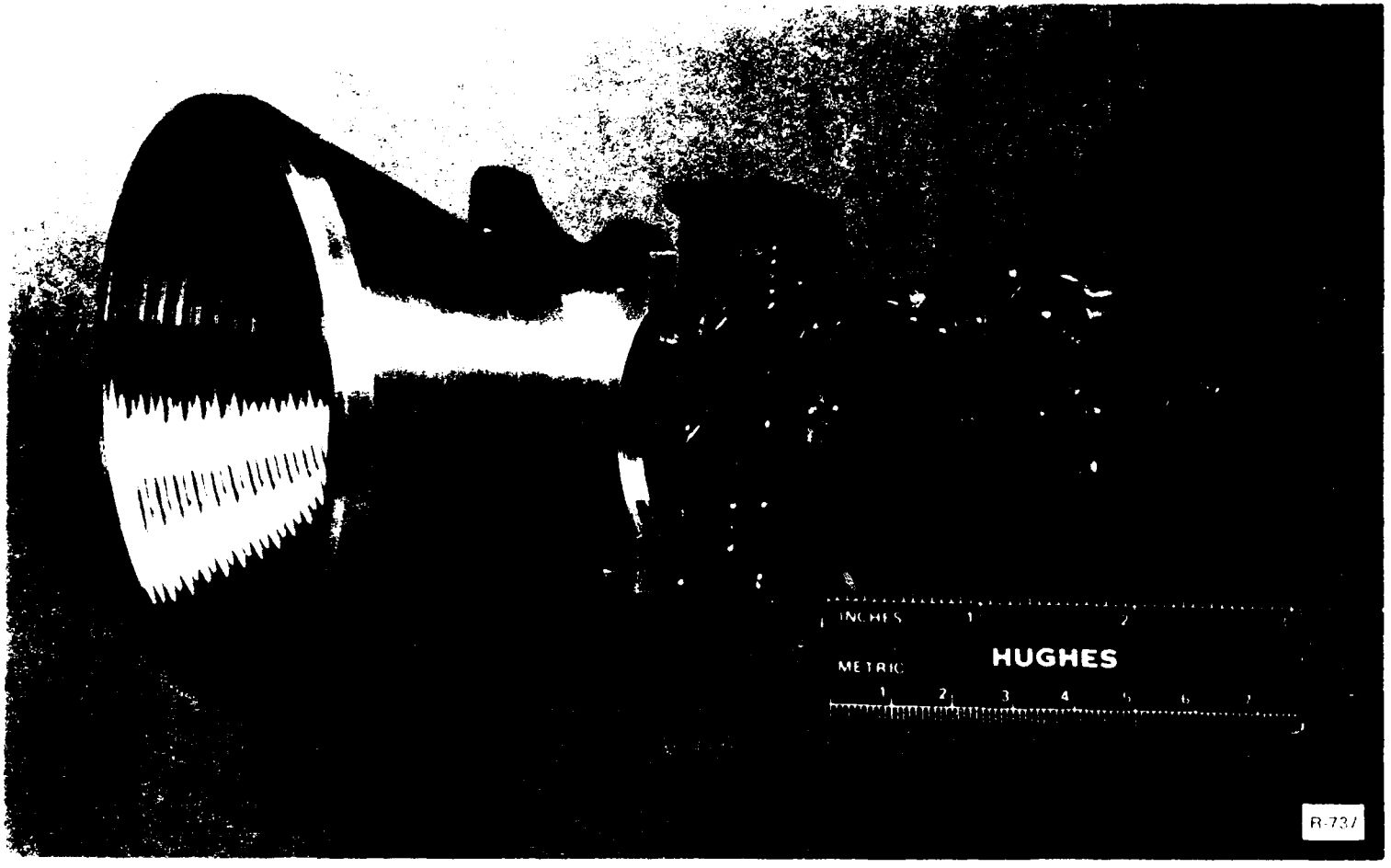

Figure II.4 The feed horn antenna of the SSM/I

Figure II.5 The sky reference reflector of the SSM/I

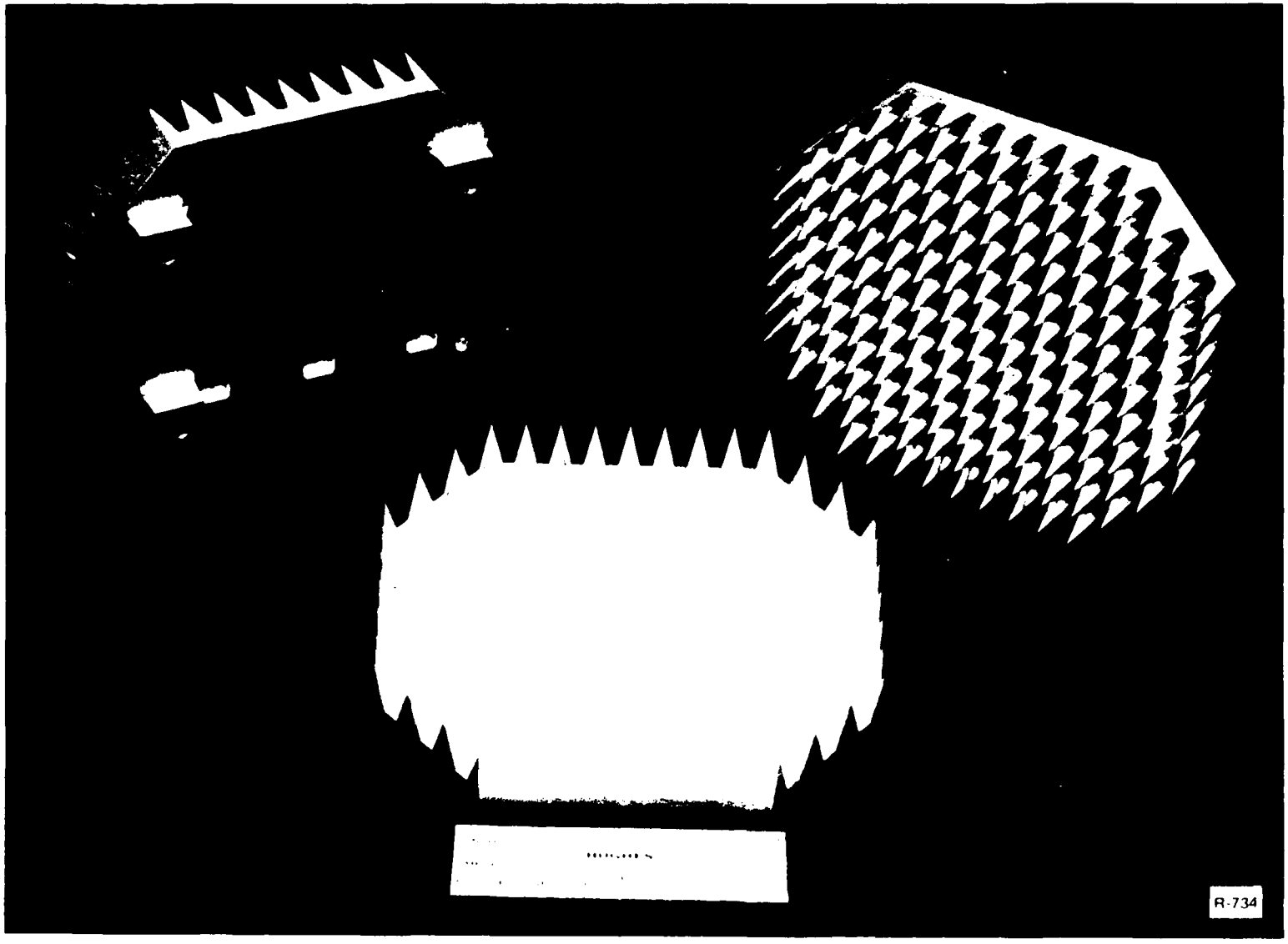

Figure II.6 The hot absorber reference of the SSM/I

PARAMETER	RADIOMETRIC PERFORMANCE			
CENTER FREQ, GHZ	19.35 ± 0.05	22.235 ± 0.05	37.0 ± 0.1	85.5 ± 0.3
POLARIZATION	VERT AND HORIZ	VERT	VERT AND HORIZ	VERT AND HORIZ
IF BANDPASS, MHZ	10 TO 250	10 TO 250	100 TO 1000	100 TO 1500
RADIOMETRIC ACCURACY, K	1.5	1.5	1.5	1.5
ΔT, K	0.8	0.8	0.6	1.1
DYNAMIC TEMP RANGE, K	375	375	375	375
EFFECTIVE FOV (3 dB ANTENNA BEAMWIDTH; INCLUDES INTEG TIME) REFERENCE, KM	70 x 45	60 x 40	38 x 30	16 x 14
INTEGRATION TIME, mS	7.95	7.95	7.95	3.89

06133-284

Figure II.7 SSM/I performance characteristics

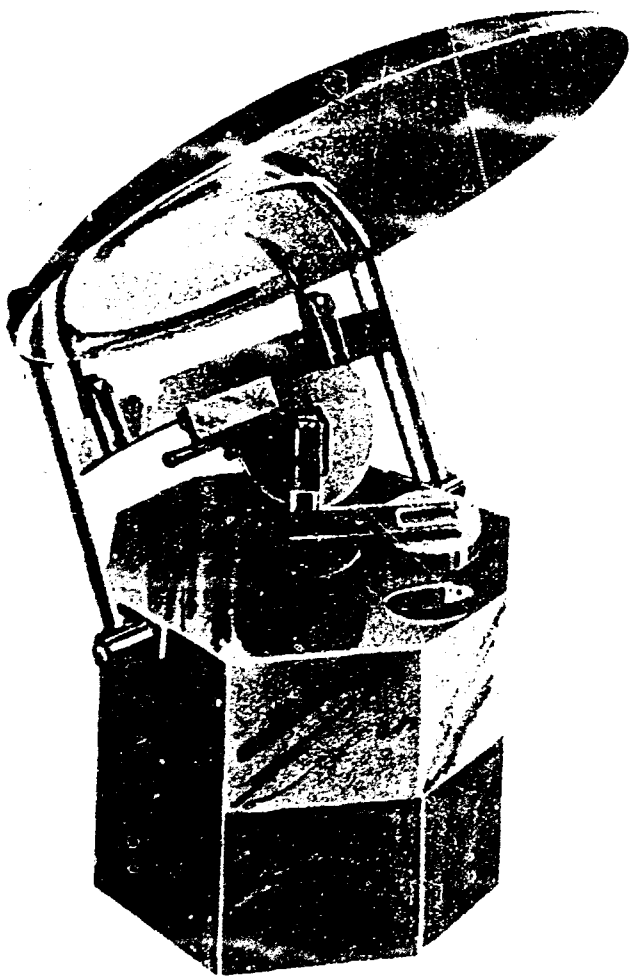

WEIGHT	107 LB
SIZE	
• ANTENNA	24 x 26 IN.
• DRUM	14 IN. DIAMETER 16 IN. HEIGHT
POWER	45 W
ORBIT	833 KM CIRCULAR 101 MINUTE PERIOD 98.7° INCLINATION — SUN SYNCHRONOUS
SWATH	1390 KM
SPACECRAFT	DMSP BLOCK 5D-2

Figure II.8 SSM/I radiometer specifications

SCAN A	
SCENE STATIONS/SCAN	**128**
PIXELS/SCAN	**576**
SCAN B	
SCENE STATIONS/SCAN	**128**
PIXELS/SCAN	**256**
SCENE STATION/ORBIT	**404,224**
PIXELS/ORBIT	**1,313,728**

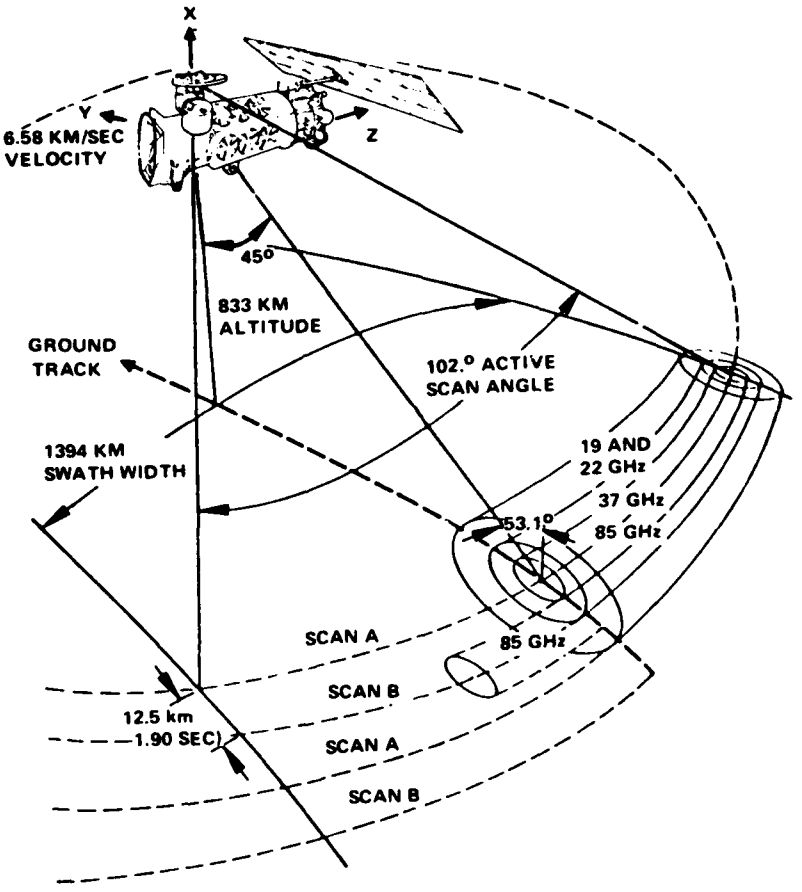

Figure II.9 SSM/I scan geometry

The hot absorber and cold sky reflector references are each sampled in the same manner as the scene data but over total angles of 8.0°, rather than 102.4°, as they occult the feed horn during the remaining portion of the scan. The scene, absorber and reflector samples along with the temperature of the absorber, various instrument parameters and zero's required to match input and output data rates result in 3636 bit blocks of data each second.

The radiometer outputs are converted to absolute antenna temperature using the hot and cold sky reference measurements and then corrected for antenna pattern effects to obtain absolute brightness temperatures. The brightness temperatures are then used with a "D" matrix retrieval algorithm to estimate various environmental parameters. The measured environmental parameters, the geometric resolution, and the range, quantization and absolute accuracy of the measurements are given in Figure II.10.

III. ENVIRONMENTAL RETRIEVAL ALGORITHM

The SSM/I environmental retrieval algorithm includes several important components: climatology and radiosondes, an interactive (radiative transfer) model, a geophysical model and the parameteric extraction algorithm. Figure III.1 shows the relationship among these elements. The geophysical model and the interaction model are employed in the brightness temperature (T_B) simulations. The D-matrix approach is used for all parameter extraction except for sea ice morphology. In that case, a deterministic approach is used. The environmental retrieval algorithm was developed at Environmental Research and Technology, Inc. (ERT) under a sub-contract from Hughes Aircraft Company. Detailed documentation of the algorithm and models was not part of the contract and is not generally available. The following sub-sections contain descriptions of the geophysical and interactive models, the environmental parameters, the climatology, and the parameter extraction algorithm as compiled from several different sources (1,2,3,4). This section serves as a comprehensive digest of the SSM/I environmental retrieval algorithm.

A. Geophysical Models

A.1 Ocean Surface Wind Speed

The calculation of the emissivity of a smooth water surface is relatively straightforward. The dielectric properties of sea water, derived from the measurements of Lane and Saxton (5) and expressed in analytic form by Chang and Wilheit (6), are used for the SSM/I algorithm. The Fresnel equations for a plane dielectric interface are used to calculate the emissivity of the smooth surface for a given view angle and polarization.

Wind driven waves and foam on the ocean surface both significantly alter the microwave emissivity of the ocean surface. The wind speed is highly variable both horizontally and vertically. Marine wind speed measured from a ship is usually referenced to a standard height of 20 meters. However, the wind speed which directly relates to roughness and foam, and the one used in the development of the physical relationships, is the friction velocity at the ocean-sea interface. The relationship developed by Cardone (7) is then used to translate it to the standard 20 meter height.

PARAMETER	DESIRED GEOMETRIC* RESOLUTION, KM	RANGE OF VALUES	QUANTIZATION LEVELS	ABSOLUTE ACCURACY
OCEAN SURFACE WIND SPEED	25	3 TO 25	1	± 2 M/S
ICE				
• AREA COVERED	25	0 TO 100	5	± 12%
• AGE	50	1ST YEAR, MULTIYEAR	1 YR, > 2 YR	NONE
• EDGE LOCATION	25	NA	NA	± 12.5 KM
PRECIPITATION OVER LAND AREAS	25	0 TO 25	0, 5, 10, 15, 20, ⩾ 25	± 5 MM/HR
CLOUD WATER**	25	0 TO 1	0.05	± 0.1 KG/M^2
LIQUID WATER***	25	0 TO 6	0.10	± 2.0 KG/M^2
PRECIPITATION OVER WATER	25	0 TO 25	0, 5, 10, 15, 20, ⩾ 25	± 5 MM/HR
SOIL MOISTURE	50	DRY – SATURATED	DRY – MOIST WET – SATURATED	NONE

* GOALS FOR SYSTEM
** <100 μm DIAMETER
*** > 100 μm DIAMETER

Figure II.10 SSM/I environmental parameters

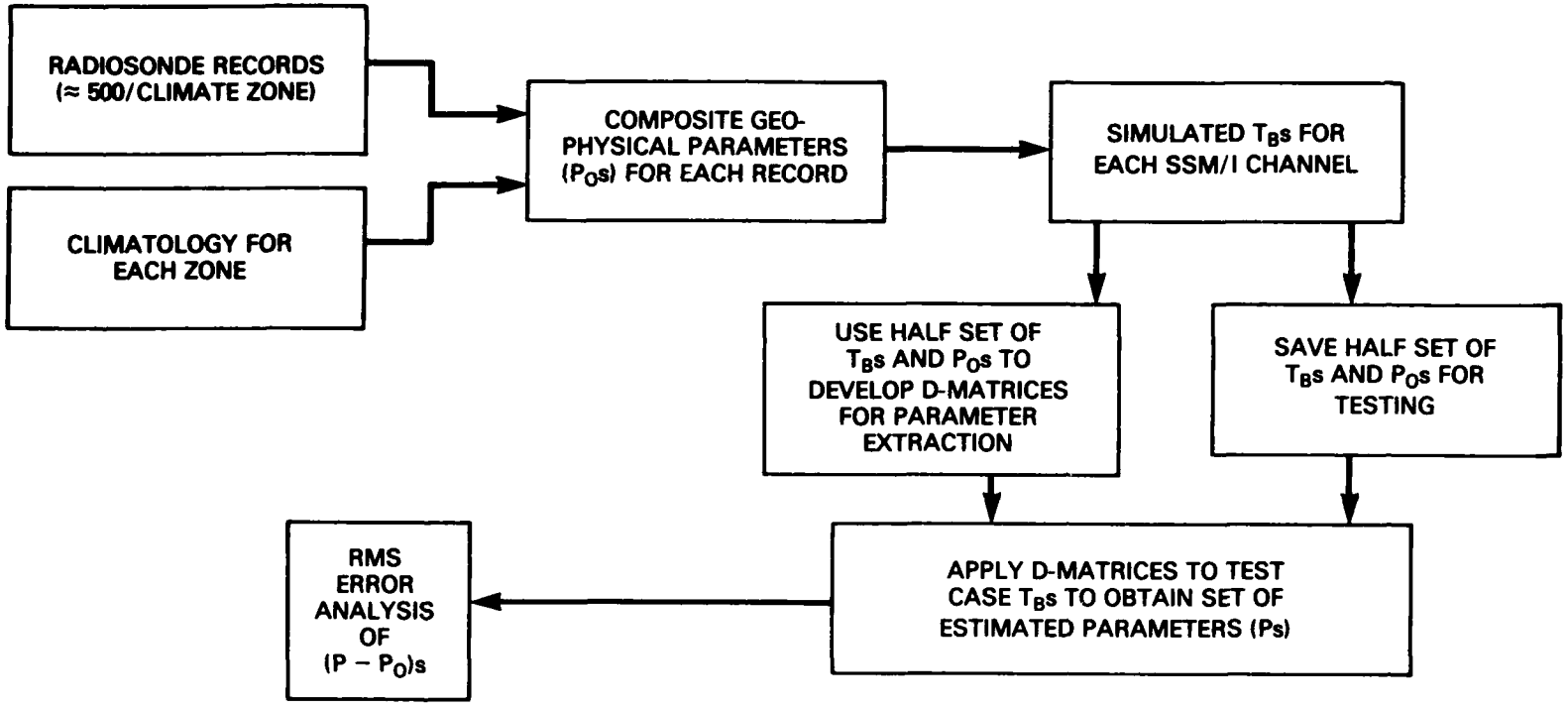

Figure III.1 SSM/I algorithm development

The roughness effect is modeled using a study by Cox and Munk (8) and treating the sea surface as a collection of plane facets large compared to the observational wavelength. The variance in sea surface slope is defined as a function of wind speed and then used for calculation of emissivity assuming a Gaussian slope distribution for the facets and using the Fresnel relations. The derived wind speed dependence of the surface slope variance, σ^2, is given by

$$\sigma^2(f) = (0.3 + 0.02\ f)\ (0.003 + 0.48\ W) \qquad \text{for } f < 35 \text{ GHz, and}$$

$$= 0.003 + 0.48\ W \qquad \text{for } f \geq 35 \text{ GHz;} \qquad \text{(III.1)}$$

where f is frequency in gigahertz (GHz) and W is the wind speed at 20 meter height in m/sec.

In the ERT model, foam is treated as partially obscuring the surface in a manner independent of polarization but dependent upon frequency. The foam fraction, K, is defined as

$$K \simeq a(1 - e^{-f/f_o})\ (W - 7) \qquad \text{for } W \geq 7 \text{ m/sec, and}$$

$$= 0 \qquad \text{for } W < 7 \text{ m/sec;} \qquad \text{(III.2)}$$

where $a = 0.006$ sec/m and f_o is 7.5 GHz. This equation is based on Nordberg's (9) observation that the brightness temperature increases linearly with wind speed exceeding 7 m/sec, and that no foam forms below that wind speed.

Figure III.2 demonstrates the response of ocean surface wind speed at 19 V and H, 22 V, and 37 V and H, assuming a tropical clear atmosphere.

A.2 Precipitation Over Ocean and Land

Precipitation size droplets are the primary contributors to atmospheric attenuation at microwave wavelengths. The attenuation results from both absorption and scattering by the hydrometeors. The magnitude of these processes depends upon wavelength, drop size distribution, and precipitation layer thickness. This leads to the potential application of microwave observations for the detection of precipitation as well as the estimation of rain rate at the surface.

At lower frequencies, such as 19.35 GHz, rain is highly absorptive and results in an apparent warm brightness temperature over cold backgrounds such as the oceans. At frequencies greater than about 80 GHz, scattering effects become predominent and result in an apparent cool brightness temperature relative to warm backgrounds such as land (10). These effects increase with increasing rain rates.

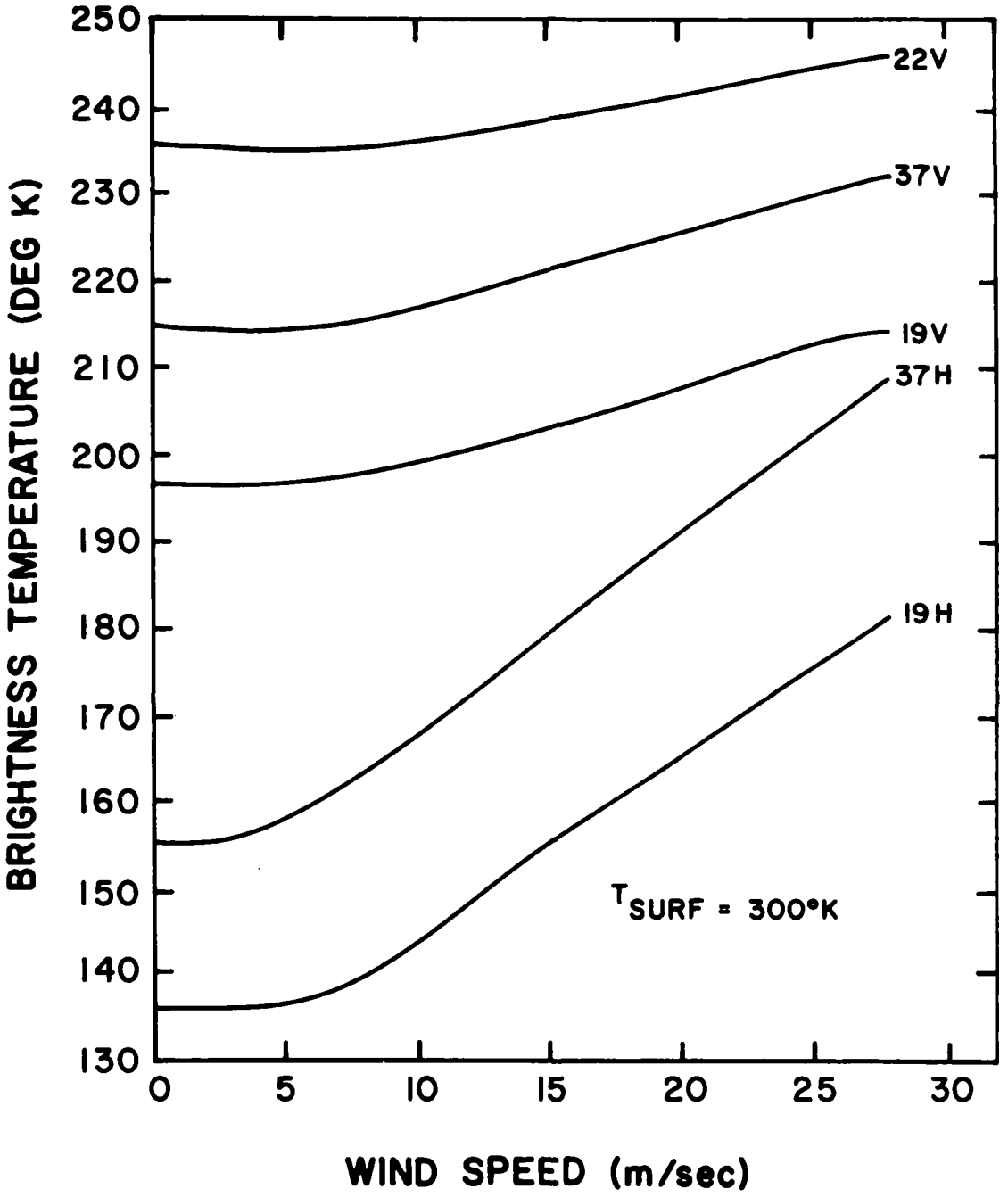

Figure III.2 Brightness temperatures function of frequency and wind speed

Some of the important physical properties of precipitation affecting microwave radiation are the drop size distribution, rain layer thickness, and the possibility of ice crystal coverage above the rain layer.

The drop size distribution employed for the SSM/I rain algorithm is derived by fitting the Deirmendjian distribution to the empirically observed spectra of Laws and Parson (11). The Deirmendjian distribution is defined as

$$n(r) = Ar^{C_1} \exp(-Br^{C_2}), \tag{III.3}$$

where n(r) is the drop size distribution in $cm^{-3}\mu m^{-1}$, r is the radius of rain drops in μm, and A and B are scale parameters.
Here,

$$A = \left(\frac{MC_2}{\frac{4\pi}{3}\rho_w 10^6}\right)\left(\frac{B}{r}\right)^{[(C_1+4)/C_2]},$$

where M is the total liquid water content in gm/m^3, and

$$M = \rho_w \int_o^\infty \frac{4\pi}{3} r^3 \eta(r)dr$$

$$B = \left(\frac{C_1}{C_2}\right) r_o^{-C_2},$$

and r_o is the mode radius in μm. The shape parameters are C_1 and C_2. The former of these, affects the distribution of the smaller radii while the latter affects the larger radii.

The analytical results from fitting the Laws-Parson empirical spectrum are

$$M = 0.0636\ (R^{.881})\ (gm/cm^3), \text{ where R is rain rate in mm/hr,}$$
$$r_o = 225 + 9.16\ (R^{.881}); \quad (r_o)_{max} = 375\ \mu m,$$
$$C_1 = 4.0, \tag{III.4}$$
$$C_2 = .70 - .00458\ (R^{.881}); \quad (C_2)_{min} = .625.$$

This formulation relates the rain rate to mode radius and liquid water density. It parameterizes the distribution as a function of rain rate only and thus simplifies the solution to the Deirmendjian distribution. On the other hand, it still retains the sensitivity of scattering to drop size, which would be lost if the simpler Marshall-Palmer distribution is used. Figure III.3 shows the good agreement between the Deirmendjian model and the Laws and Parson distributions.

For weak storms with low rain rates, $R \leq 8$ mm/hr, the ceiling for the rain layer does not exceed the 0 C isotherm. For more intensive convective storms, the ceiling is higher with a supercooled water layer on top. The

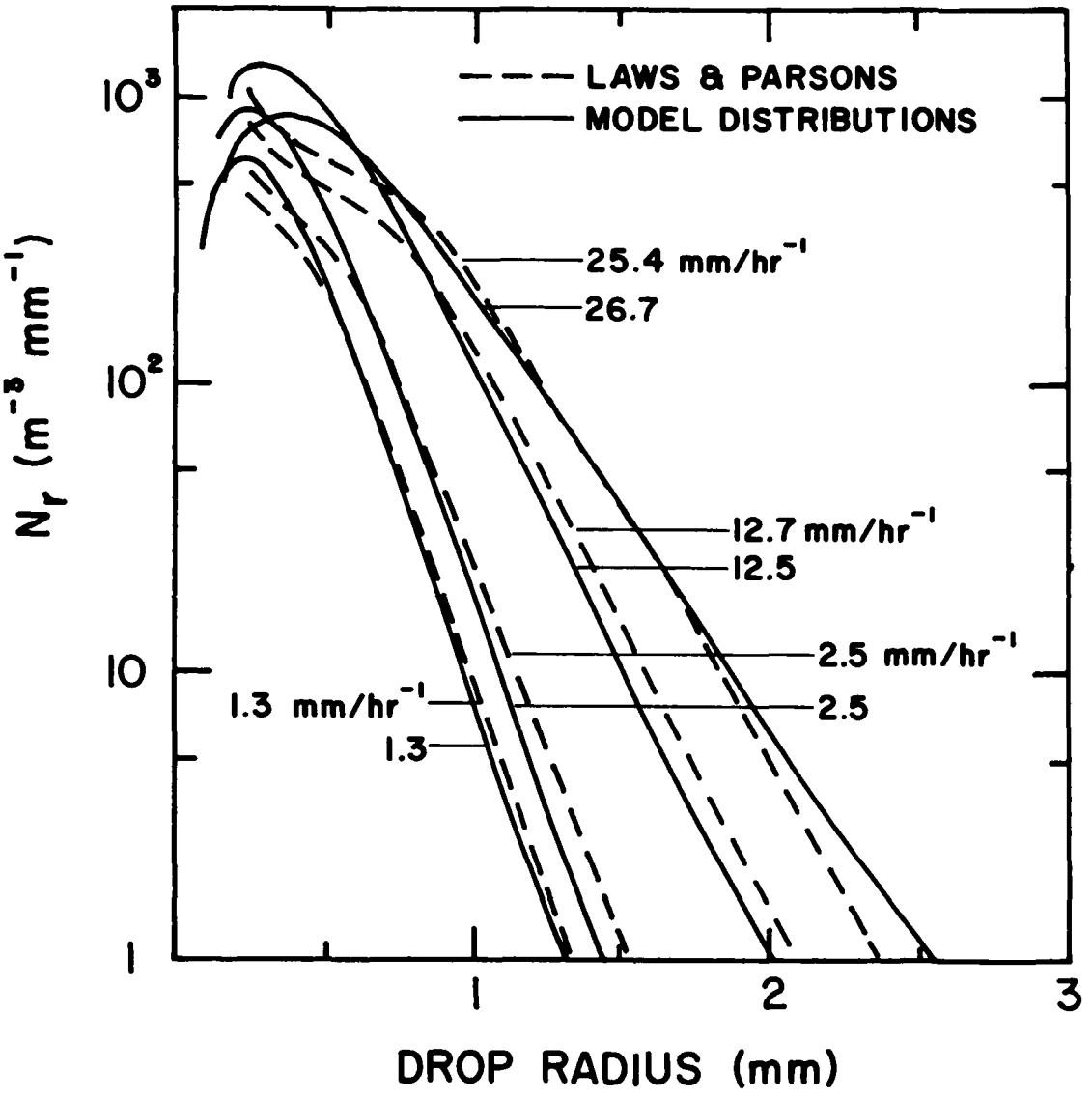

Figure III.3 The matching of the Deirmendjian raindrop-size distributions used in model computations to the observed Laws and Parsons distributions.

thickness of this layer depends on the intensity of convection. Climatology using categories of latitudes (tropics, mid-latitudes and Arctic regions) and surface types (land and ocean) is used to provide the estimation of the supercooled water layer thickness as a function of rain rate. The thickness of the supercooled layer, ΔZ, for rain rates in excess of 8 mm/hr, is given as

$$\Delta Z = (R - 8.0)\, Z_{inc},$$

and (III.5)

$$\Delta Z \leq Z_{max},$$

where Z_{inc} and Z_{max} are determined from climatology (1).

At lower frequencies the absorption effect of ice particles is insignificant, but large ice or snow crystals, which may occur on the top of a storm, can cause significant scattering effects at 85.5 GHz. From simulation studies, it is evident that layers of ice particles having a size of 400 μm would cause the loss of all sensitivity to rain rate. With 200 μm particle size, the effect could also be significant depending on the layer thickness. For most rain conditions, the typical ice particle size is 100 μm, which does not cause significant attenuation at 85.5 GHz. A 1 km thick cloud layer of 200 μm ice particles would be considered unusually severe (1).

Brightness temperature calculations are based on the radiative transfer theory and the atmoshpere and rain models. The brightness temperature versus rain rates over mid-latitude ocean and over mid-latitude land are presented in Figures III.4 and III.5. These calculations include the presence of supercooled water layers for rain rates above 8mm/hr. The 19.35 and 37.0 GHz frequencies are used for retrieval of rain over ocean, while the 37.0 and 85.5 GHz are used over land.

A.3 Cloud Water Over Ocean and Land

Cloud water is defined to consist of droplets smaller than 100 m in diameter. Droplets this size produce negligible scattering at the SSM/I frequencies and only absorption due to the mass of water present need be considered. The absorption coefficient, γ, in nepers/m for droplets with diameter small compared to a wavelength is given by Staelin (12) as

$$\gamma = \frac{1.0016 \times 10^{4} \quad m \quad 10^{0.0122(291-T)}}{\lambda^{2}}, \qquad \text{(III.6)}$$

where m is liquid water content gm/m^3; T is atmospheric temperature in K and λ is wavelength in cm.

The water vapor in the cloud is taken as the saturation value. The absorption coefficient for water vapor is computed using the Van-Vleck and

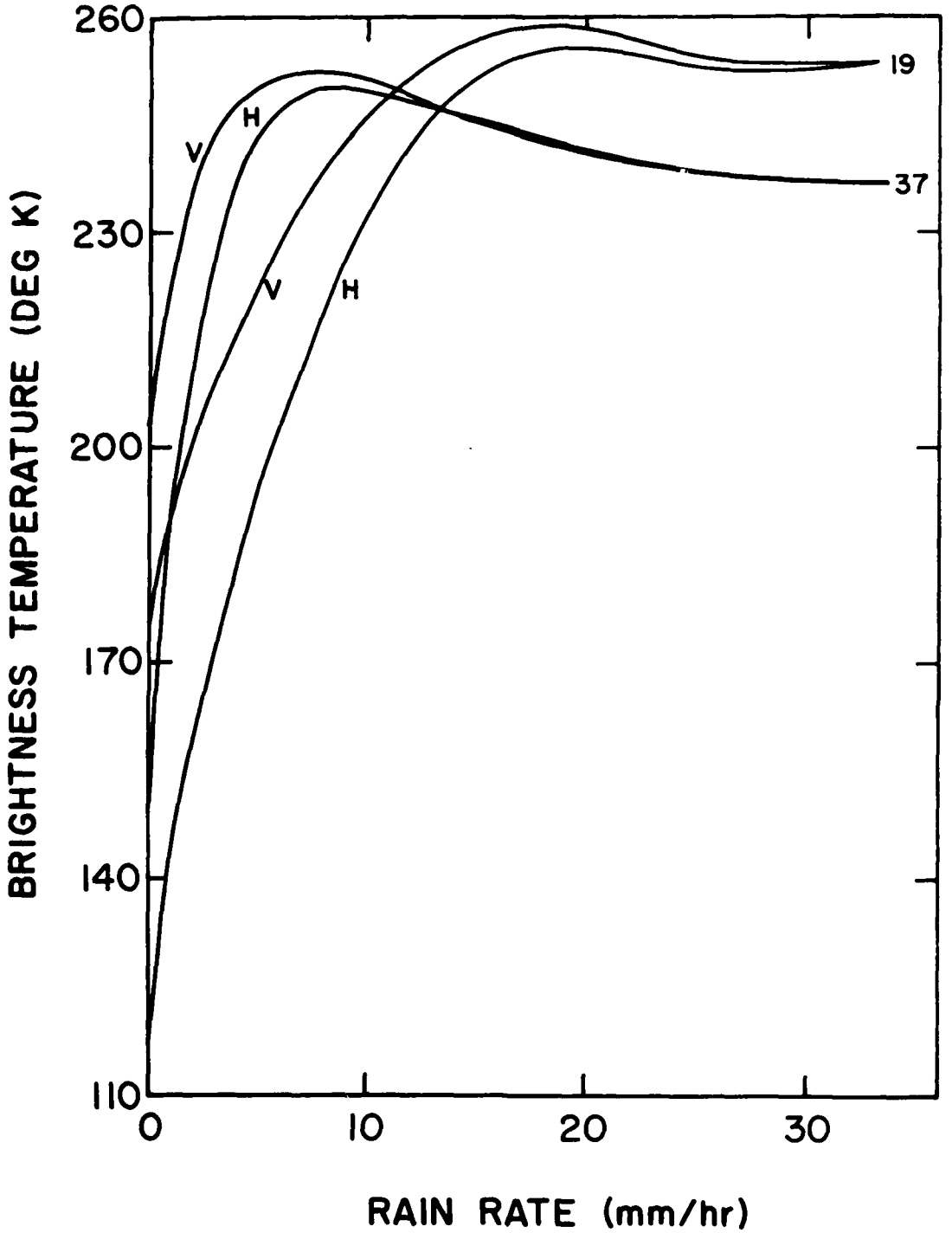

Figure III.4 Brightness temperature vs. rain rate over mid-latitude ocean background at 19.35 and 37 GHz, vertical and horizontal polarizations (look angle = 50°).

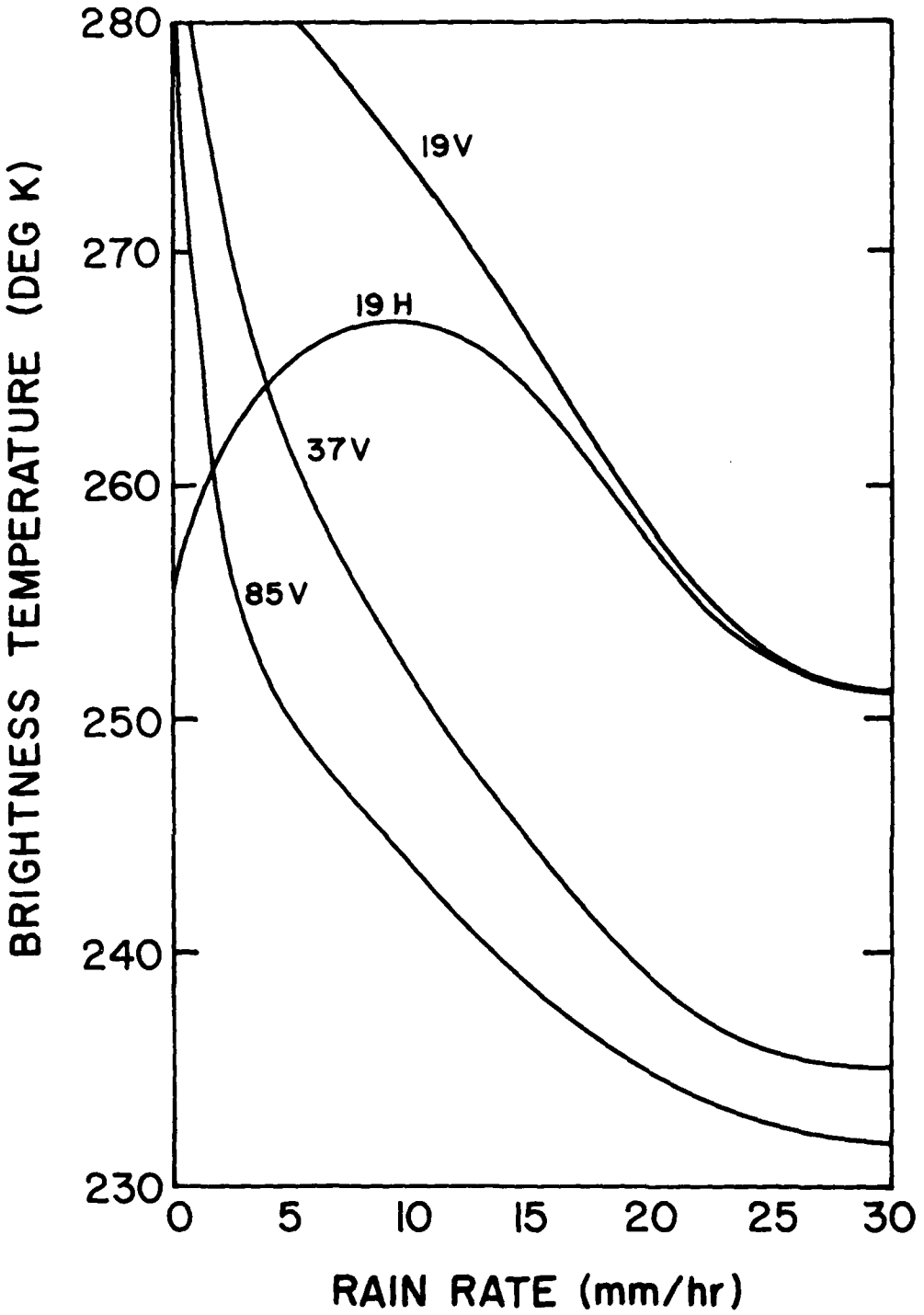

Figure III.5 Brightness temperature vs. rain rate over mid-latitude land at 85.5, 37 and 19.35 GHz. The look angle is assumed to be 50^{o}.

Weisskopf (19) collision broadened line shape with an empirical correction term for the wings of the line (20). The absorption coefficient of oxygen is computed using line shape factors defined by Rosenkranz (21). These are computed for all parameters for each level and integrated using the radiative transfer equation to provide brightness temperatures. The response due to cloud water at 19, 22, and 37 GHz over a mid-latitude ocean background is shown in Figure III.6. The figure is an idealized demonstration assuming the existence of only one type of cloud.

In general, the retrieval of cloud water over the ocean can be achieved with a high degree of accuracy due to the fact that the ocean surface is a cold background in the microwave range, and is relatively homogeneous. The retrieval of cloud water over land can be difficult because the land background is much warmer than the ocean and results in less contrast between cloud and background and because the variations in the land background are significant relative to the cloud contrast. As a result, cloud signatures frequently fall within the environmental noise range.

When rain occurs, the sensitivity of the algorithm to cloud water is lost. Criteria including the 85.5 GHz vertical polarization brightness temperature, and the brightness temperature difference between the horizontal and vertical polarizations at 85.5 GHz, have been set to determine whether rain exists over land. Similar criteria using 37.0 GHz data have been chosen for ocean cases. These are used to determine whether cloud water or rain rate is to be retrieved. The brightness temperature criteria are given for different latitude regions and seasons. Those for mid-latitude land for spring and autumn and tropical ocean for summer are illustrated in Figures III.7 and III.8.

A.4 Soil Moisture

The soil moisture model developed for SSM/I is based on the concept that thermal microwave radiation in soils results from the random, microscopic current loops within the soil volume (13). The intensity of radiation at a given point depends on the local dielectric constant and the physical temperature of the soil. Moisture produces a marked increase in both the real and the imaginary parts of the dielectric constant of soil, leading to a decrease in the soil emissivity. Experimental observations and theoretical calculations indicate that the emissivity of soil at microwave frequencies can range from > 0.9 for dry soils to ≤ 0.6 for very moist soils.

A generalized incoherent layered surface model (24) was used to simulate expected SSM/I soil moisture signatures. In this model, layers of soil with different moisture contents are modeled as multilayer media, with the reflection coefficients between layers and opacities within the layer calculated from the dielectric properties of the medium.

For a plane dielectric-air interface the Fresnel coefficients are

$$F_H = \frac{\cos\theta - \sqrt{\varepsilon - \sin^2\theta}}{\cos\theta + \sqrt{\varepsilon - \sin^2\theta}} \qquad \text{(III.7)}$$

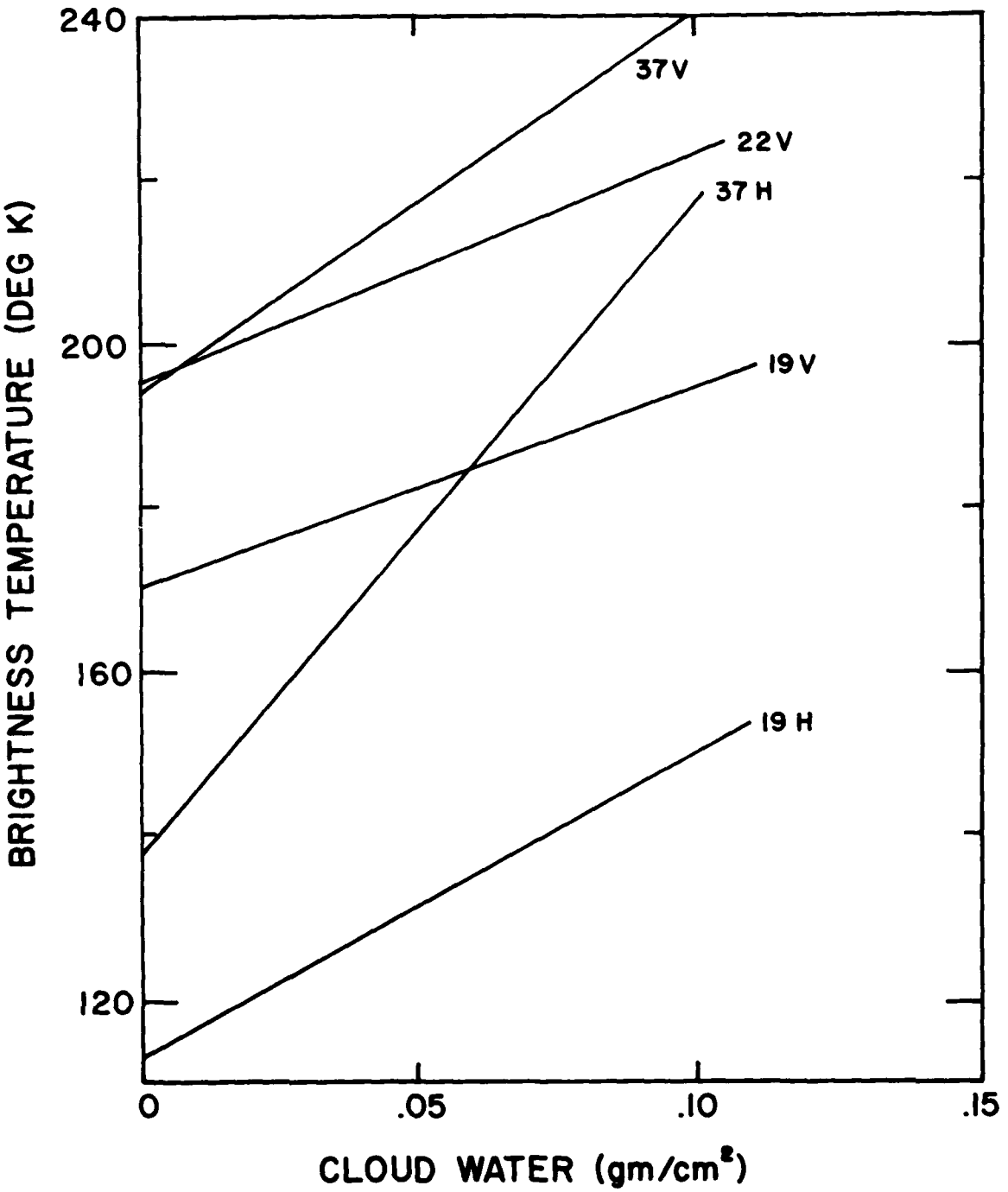

Figure III.6 Brightness temperature vs. cloud water over mid-latitude ocean

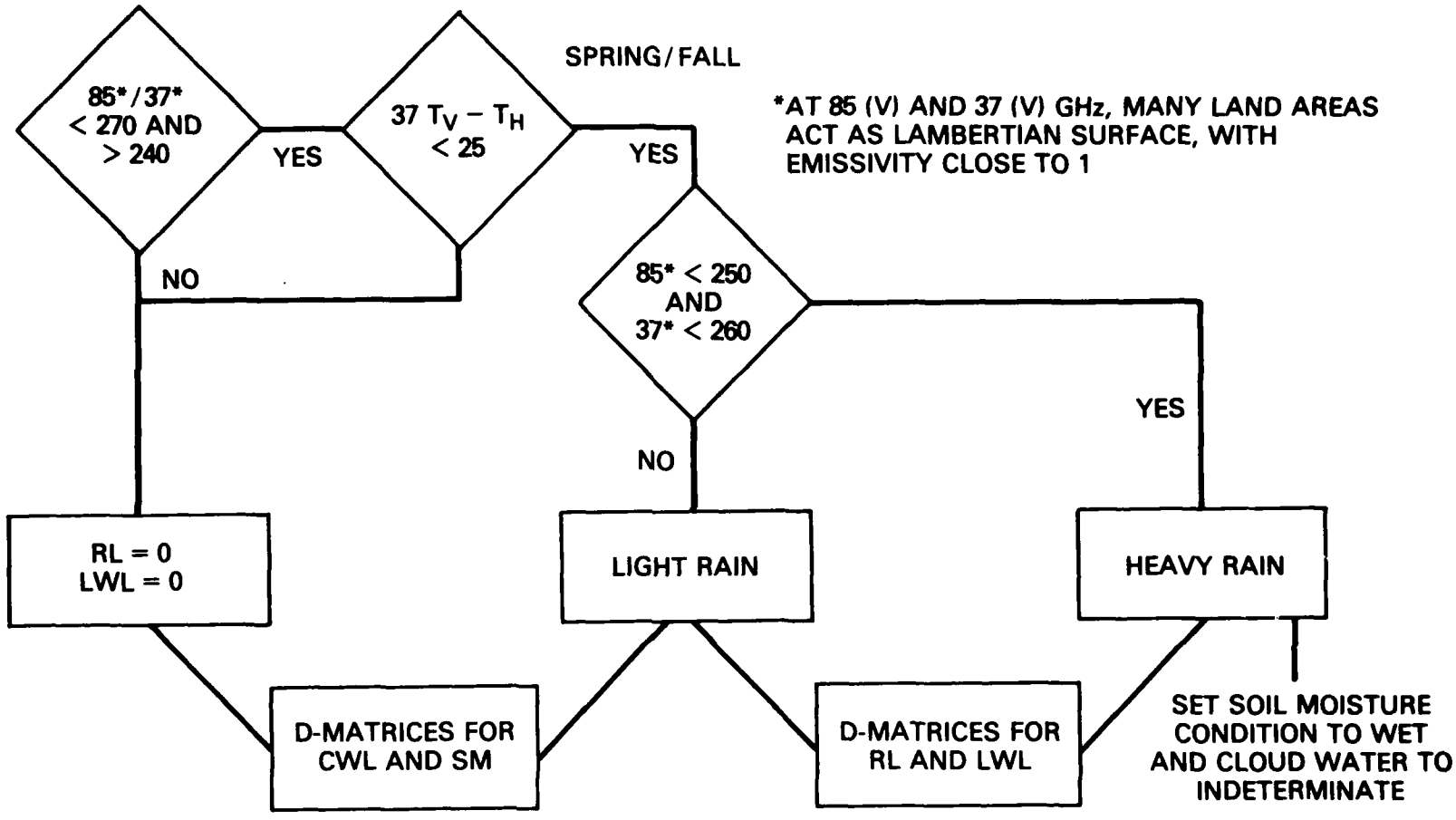

Figure III.7 Mid-latitude region algorithm for land

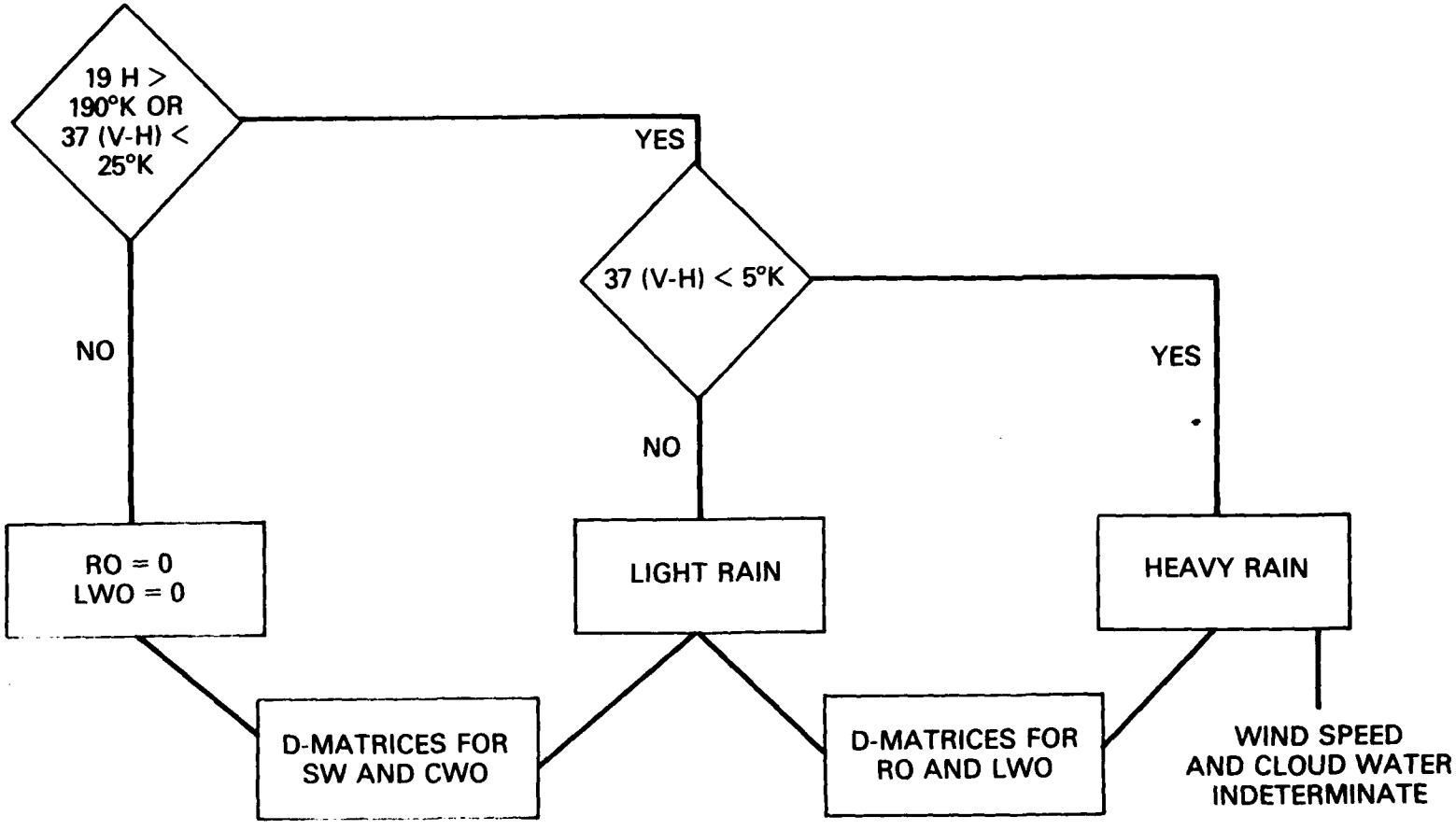

Figure III.8 Algorithm for tropical ocean summer

$$F_V = \frac{\varepsilon \cos\theta - \sqrt{\varepsilon - \sin^2\theta}}{\varepsilon \cos\theta + \sqrt{\varepsilon - \sin^2\theta}} \qquad \text{(III.8)}$$

where the dielectric constant of soil is ε. The angle of incidence is θ and the horizontal and vertical polarizations are denoted by H and V. The reflection coefficient is the square of the absolute value of the Fresnel coefficient.

$$R_H = |F_H|^2 \qquad \text{and } R_V = |F_V|^2 \quad . \qquad \text{(III.9)}$$

The soil moisture model uses existing measurements of the dielectric properties of the soil. The layered surface is combined with the radiative transfer equations of the atmosphere to obtain brightness temperatures for the generation of the inversion algorithms.

Figure III.9 gives the predicted emissivity at 1.43, 19 and 37 GHz as a function of soil moisture. The SSM/I soil moisture retrieval uses only the 19 GHz H and V channels.

Choudhary and Schumugge (14) developed a simple correction factor to the reflectivity to take into account the surface roughness effect. The corrected reflection coefficient is given by

$$R'(\theta) = R(\theta) \exp(-h \cos^2\theta),$$

where (III.10)

$$h = 4\sigma^2 (2\pi/\lambda)^2,$$

σ^2 is the variance of the surface roughness, λ is the observational wavelength and h at 19 GHz is assumed to vary between 0 and 0.6.

A.5 Sea Ice

A detailed geophysical model is not used for sea ice since the sea ice parameters are not obtained from the general "D" matrix retrieval algorithm employed for the other geophysical parameters but rather are obtained from deterministic equations with empirically determined constants. The upwelling brightness temperature sensed by the SSM/I radiometer from a scene containing various amounts and types of sea ice may be expressed as

$$T_{Bp} = e^{-\tau} \left[C \cdot F \left(\varepsilon_{fp} T_f + (1-\varepsilon_{fp}) T_{sky}\right) + C \cdot (1-F) \left(\varepsilon_{mp} T_m + (1-\varepsilon_{mp}) T_{sky}\right)\right.$$

(III.11)

$$\left. + (1-C) \left(\varepsilon_{wp} T_w + (1-\varepsilon_{wp}) T_{sky}\right)\right] + T_{atm}$$

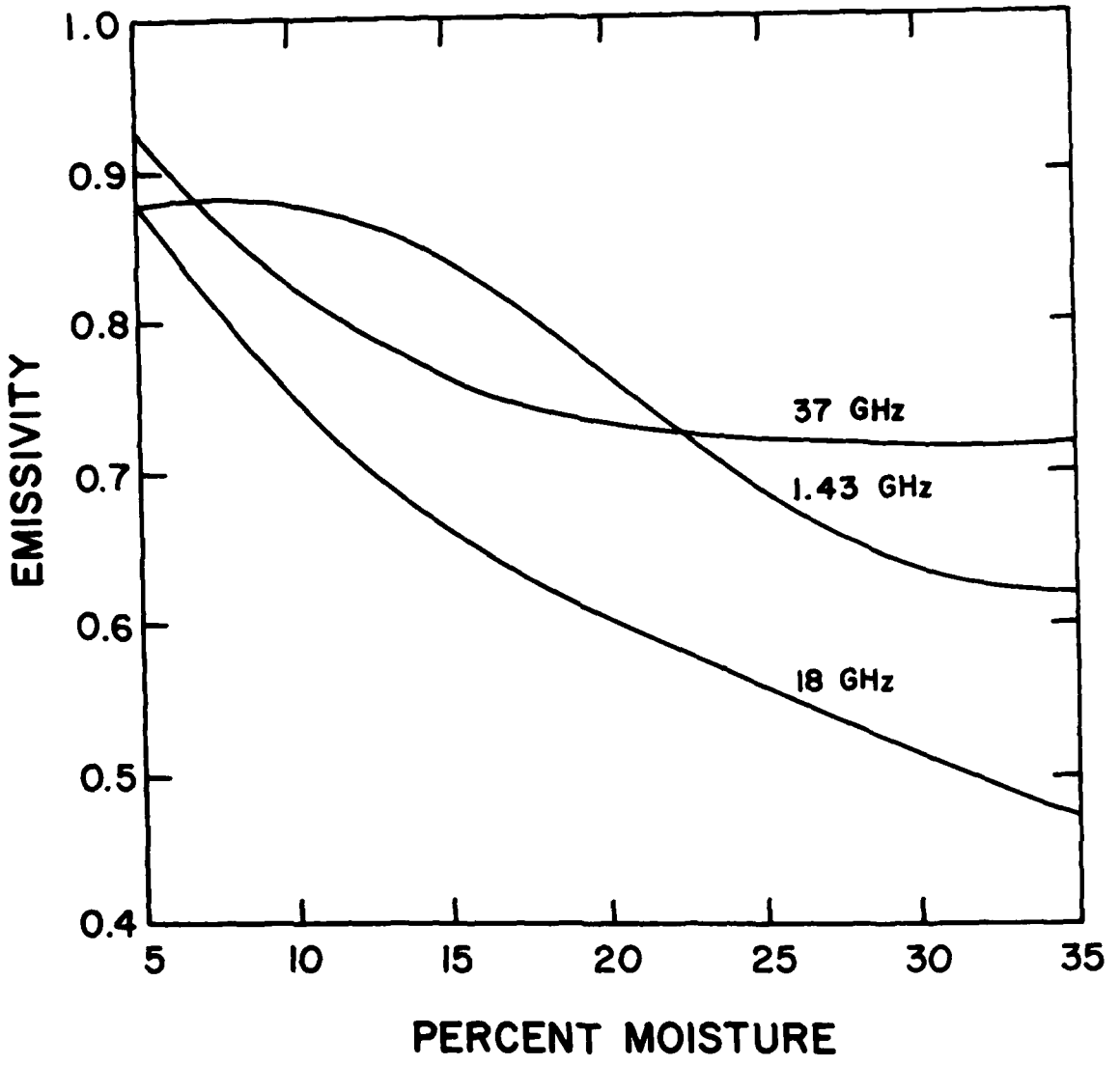

Figure III.9 Predicted emissivities at 37, 18, and 1.43 GHz for various soid moisture contents

where τ is total atmospheric opacity; p indicates polarization (H or V), C is the fraction of sea ice including all ice types; F and M are fractions of first year ice and multiyear ice relative to the total ice present and F+M=1. The emissivities are given by ε, and T is the surface temperatures in Celsius. Subscripts f, m, and w indicate first year ice, multiyear ice, and sea water. T_{sky} is the incident sky temperature at the surface, and T_{atm} is atmospheric contribution to the upwelling radiation.

The difference between the vertical and horizontal emissivities at 37 GHz (see Table III.1) exhibits significantly less dependence on ice age than the corresponding 19.35 GHz emissivity differences or the vertical and horizontal components themselves at either frequency. This property is employed to obtain the ice concentration using only the difference in the vertical and horizontal 37 GHz brightness temperatures through the deterministic inversion method.

The algorithms used to extract sea ice concentration and ice temperature are given by

$$C = a_o + a_1 [T_{BV}(37) - T_{BH}(37)] \qquad \text{(III.12)}$$

$$= [(a_2 + a_3 T_{BV}(37)]/C + a_4 \qquad \text{(III.13)}$$

Ice type is determined by the derived temperature T in the following manner:

FY if $T > T_o$,

MY if $T < T_o$.

The coefficients a_o thru a_4, as well as T_o are different for each season of the year and are

	a_o	a_1	a_2	a_3	a_4	T_o
winter	1.165	-0.0206	-217.70	1.1050	192.28	218.0
spring	1.164	-0.0176	-217.70	1.1050	192.28	218.0
summer	1.164	-0.0176	-219.06	1.1050	193.64	228.0
autumn	1.163	-0.0276	-219.06	1.1050	193.64	228.0

The ice edge locations is determined using a two dimensional interpolation technique. If a pixel is determined to be ice by the above algorithm, the four cardinal adjacent pixels (two perpendicular and two along the scan) will also be tested. If any of these four pixels is found to be water, the center pixel will be flagged as the ice edge.

B. Interaction Model

The geophysical models define the physical and electromagnetic properties of the surface and atmospheric constituents. The interaction model determines the radiative transfer properties of the total surface-atmospheric system. The liquid water present in the system dominates the radiative transfer calculation. When only very small droplets

Table III.1 Emissivity of ice

ICE TYPE	MY		FY ICE		FY THIN ICE		WATER CALM SEA	
POLARIZATION**	V	H	V	H	V	H	V	H
FREQ, GHZ								
19.35	0.86	0.73	0.97	0.84	0.96	0.78	0.60	0.33
37	0.69	0.64	0.97	0.95	0.96	0.87	0.70	0.40
37 (V-H)	0.05		0.02		0.09		0.30	

**V – VERTICAL; H – HORIZONTAL; 50° EARTH INCIDENCE ANGLE

in the form of clouds are present, the calculations are relatively simple because only absorption effects need be considered. However, when scattering is present, e.g., in the case of precipitation, a much more complicated scheme must be employed. The Mie theory is employed to evaluate the extinction coefficients and a variational, iterative approach (16, 17) is used to solve the radiative transfer equation.

The radiative transfer equation, using the Rayleigh-Jeans approximation for a blackbody, can be written as

$$\frac{dT_B(A,\theta)}{dr'} = T_B(A,\theta) - T(Z), \qquad \text{(III.14)}$$

where T_B is the brightness temperature and T is the physical temperature in degrees K; r' is the total opacity of the atmosphere along the line of sight (in nepers); Z is the height and θ is the look angle. When no scattering is present, T_B sensed by the satellite can be written as (18)

$$T_B(Z,) = T_{B_1}(Z,) + [(1-R)\, T_G + R\, T_{B_2}] \exp(-r') \qquad \text{(III.15)}$$

where T_{B_1} is the upward atmospheric emission; R is the effective surface reflectivity; T_G is the surface temperature, and T_{B_2} is the downward atmospheric emission plus the attenuated sky background emission. Intergrating over the entire atmospheric yields.

$$T_{B1} = \int_o^H T(z)\gamma(z) \exp\left[- \int_z^H \gamma(z') \sec\theta \, dz'\right] \sec\theta dz,$$

and (III.16)

$$T_{B2} = T_{sky} e^{-\tau'} + \int_o^H T(z)\gamma(z) \cdot \exp\left[- \int_o^\xi \gamma(z')\sec\theta dz'\right] \sec\theta \, dz$$

where $\tau' = \int_o^H \gamma(z) \sec dz$. Here H is the height of the radiometer and γ is the total extinction coefficient at height z.

The Mie scattering theory is the formalism used to account for the coupling of the absorption and multiple scattering effects when rain is present. It is based on the diffraction of a plane monochromatic wave by a sphere with a homogeneous complex index of refraction. The absorption in the sphere and the scattered wave are calculated to provide the extinction coefficient and single scatter albedo.

$$Q_E = Q_A + Q_S,$$
$$\omega_O = Q_S/Q_A \ , \qquad \text{(III.17)}$$

where the Q's are efficiency factors defined as the ratio of actual to geometric cross sections. A, S, and E indicate absorption, scattering and

extinction. ω_o is the single scattering albedo. The extinction coefficient is derived by integrating the efficiency factor over the drop size distribution encountered in the geophysical model for rain.

$$\gamma_E = \int N(r)\, Q_E\, r^2\, dr \qquad \text{(III.18)}$$

Note that Q_E is a function of wavelength, temperature and drop size. The radiative transfer equation is now

$$\frac{dT_B(z,\theta)}{dr'} = T_B(z,\theta) - T_S(z,\theta) \qquad \text{(III.19)}$$

The difference between this and equation (III.14) is that the source function is no longer the physical temperature. Equation (III.19) can be written as

$$\mu \frac{dT_B(\tau,\mu)}{d\tau} = T_B(\tau,\mu) - T_S(\tau,\mu) \qquad \text{(III.20)}$$

where $\mu = \cos\theta$ and $\tau = r'/\mu$.

$$T_S = [1-\omega_o(\zeta)]\, T(\tau,\mu) - \frac{\omega_o(\tau)}{2}\int_{-1}^{1} P(\mu,\mu')\, T_B(\tau,\mu')\, d\mu' \qquad \text{(III.21)}$$

where P is phase function. It is reduced to 1 in the isotropic scattering case. It can be shown that the integral equation for the source function T_S including the boundaries i

$$T_S(\tau) = \left[1-\omega_o(\tau)\right]\left[T-T_{sky}e^{-\tau}\right] + \frac{\omega_o(\tau)}{2}\int_o^{\tau^*} T_S(\tau)\, E_1(|\tau-\tau|)d\tau$$
$$+ \frac{\omega_o(\tau)}{2} E_2(\zeta^*-\zeta)\left[(1-R)T_G + R\int_o^{\tau^*} T_S(\tau)\exp-\left[\frac{(\tau^*-\tau)}{\mu}\right]\frac{d\tau}{\mu}\right] \qquad \text{(III.22)}$$

where τ^* is total optical depth of the atmosphere and E_n is

$$E_n(x) = \int_o^1 \exp(-x/\mu)\mu^{n-2} d$$

The variational-iterative approach (16,17) is then used to solve for the integral for T_S. The method essentially finds the "extremum" of a function in N-dimensional parameter space. It is a fast and accurate technique for handling large ensembles of data.

C. The Retrieval Technique and Climatology.

The statistical inversion method is used for retrieving the geophysical parameters with the exception of the ice parameters, from the brightness temperatures. The method determines the statistical correlations between an ensamble of sets of brightness temperatures derived from the environmental model and the associated environmental parameters. The resulting

correlation cofficients are contained in the so-called D-matrix. This technique assumes a linear relationship between the T_B's and the physical parameters.

$$\underline{P}^* = \underline{D} \quad \underline{t} \ , \tag{III.23}$$

Where $\underline{P}^*$ is the vector of estimates of the parameters, $\underline{t}$ is the vector of brightness temperatures and $\underline{D}$ is the D-matrix.

C.1 Averaging technique for each parameter

Another feature used in the inversion process is to "tune" the D-matrix to the average value of each parameter. Though the resulting inversion is still linear in brightness temperature, $\underline{D}$ is now focussed on a correlated deviation from the statistically averaged values of the parameters. The D-matrix is determined from the least squares process based on the actual parameters and the corresponding simulated brightness temperatures.

C.2 Separate inversion scheme for each climatology.

In order to minimize non-linearities between the TB's and the environmental parameters to be derived, and hence to enhance the accuracy of the retrievals the earth is divided geographically into three major regions over four seasons (see Table III.2). Transition zones are also designed to avoid drastic transition between the neighboring regions. Stations, representative of each climate region, are selected for the collection of a atmospheric radiosondes and surface observations necessary for the calculation of the brightness temperatures needed for the construction of the D-matrices. The stations selected are shown in Table III.3.

C.3 Piece-wise Scheme for regression

Another type of non-linearity encountered in the retrieval of the geophysical parameters involves the relationship between the parameter and brightness temperature. The radiative signatures, particularly rain rate, are highly non-linear. The signatures for no rain, light rain, and heavy rain are very different. A piece-wise decision test for rain was designed. The algorithm for the estimation of rain over ocean is shown in Figure III.8. The criterion for no rain, light rain, and heavy rain are the 37.0 GHz vertical polarization and the difference between the vertical and horizontal polarization brightness temperatures at 37.0 GHz. The criteria for rain over land are based on brightness temperatures from both the 37.0 and the 85.5 GHz channels. (See Figure III.9.) For each of the categories, seasons and locations, a separate D-matrix is available for retrieval purposes.

Table III.2 Climate types defined for the SSM/I

	DEGREES LATITUDE	SEASONS	BACKGROUNDS
TROPICAL	$0^{o} - 20^{o}$	WARM (JUN – NOV) COOL (DEC – MAY)	LAND, OCEAN
TRANSITION	$20^{o} - 25^{o}$	MULTISTEP AVERAGING BETWEEN TROPICAL AND MIDLAT	
MIDLAT	$25^{o} - 60^{o}$*	SPRING/FALL SUMMER (JUN – AUG) WINTER (NOV – FEB)	LAND, OCEAN
TRANSITION	SIMILAR TO PROCEDURE BETWEEN TROPICS AND MIDLAT		
ARCTIC	60^{o}* – 90^{o}	COOL (MAY – OCT) COLD (NOV – APR)	LAND, OCEAN (INCLUDING SEA ICE)

*EXCEPT FOR POSSIBLE SEA ICE AREAS, BOUNDARIES ARE DEFINED ACCORDING TO ICE DYNAMICS

Table III.3 Stations selected to represent the climate types

REGION	STATIONS	LAT	LONG	CLIMATE TYPE
Tropics-Land	Kwajalein	8°43'N	167°44'E	Warm/Moist
	Bogota, Columbia	4°42'N	74° 9'W	High Altitude
	Niamey, Niger	13°29'N	2°10'E	Warm/Dry
Tropics-Ocean	Kwajalein	8°43'N	167°44'E	Warm/Moist
Mid-Lat Land	Rapid City, S.D.	44°3'N	103° 4'W	Temp/Dry
	Victoria, TX	28°51'N	96°55'W	Warm/Moist
	Spokane, Wash.	47°37'N	117°31'W	Cool/Dry
Mid-Lat Oceans	OVSC-Ocean Sta.	52°45'N	35°30'W	Cool
	Kindley AFB, Bermuda	32°22'N	64°41'W	Warm
Arctic-Land	Fairbanks, Alaska	64°49'N	147°52'W	Cold/Dry
	Bethel, Alaska	60°47'N	161°48'W	Cold/Dry
Arctic-Ocean	OVSM-Ocean Sta.	66° 0'N	2° 0'E	Cold

References

1. Burke, H. K., and K. C. Jones, "Models of Environmental Parameters for the SSM/I Program," Environmental Research and Technology, Inc., February 1980.

2. Burke, H. K., A. J. Bussey, K. C. Jones, N. K. Tripps and J. Ho, "Inversion Algorithm for Environmental Parameter Extraction of the SSM/I Program," Environmental Research and Technology, Inc., February 1980.

3. "Proposal for Microwave Environmental Sensor System (SSM/I); Vol. I. Technical Proposal," Hughes Airicraft Companry, Hughes RFP No. F04701-78-R-0094, January 1979.

4. "Special Sensor Microwave/Imager (SSM/I) Critical Design Review; Vol. II. Ground Segment," Hughes Aircraft Company, HS 256-0006-0150, March 1980.

5. Lane, J. A. and J. A. Saxton, "Dielectric Dispersion in Pure Polar Liquids at Very High Radio Frequencies, III. The Effect of Electrolytes in Solution," Proc. Roy. Soc., London A, 214, pp. 531-545, 1952.

6. Chang, A. T. C. and T. Wilheit, "Remote Sensing of Atmospheric Water Vapor, Liquid Water, and Wind Speed at the Ocean Surface by Passive Microwave Techniques from the NIMBUS-5 Satellite," Radio Science, 1979, p. 793.

7. Cardone, V. J., "Specification of the Wind Field Distribution in the Marine Boundary Layer for Wave Forecasting," Report TR 69-1, Geophys. Sci. Lab., New York University, 1969.

8. Cox, C. and W. Munk, "Measurement of the Roughness of the Sea Surface from Photographs of the Sun's Glitter," J. Optical Society of America, Vol. 44, No. 11, 1954, p. 838.

9. Nordberg, W., et al., "Measurements of Microwave Emission from a Foam Covered Wind Driven Sea," J. Atmos. Sci., Vol. 28, p. 429, 1971.

10. Savage, Richard C., "The Transfer of Thermal Microwaves Through Hydrometeors," Ph.D. Thesis, University of Wisconson-Madison, 1976.

11. Laws, J. O., and D. A. Parson, "The Relation of Raindrop Size to Intensity", Trans. American Geophys. Union, Vol.24, p. 452, 1943.

12. Staelin, D. H., et al., "Remote Sensing of Atmospheric Water Vapor and Liquid Water with the NIMBUS-5 Microwave Spectrometer," J. Appl. Met., Vol. 15, pp. 1204-1214, 1976.

13. Stogryn, A., "The Brightness Temperature of a Vertically Structured Medium," Radio Science, Vol. 5, No. 12, pp 1397-1406, December 1970.

14. Choudhury, B. J., T. J. Schmugge, A. Cheng, and R. W. Newton, "Effect of Surface Roughness on the Microwave Emission From Soils," J. of Geophy. Res., Vol. 84, No. C9, September 1979, p. 5699.

15. Gloersen, P., et al., "Time-Dependence of Sea-Ice Concentration and Multiyear Ice Fraction in the Arctic Basin," Boundary-Layer Met., Vol. 13, 1978, p. 339.

16. Sze, N. D. "Variational Methods in Radiative Transfer Problems," J. Quant. Spectroe, Radiat. Transfer, Vol. 16, 1976, p. 763.

17. Burke, H.-H. K., and N. D. Sze, "A Comparison of Variational and Discrete Ordinate Methods for Solving Radiative Transfer Problems," J. Quant. Spectrosc. Radiat. Transfer, Vol. 17, 1977, p. 783.

18. Gaut, N. T. and E. C. Reifenstein III, "Interaction Model of Microwave Energy and Atmospheric Variables," Final Report, Environmental Research and Technology, Inc., Corcord, Massachusetts, 1971.

19. Van Vleck, J. H. and V. F. Weisskopf, "On the Shape of Collision-Broadened Lines", Rev. Mod. Phys., Vol. 17, 1945, p. 227.

20. Gaut, N. E., "Studies of Atmospheric Water Vapor by Means of Passive Microwave Techniques", Research Laboratory for Electronics, Tech. Report 467, Massachusetts Institute of Technology, 1968.

21. Rosenkranz, P. W., "Shape of the 5 mm Oxygen Band in the Atmosphere," IEEE Trans. Antenna and Propagation, Vol. AP-23, No. 4, 1975, p. 498.

Appendix A

NRL comments on the ERT SST
Study for the SSM/I
December 1981

Robert C. Lo and James P. Hollinger
Space Sensing Applications Branch
Naval Research Laboratory
Washington, D. C. 20375

NRL COMMENTS ON THE ERT SST STUDY FOR THE SSM/I

Robert C. Lo and James P. Hollinger
Space Sensing Applications Branch
Naval Research Laboratory
Washington, DC 20375

In anticipation of the presentation of the sea surface temperature (SST) studies by Environmental Research and Technology, Inc. (ERT), at El Segundo, CA on November 24, 1981 NRL requested and received copies of the report. In the few days available before the presentation NRL examined the report and conducted a number of comparison studies; particularly in the area of sensitivity of the SSM/I instrument to changes in the SST. Results analogous to Figures 2-1 to 2-6 of the ERT report (Ref. 1) are attached as Figures 1 to 6. These were simulated using an environmental model previously developed at NRL (Ref. 2). The set of figures were presented to ERT's Dr. K. Hardy and Commander F. Wooldridge of NSSA at the conference. Note that the rain cases shown in the ERT figures are not included in Figures 5 and 6 because the NRL model does not yet contain a rain algorithm. Comparing figures 1 through 6 with the corresponding figures in the ERT report, shows that the two sets are in general agreement. The only significant discrepancy between them are the curves representing 15 m sec^{-1} wind in Figures 3 and 4. Dr. K. Hardy of ERT, who made the presentations at the November 24th conference, stated that the ERT 15 m sec^{-1} curves are in error.

The D-matrix algorithm previously developed at NRL is distinctly different from that used by ERT. Trade off studies were done at NRL in 1978 during the definition study phase of the SSM/I (Ref. 3). Included in these studies is a sensitivity study of radiometric noise on SST estimations. The climatic data selected for this sensitivity study were mid-latitude summer (see Ref. 3). The study used 5 frequencies with 2 polarizations each (i.e. 14.5 H,V and 22.2 H in addition to the SSM/I frequencies). This early study indicates that in order to obtain a SST retrieval error of 1.6 K from climatic data with an a priori uncertainity of 3.8 K, as in the ERT report, no radiometer noise can be present. Assuming a realistic radiometric noise of about 0.8 K, as specified in the ERT report, the retrieval error would be approximately 3.2 K. Current but preliminary studies based on an updated D-matrix model for the SSM/I developed at NRL confirm this result. On this basis it appears that the 1.6 ΔK accurracy indicated in the ERT study might be too optimistic. NRL suggested at the meeting that ERT should perform a sensitivity study concerning the effects of radiometric noise.

The following are some other observations made while examining the ERT report.

1. The surface air temperature is used in place of SST for the climatic SST data set since the actual SST data were not available. This artificially introduces a greater variance in the SST. Since regression models tend to be more sensitive to variables with greater variance the accuracy obtained by the ERT model may be less if actual SST data were used.

2. The climatic data are taken from two stations chosen to represent warm mid-latitude and cool mid-latitude ocean conditions. From Figures 3-2 to 3-4 of the ERT report (Ref. 1), the data appear to represent a bi-model sample. This may be inadequate for the linear regression model which implies a normal distribution. The effect of the bi-model sample is usually an over-estimate of the a priori variance in the SST.

3. The ERT model uses half of the climatic data set to arrive at the D-matrix and the other half to verify the algorithm. It appears that a more independent set of climatic data should be employed. For example, those taken from a third station in the mid-latitude ocean.

4. The verification of the model through the climatology is of the nature of internal verification showing model self-consistency. External verification is also necessary to establish that the model is not only self-consistent but also relates to reality. An independent benchmark set of, say, mid-latitude ocean SST and the corresponding TB's at the SSM/I frequencies ought to be collected. These should be tested with the D-matrix produced from the ERT model. This benchmark set should include cases of warm and cool mid-latitude ocean. Since the ERT model produces D-matrixes for other climates benchmark data sets for all of these climates should be collected for tests. Only then can an understanding of the ERT model's real performance be achieved.

Among those in the audience when Dr. Hardy presented the SST algorithm and an algorithm for the retrieval of land surface temperature (LST) (Ref. 4) and who made significant remarks concerning the SST algorithm were Mr. F. Wentz of Wentz & Associates, Dr. E. Njoko of Jet Propulsion Laboratory and Mr. J. Cornelius of Fleet Numeric Oceanic Center. Dr. Robert C. Lo (Code 7911L) represented NRL at the meeting.

Dr. Hardy presented simulation results which indicate the sensitivity of 19.35 GHz TB to SST and wind speed. Changes in TB (ΔTB) corresponding to a change of 20 K in SST for three different wind speeds were presented. Similar simulations* of ΔTB for thin clouds, thick clouds and rain were also presented. The approach for the SST retrieval and the climatic data base employed, were then presented. The following is a list of some of the relevant comments made during the meeting.

1. ERT cloud and rain models assume single scattering. This assumption is not adequate for thick cloud and rain cases. Multiple scattering should be included in the considerations. (Njoko)

2. From the sensitivity studies, the relationship between SST and T_B at the SSM/I frequencies is apparently non-linear, while the ERT model implies linearity. The estimated 1.6 K accuracy appears to be too small under such a situation. (Wentz)

*For SST retrieval, rain cases were excluded using pre-determined criteria.

3. Analysis of data from SEASAT SMMR, which includes lower frequency channels approximately 3 times more sensitive to SST While several times less sensitive to the atmospheric effects than the SSM/I higher frequency channels, indicates an accuracy of 1.0 K for SST estimates given an instrumental RMS error of 0.2 K. Based on the SEASAT results, the fact that instrumental error for SSM/I was assumed to be about 1.0 K and assuming similiar algorithms, the retrieval accuracy should be about 4 K (Njoko, Wentz).

4. The SST used in the ERT algorithm was in fact air temperature at the surface rather than the skin temperature of the sea surface since the SST was not available. This results in a much larger variance of SST than what would actually be expected from the two stations if the SST had been measured directly. Questions were raised as to whether the artifically large variance led to a good result. (Wentz) Some discussion was also made concerning implied surface stability from decoupling SST from air temperature. (Wentz, Njoko) No definite conclusions were reached concerning these points, due to the lack of data and comparison studies. Another question was raised about using surface air temperature, for it is usually closely related to water vapor burden in the lower troposphere. (Cornelius) However, the ΔSST (actually radiosonde measurements of surface air temperature minus predicted SST) was plotted against the integrated water vapor, which is another parameter estimated by the D-matrix algorithm. No clear correlation is indicated in the plot. This appears to indicate that even using the air temperature, the algorithm is relatively independent of water vapor. By the same means, estimated SST appears to be independent of wind speed and integrated cloud water.

Additional Comments are:

5. That a sensitivity study as to model certainty should be performed. The result from the model is highly dependent on the input climatology. It is important to understand how reliable the model parameter estimates are when certain error exist in the climatology. (Njoko)

6. A sensitivity study of the model to instrumental noise should be done. (Lo)

7. Climatology data should be collected from more stations to constitute a more representative data base for the mid-latitude ocean. (Wentz)

It is observed that besides NRL, none of the critics in the audience has done an in depth comparison of the ERT model with their own. The evaluation and comments, valuable as they were, were more qualitative than quantitative.

In summary it appears that in its present state the ERT model has the following shortcomings.

1. Using air temperature rather than the SST for retrieval and evaluation.

2. Not enough sensitivity studies done concerning the model uncertainty, therefore, not enough understanding as to how well the model could perform.

3. Not adequate cloud model for thick clouds and rain cases.

4. Not enough understanding as to the effect of the linear assumption to the basically non-linear problem.

5. Not enough data for climatology.

6. Not adequately verified with independently collected data.

A possible explanation for the discrepancy in the sensitivity of the ERT and the NRL models to radiometer noise is in the way the noise was introduced into each model. Further comparison of this aspect is needed.

NRL strongly recommends that the SST retrieval algorithm be incorporated in the SSM/I retrieval since it is of relatively very low cost and will be the only SST test bed in the known future. NRL concurs with other critics that the environmental models are not yet fully understood, that the techniques for retrieval need further development and refinements and that the climatological data base needs to be increased. It is for these very reasons that the SST algorithm should be included in order that experience and data can be gained to improve our knowledge in these very areas. Only in this way can the NAVY develop the capability for accurate spaceborne sensing of SST as required. The algorithm is constructed in such a way that improvements can be incorporated and tested fairly easily in the operational system. NRL also recommends that sets of benchmark TB observations with corresponding atmospheric and surface truth data at the SSM/I frequencies be collected which include all climate conditions considered by the ERT model. The algorithm should be tested against this data set. Finally, NRL recommends that model validity be tested as well as sensitivity tests be done for radiometric noise effects on SST retrieval errors.

List of Figures

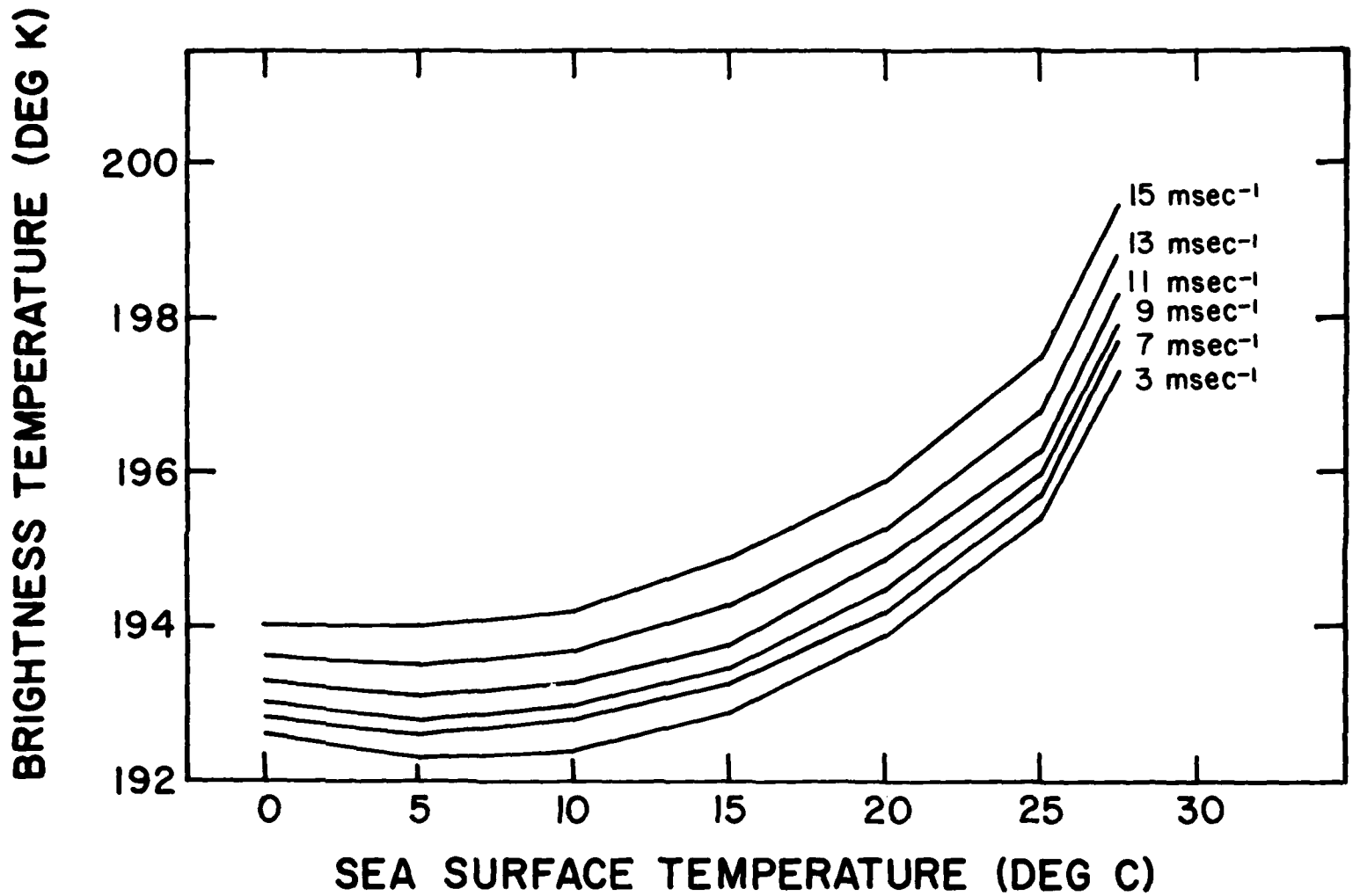

Figure 1 The variation of the 19.35 GHz vertical brightness temperature with sea surface temperature for several wind speeds.

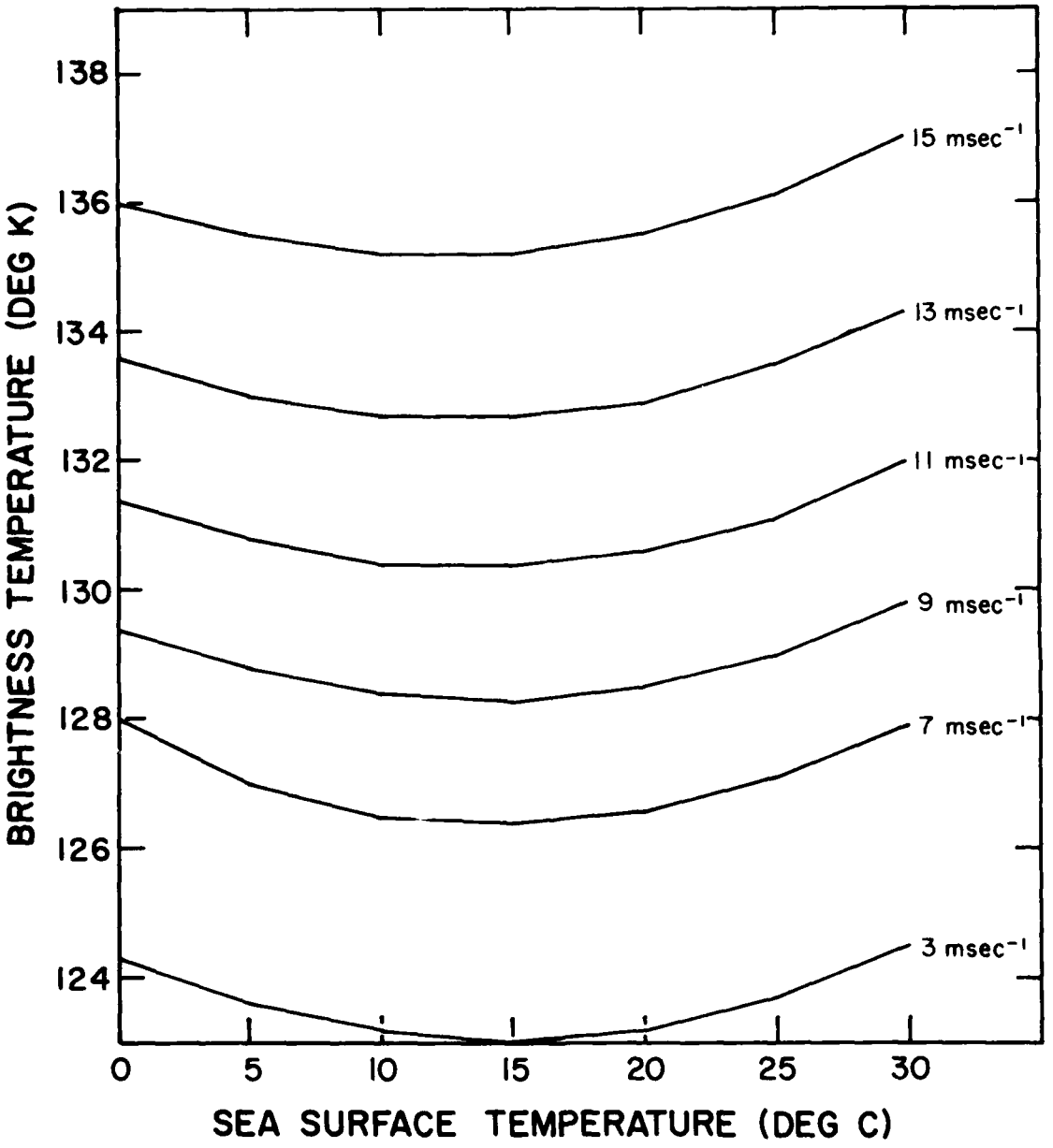

Figure 2 The variation of the 19.35 GHz horizontal brightness temperature with sea surface temperature for several wind speeds.

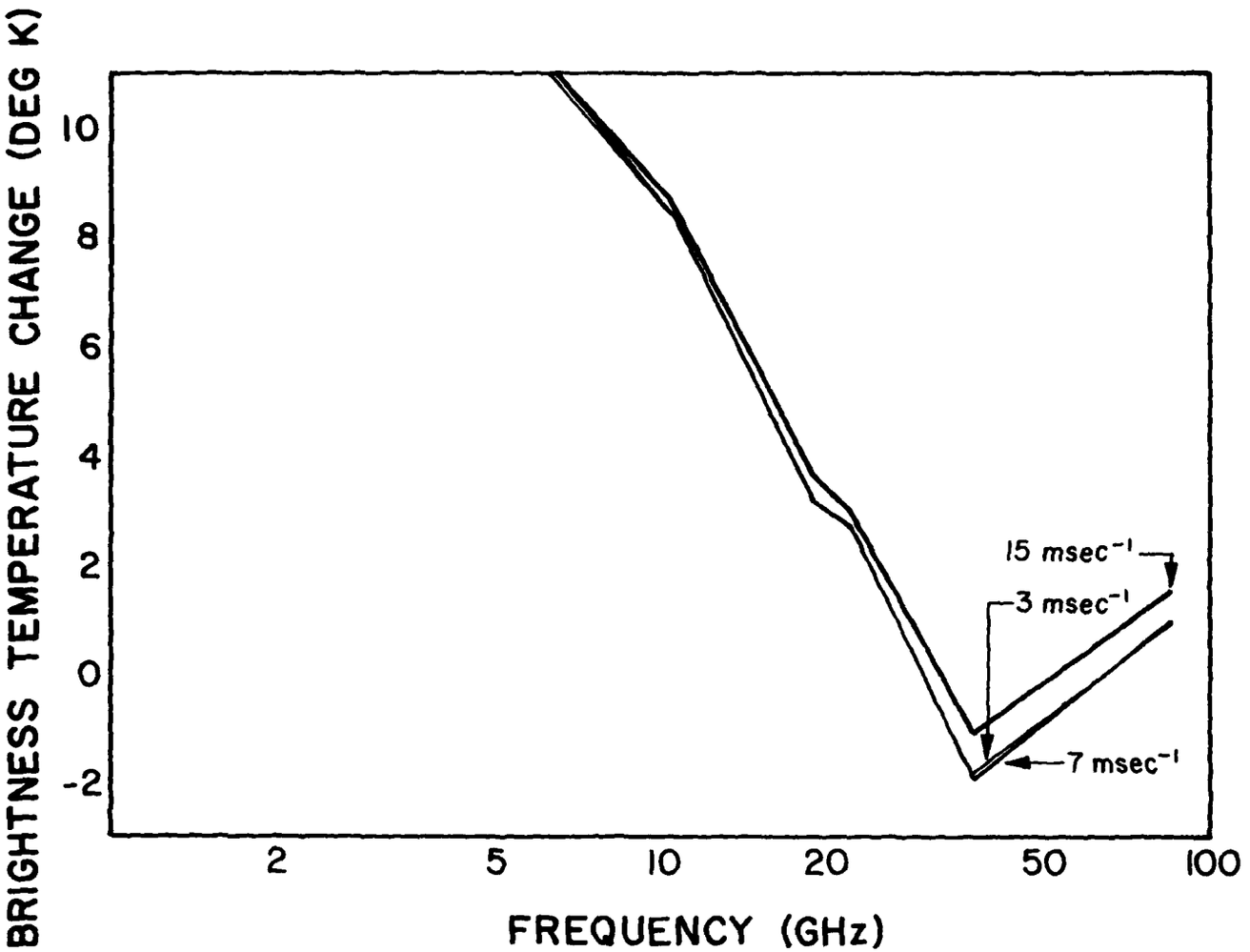

Figure 3 Change in the vertical brightness temperature for a change in sea surface temperature from 5 to 25C for three different wind speeds.

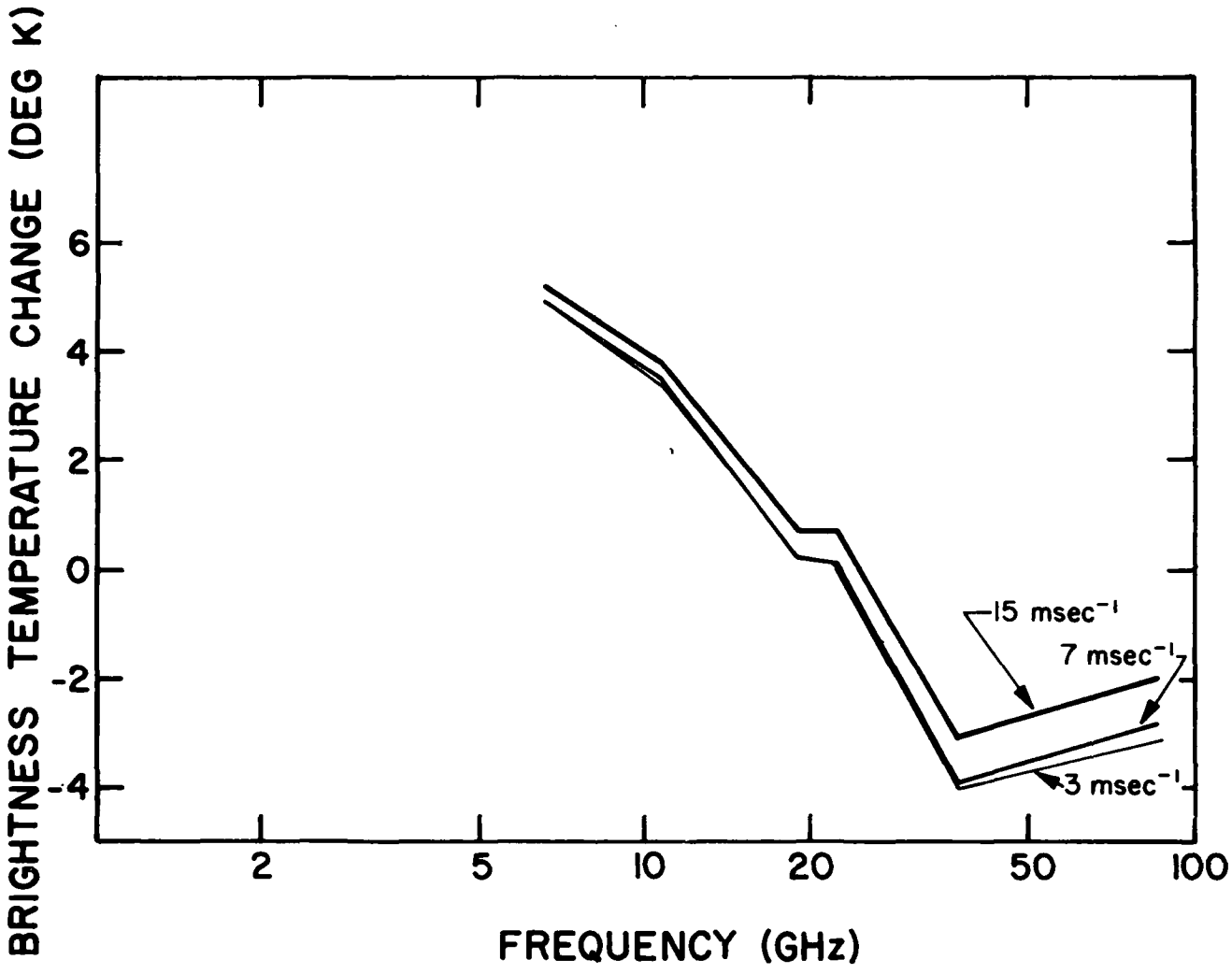

Figure 4 Change in the horizontal brightness temperature for a change in sea surface temperature from 5 to 25C for three different wind speeds.

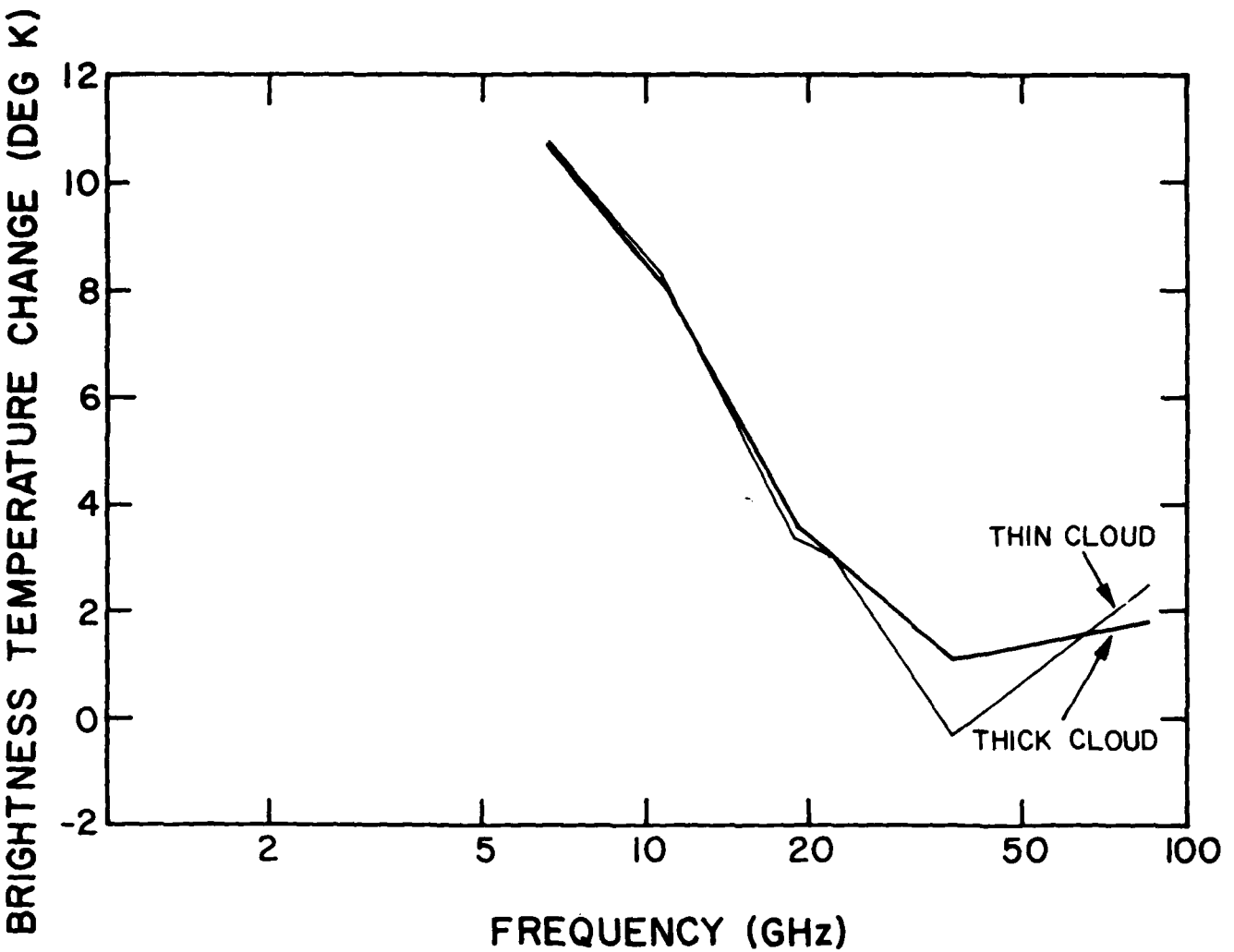

Figure 5 Change in the vertical brightness temperature for a change in sea surface temperature from 5 to 25C for two different and atmospheric conditions.

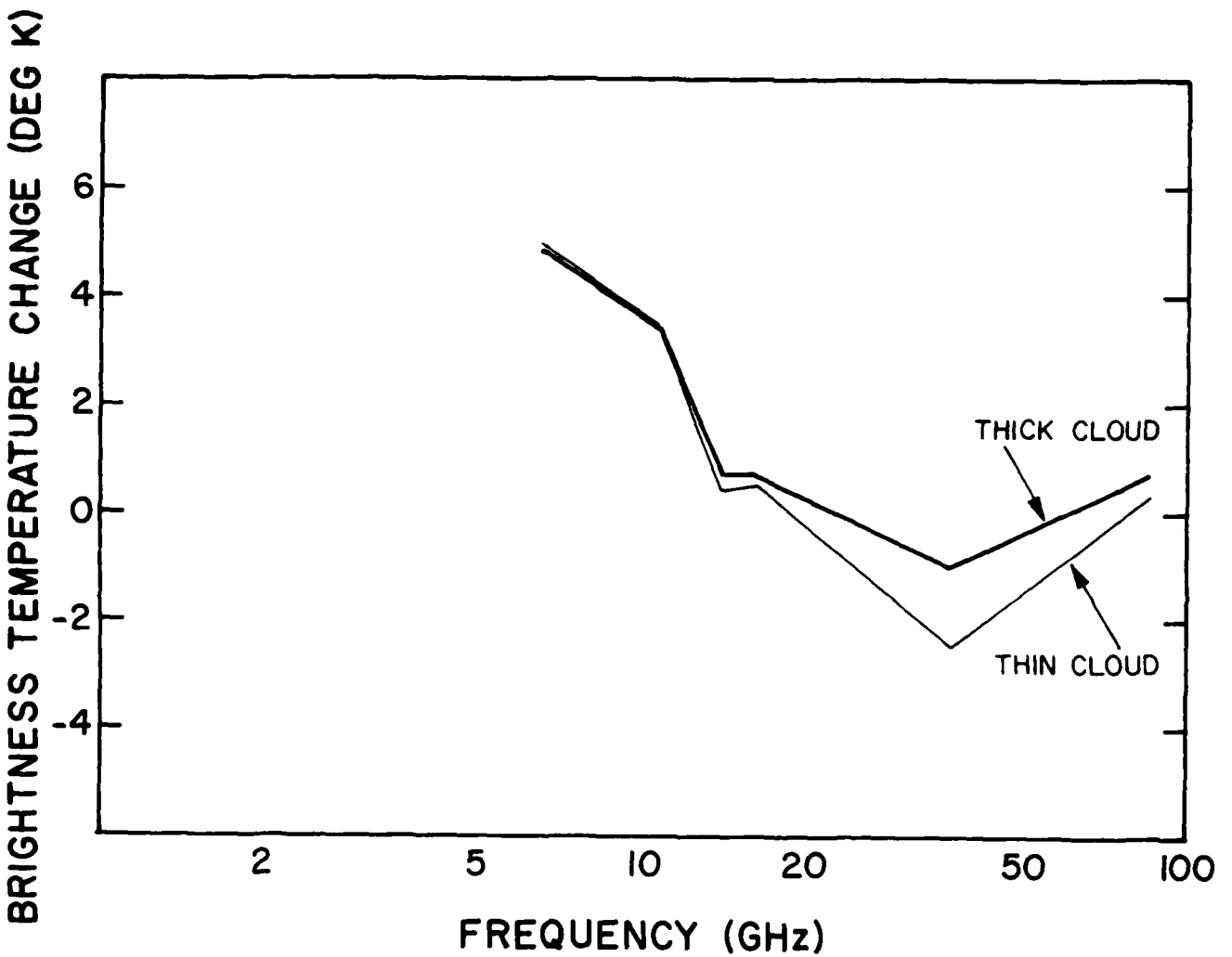

Figure 6 Change in horizontal brightness for a change in sea surface temperature from 5 to 25C for two different atmospheric conditions.

References

1. Hardy, K. R., et al. " A Study of Sea Surface Temperature Estimates Using the SSM/I", ERT Document No. P-B088-F, October 29, 1981.

2. Wisler, M. M., and J. P. Hollinger. "Estimation of Marine Environmental Parameters Using Microwave Radiometric Remote Sensing Systems", NRL Memorandum Report 3661, November 1977.

3. Hollinger, J. P., et al. "Joint Services 5D-2 Microwave Scanner Definition Study", NRL Memorandum Report 3807, August 1978.

4. Hardy, K. R., et. al. "A Study of Land Surface Temperature Estimates Using the SSM/I", ERT Document No. P-B144-F, November 16, 1981.

Appendix B

Selection of Optimal Combination of Frequencies for the Special Sensor Microwave Imager (SSM/I) Environmental Retrievals

April 1982

Robert C. Lo and James P. Hollinger
Space Sensing Applications Branch
Naval Research Laboratory
Washington, D. C. 20375

SELECTION OF OPTIMAL COMBINATIONS OF FREQUENCIES FOR THE SPECIAL SENSOR MICROWAVE IMAGER (SSM/I) ENVIRONMENTAL RETRIEVALS

Robert C. Lo and James P. Hollinger
Space Sensing Applications Branch
Aerospace Systems Division
Naval Research Laboratory
Washington, DC 20375

I. Introduction

The SSM/I brightness temperature observations are related to the environmental parameters as independent variables through the so-called 'D' matrices of regression coefficients. Some of the most important parameters for ocean retrievals are wind speed, sea surface temperature, columnar density of water vapor, and liquid water contained in clouds. The best estimation of each parameter is expected when all seven SSM/I channels are used. However, limitations of the computing facility dedicated for the SSM/I project, dictated the use of at most four channels for each environmental parameter (6).

The purpose of this study is to evaluate the retrieval performance of all four-channel subsets from the seven SSM/I channels, and to determine the optimum subset for each environmental parameter. The performance of a certain frequency combination depends on the instrumental noise (1), (2), the geophysical model and the climate statistics utilized for the derivation of the 'D' matrices. A model originally designed by Wisler and Hollinger (1) is used for this study. The climate statistics were compiled by Wentz for the SSM/I definition study (3). They include all four seasons for three locations representing high, middle, and low latitudes. Instrumental noise is simulated. The environmental parameters examined in this study are the sea surface temperature, wind speed and the columnar densities of cloud liquid water and water vapor.

II. Approach

All four-channel subsets are evaluated for the sake of completeness. The total number of possible combinations is ${}_7C_4 = 7!/(4!3!) = 35$ and the channels included in each of the combinations are listed in Table 1. The criteria chosen for the evaluations are the residual RMS errors of the parameter for a certain frequency combination, and a quantity called the confidence factor which is defined as:

$$CF = 1 - \sqrt{(\sigma 2 - \sigma_r^2)/\sigma^2} \qquad \text{(II.1)}$$

Table 1

Listing of Frequency Combinations

Combination No.	Channels			
1	19.3 H	19.3 V	22.2 V	37.0 H
2	19.3 H	19.3 V	22.2 V	37.0 V
3	19.3 H	19.3 V	22.2 V	85.5 H
4	19.3 H	19.3 V	22.2 V	85.5 V
5	19.3 H	19.3 V	37.0 H	37.0 V
6	19.3 H	19.3 V	37.0 H	85.5 H
7	19.3 H	19.3 V	37.0 H	85.5 V
8	19.3 H	19.3 V	37.0 V	85.5 H
9	19.3 H	19.3 V	37.0 V	85.5 V
10	19.3 H	19.3 V	85.5 H	85.5 V
11	19.3 H	22.2 V	37.0 H	37.0 V
12	19.3 H	22.2 V	37.0 H	85.5 H
13	19.3 H	22.2 V	37.0 H	85.5 V
14	19.3 H	22.2 V	37.0 V	85.5 H
15	19.3 H	22.2 V	37.0 V	85.5 V
16	19.3 H	22.2 V	85.5 H	85.5 V
17	19.3 H	37.0 H	37.0 V	85.5 H
18	19.3 H	37.0 H	37.0 V	85.5 V
19	19.3 H	37.0 H	85.5 H	85.5 V
20	19.3 H	37.0 V	85.5 H	85.5 V
21	19.0 V	22.2 V	37.0 H	37.0 V
22	19.0 V	22.2 V	37.0 H	85.5 H
23	19.0 V	22.2 V	37.0 H	85.5 V
24	19.0 V	22.2 V	37.0 V	85.5 H
25	19.0 V	22.2 V	37.0 V	85.5 V
26	19.0 V	22.2 V	85.5 H	85.5 V
27	19.0 V	37.0 H	37.0 V	85.5 H
28	19.0 V	37.0 H	37.0 V	85.5 V
29	19.0 V	37.0 H	85.5 H	85.5 V
30	19.0 V	37.0 V	85.5 H	85.5 V
31	22.2 V	37.0 H	37.0 V	85.5 H
32	22.2 V	37.0 H	37.0 V	85.5 V
33	22.2 V	37.0 H	85.5 H	85.5 V
34	22.2 V	37.0 V	85.5 H	85.5 V
35	37.0 H	37.0 V	85.5 H	85.5 V

The seven SSM/I channels are 19.0 H, 19.0 V, 22.2 V, 37.0 H, 37.0 V, 85.5 H and 85.5 V.

Where σ^2 is the natural variance of a parameter given as a climate statistic, σ_r^2 is the variance predicted by the retrieval model and is part of the model output and $\sqrt{\sigma^2 - \sigma_r^2}$ is the residual RMS error. The confidence factor is then a measure of the fraction of the error explained by the retrieval model. If it is unity, the estimation is perfect, and if it is zero, the scheme is completely unable to retrieve the environmental parameters.

The RMS error and the confidence factor for each of the 35 frequency combinations are examined with respect to different climate conditions assuming the same instrumental noise. They are then examined with respect to changes in the instrumental noise for a given climate. The noise for the 85.5 GHz channels is assumed to be one-half those of the other channels since its linear resolution is one-half of the other frequencies. It is assumed that four samples will be averaged together for use with a single sample of each of the other channels. The two frequency combinations which exhibit the best overall performance are then recommended for each parameter.

II.A. Sea Surface Temperature

The residual RMS and confidence factors for Azores Summer with instrumental noise of 0.5 K are listed in Table 2. The RMS error is also plotted in Figure 1. Based on the RMS error and confidence factor values, the best frequency combination is determined to be number 26 which is composed of the 19 V, 22 V, 85 H and 85 V channels. Numbers 30 and 10 which, substitute the 37 V and 19 H, respectively, for the 22 V channel, are the next best choices. The same examination is performed for all 11 remaining climates. The climate statistics used for the development of the SSM/I algorithm by the Environmental Research and Technology, Inc. (ERT) (4) are included as an additional climatology. The natural variance of sea surface temperature introduced by use of the ERT climatology is much greater than for any of the Wentz climates. The ERT climatology implies that the sea surface temperature is equal to the measured air temperature. This is an inappropriate assumption but it does afford an evaluation of the performance of the retrieval scheme under large variance conditions. The best three frequency combinations for each of the cases are shown in Table 3 together with the associated RMS error and confidence factor values. The retrievals for Azores Summer climatology are also shown in Table 3 with simulated instrumental noise of 0.1 and 1.0 K. In general, a larger natural variance leads to a better estimation in the sense that the confidence factor tends to be greater. Retrievals are also sensitive to the instrumental noise. For example, it is greatly improved as the instrumental noise decreases from 0.5 to 0.1 K.

Even a cursory examination of Table 3 will reveal the fact that none of the frequency combinations is best for every climate condition. In order to choose a combination which has the best over-all performance, the confidence factor and the RMS error, averaged over all the climate conditions, are used as the criteria of selection. The best frequency combination selected for

Table 2

RMS and CF of SST for Climate 7 and IN of 0.5

Combination No.	Residual RMS	CF
1	0.7377	0.0313
2	0.7394	0.0290
3	0.7385	0.0302
4	0.7455	0.0210
5	0.7469	0.0191
6	0.7474	0.0186
7	0.7322	0.0385
8	0.7470	0.0190
9	0.7299	0.0415
10	0.7125	0.0644
11	0.7586	0.0038
12	0.7583	0.0042
13	0.7309	0.0401
14	0.7598	0.0022
15	0.7449	0.0218
16	0.7219	0.0520
17	0.7580	0.0045
18	0.7277	0.0444
19	0.7195	0.0551
20	0.7227	0.0510
21	0.7377	0.0313
22	0.7377	0.0313
23	0.7276	0.0445
24	0.7406	0.0275
25	0.7319	0.0389
26	0.7073	0.0712
27	0.7528	0.0114
28	0.7221	0.0518
29	0.7126	0.0642
30	0.7102	0.0673
31	0.7584	0.0041
32	0.7367	0.0325
33	0.7261	0.0465
34	0.7258	0.0469
35	0.7434	0.0238

Natural standard deviation = 0.7615
Residual RMS for all 7 channels = 0.7029

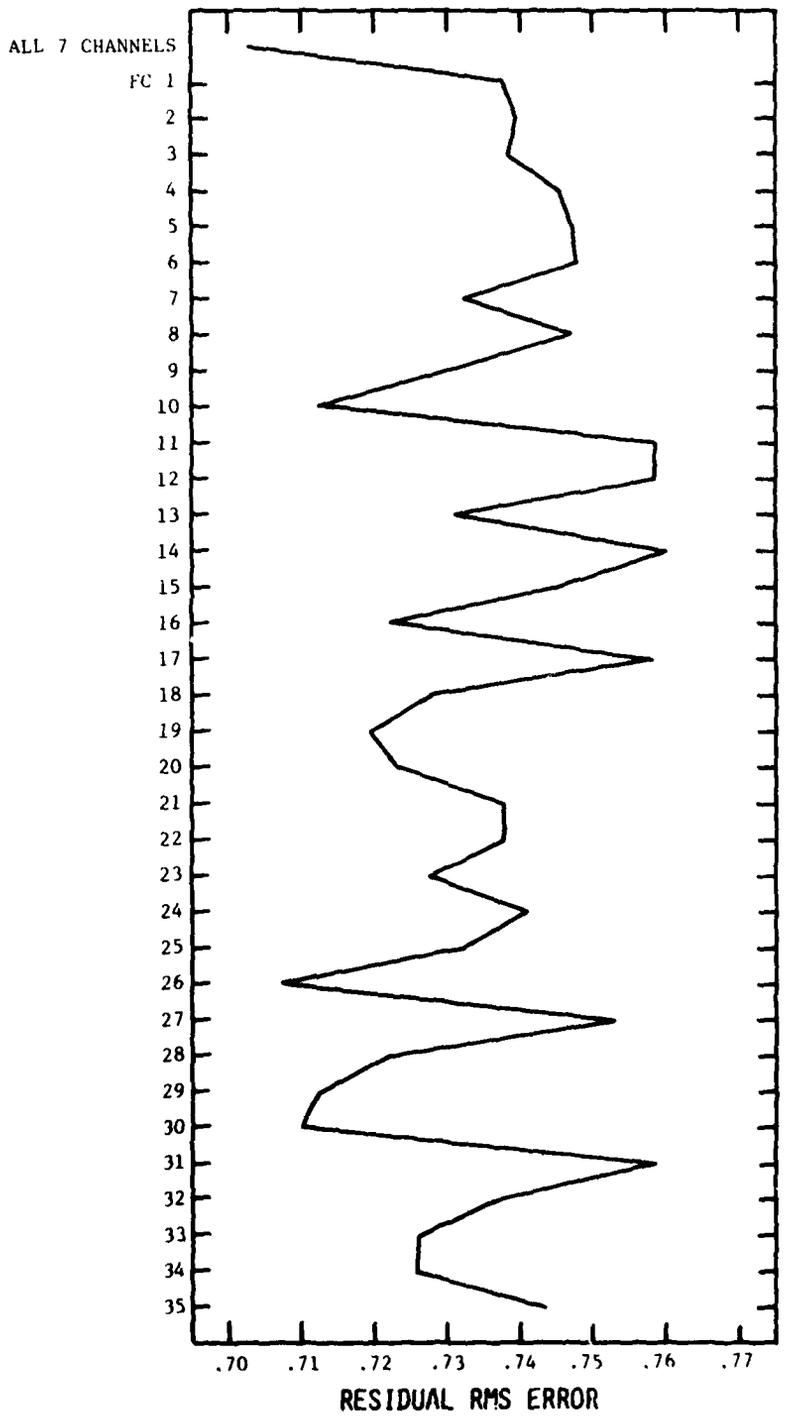

Figure 1 Residual RMS Error of SST for Azores, Summer

Table 3

Frequency Combination Selection Study for SST (C)

Instrumental Noise = .5 (19.35, 22.235, 37 GHz) and .25 (85.5 GHz)

	Original		First Choice			Second Choice			Third Choice	
	RMS (C)	FC	RMS (C)	CF	FC	RMS (C)	CF	FC	RMS (C)	CF
Jan Mayen										
Winter	.2030	18	.2011	.0092	13	.2012	.0089	32	.2015	.0073
Spring	.7783	20	.6989	.1021	16	.7052	.0939	10	.7062	.0926
Summer	.5953	18	.5592	.0606	32	.5660	.0492	34	.5663	.0487
Autumn	1.2670	33	1.0742	.1522	13	1.0925	.1377	23	1.0946	.1361
Azores										
Winter	.3403	18	.3359	.0130	30	.3360	.0126	13,19	.3363	.0116
Spring	1.4930	30	1.2096	.1898	26	1.2243	.1800	10	1.2319	.1749
Summer	.7615	26	.7073	.0712	30	.7102	.0673	10	.7125	.0644
Autumn	1.3850	30	1.1466	.1721	28	1.1519	.1683	18	1.1553	.1659
Truk										
Winter	.2127	29	.2112	.0073	7,23,28	.2112	.0072	10	.2114	.0060
Spring	.2628	28	.2598	.0115	23	.2598	.0114	29	.2598	.0113
Summer	.0822	7	.0821	.0012	28	.0821	.0010	9,13,22,29	.0822	.0008
Autumn	.2576	7	.2547	.0112	28	.2548	.0108	29	.2548	.0107
ERT SST	3.800	18	1.9719	.4811	10	1.9904	.4762	19	1.9919	.4758
Azores Summer										
IN = 0.1	.7615	20	.3978	.4775	16	.3992	.4758	29	.4032	.4705
IN = 1.0	.7615	29	.7431	.0241	26	.7441	.0228	10	.7442	.0227

sea surface temperature is number 10. The first runner-up is number 29. The RMS error and confidence factor of all the climate conditions for these two combinations are listed in Table 4. From the RMS values, it appears that the estimation of sea surface temperature is reasonable. They are all under 1.5 C except for the ERT case when the estimated RMS error is around 2.0 C. But the confidence factors are often less than 0.1, indicating that the SSM/I is not well suited for the estimation of sea surface temperature. The reasonable residual RMS error values are due to the fact that the natural variance for each of the climate conditions is small and is within the SSM/I specification value. The relatively higher confidence factors values for the ERT case are due to the assumption of an unrealistically large initial RMS errors. The confidence factors are also relatively high for the case when instrumental noise is equal to 0.1 K. But the actual noise of the SSM/I is much closer to 0.5 than 0.1 K.

Note that both the 85.5 GHz polarizations are included in combination number 10 as well as number 29. This may partly be due to the smaller instrumental noise attributed to these channels. The selections made here are appropriate only for the case when 85.5 GHz data are averaged to match resolution with the other channels before retrieval.

II.B. Wind Speed

In the same fashion as for sea surface temperature, the best three frequency combinations for all the climate and noise conditions are listed in Table 5 for wind speed retrieval. Again, no single combination is best for all cases. Based on the mean RMS error and confidence factor values, the best over-all combination selected is number 2 (19 H, 19 V, 22 V, 37 V) with number 11, where 37 H is substituted for 19 V, as the second best. The RMS errors and confidence factors for all the conditions associated with these two combinations are listed in Table 6. The greatest RMS error found among all cases is less than 1.5 m/sec, which is quite acceptable. And the confidence factors of about 0.6 indicate that the retrieval of wind speed is much more reliable than that of sea surface temperature.

II.C. Columnar Density of Water Vapor and Liquid Water

The best two frequency combinations for water vapor and liquid water densities are selected in a fashion similar to the other parameters. Tables 7 and 8 contain the results for water vapor density. Tables 9 and 10 contain the results for cloud liquid water. As can be seen, the retrieval model is extremely sensitive to these two parameters. Especially in the case of liquid water, every combination appears to yield good retrieval results. The best combinations for water vapor are number 1 (19 H, 19 V, 22 V, 37 H) and 13 where 85 V is substituted for the 19 V channel. The worst residual RMS error found in the results of these two combinations is around 0.1 gm/cm^2 which is much better than the SSM/I specification. The overall best combinations for liquid water are numbers 3 (19 H, 19 V, 22 V, 85 H) and 14 where 37 V is substituted for 19 V. The largest residual RMS error found for these two combinations is 0.004 gm/cm^2; again much better than the SSM/I specification. The confidence factors are greater than 0.9 for both these environmental parameters indicating that they may be very reliably and accurately determined by the SSM/I.

Table 4

The Best Two Frequency Combinations for SST(C)

Instrumental Noise = .5 (19.35, 22.235, 37 GHz) and .25 (85.5 GHz)

	FC 10		FC 29	
	RMS(C)	CF	RMS(C)	CF
Jan Mayen				
Winter	.2017	.0065	.2021	.0045
Spring	.7062	.0926	.7478	.0392
Summer	.5720	.0392	.5811	.0239
Autumn	1.1674	.0786	1.1200	.0880
Azores				
Winter	.3365	.0113	.3370	.0097
Spring	1.2319	.1749	1.2378	.1709
Summer	.7125	.0644	.7126	.0642
Autumn	1.1722	.1537	1.1776	.1498
Truk				
Winter	.2114	.0060	.2112	.0073
Spring	.2611	.0063	.2598	.0113
Summer	.0822	.0005	.0822	.0008
Autumn	.2555	.0083	.2548	.0107
ERT	1.9904	.4762	2.0711	.4550
Azores Summer				
IN = 0.1	.4141	.4562	.4032	.4775
IN = 1.0	.7442	.0227	.7431	.0241
Average	.6706	.1064	.6756	.1020

Table 5

Frequency Combination Selection Study for WS (m/sec)

Instrumental Noise = .5 (19.35, 22.235, 37 GHz) and .25 (85.5 GHz)

	Original RMS (m/sec)	FC	First Choice RMS (m/sec)	CF	FC	Second Choice RMS (m/sec)	CF	FC	Third Choice RMS (m/sec)	CF
Jan Mayen										
Winter	4.0772	14	.9930	.7565	2	.9948	.7560	15	.9989	.7550
Spring	4.5889	12	.8530	.8141	13	.8999	.8039	15	.9005	.8038
Summer	3.0800	12	.8448	.7257	15	.8694	.7177	2	.8764	.7155
Autumn	3.4692	2	1.0336	.7021	11	1.0624	.6938	14	1.0790	.6890
Azores										
Winter	3.4100	12	.8174	.7603	15	.8553	.7492	2	.8564	.7489
Spring	2.1632	12	.7985	.6309	11	.8545	.6050	2	.8664	.5995
Summer	2.1030	12	.8061	.6167	11	.8740	.5844	13	.8741	.5843
Autumn	3.0559	2	.9387	.6928	11	.9406	.6922	14	.9471	.6901
Truk										
Winter	1.7369	11	.9417	.4578	2	.9457	.4555	3	.9832	.4339
Spring	2.4051	2	1.1848	.5074	11	1.2084	.4976	15	1.2510	.4798
Summer	4.3408	2	1.3666	.6852	5	1.4086	.6755	15	1.4465	.6668
Autumn	2.1802	11	1.1066	.4924	2	1.1128	.4896	5	1.1605	.4677
ERT SST	5.6	11	.9124	.8371	15	.9173	.8362	2	.9259	.8347
Azores Summer										
IN = 0.1	2.1030	12	.2225	.8942	16	.2267	.8922	15	.2278	.8917
IN = 1.0	2.1030	12	1.3311	.3670	13	1.3846	.3416	11	1.4098	.3296

Table 6

The Best Two Frequency Combinations for WS (m/sec)

Instrumental noise = .5 (19.35, 22.235, 37 GHz) and .25 (85.5 GHz)

	FC 2		FC 11	
	RMS (m/sec)	CF	RMS (m/sec)	CF
Jan Mayen				
Winter	.9948	.7560	1.0307	.7472
Spring	.9326	.7968	.9502	.7929
Summer	.8764	.7155	.8996	.7079
Autumn	1.0336	.7021	1.0624	.6938
Azores				
Winter	.8564	.7489	.8689	.7452
Spring	.8664	.5995	.8545	.6050
Summer	.8915	.5761	.8740	.5844
Autumn	.9387	.6928	.9406	.6922
Truk				
Winter	.9427	.4555	.9417	.4578
Spring	1.1848	.5074	1.2084	.4976
Summer	1.3666	.6852	1.4164	.6737
Autumn	1.1128	.4896	1.1066	.4924
ERT SST	.9259	.8347	.9124	.8371
Azores Summer				
IN = 0.1	.2288	.8912	.2329	.8892
IN = 1.0	1.4243	.3227	1.4098	.3296
Average	.9720	.6516	.9806	.6498

Table 7

Frequency Combination Selection Study for VAP (gm/cm^2)

Instrumental Noise = .5 (19.35, 22.235, 37 GHz) and .25 (85.5 GHz)

	Original RMS (gm/sec^2)	FC	First Choice RMS (gm/cm^2)	CF	FC	Second Choice RMS (gm/cm^2)	CF	FC	Third Choice RMS (gm/cm^2)	FC
Jan Mayen										
Winter	.2859	12	.0491	.8283	13	.0492	.8278	1	.0494	.8272
Spring	.3935	1	.0430	.8908	13	.0435	.8896	12	.0436	.8893
Summer	.5441	1	.0424	.9221	12,13	.0428	.9213	3	.0429	.9212
Autumn	.3253	12	.0524	.8390	13	.0535	.8355	11	.0539	.8343
Azores										
Winter	.4332	1	.0425	.9019	3	.0437	.8992	12,13	.0437	.8991
Spring	.5523	13	.0491	.9111	23,26	.0494	.9106	4,25	.0497	.9101
Summer	.5283	1	.0519	.9017	13	.0527	.9002	3	.0528	.9001
Autumn	.5393	26	.0523	.9031	13	.0527	.9022	23	.0535	.9009
Truk										
Winter	.9616	1	.0633	.9342	3	.0644	.9331	26	.0653	.9321
Spring	.9032	26	.0787	.9129	1	.0834	.9077	3	.0839	.9071
Summer	.5065	26	.0844	.8334	22	.0949	.8126	24	.0951	.8123
Autumn	.7200	26	.0760	.8944	3	.0764	.8938	1	.0765	.8937
ERT SST	.5283	32	.0650	.8770	15	.0650	.8769	16	.0669	.8733
Azores Summer										
IN = 0.1	.5283	33	.0145	.9726	23	.0146	.9723	16	.0148	.9719
IN = 1.0	.5283	3	.0925	.8249	13	.0961	.8181	12	.0964	.8175

Table 8

The Best Two Frequency Combinations For VAP (gm/cm^2)

Instrumental Noise = .5 (19.35, 22.235, 37 GHz) and 25 (85.5 GHz)

	FC 1		FC 13	
	RMS (gm/cm^2)	CF	RMS (gm/cm^2)	CF
Jan Mayen				
Winter	.0494	.8272	.0492	.8278
Spring	.0430	.8908	.0435	.8896
Summer	.0424	.9221	.0428	.9213
Autumn	.0544	.8329	.0535	.8355
Azores				
Winter	.0425	.9019	.0437	.8991
Spring	.0519	.9061	.0491	.9111
Summer	.0519	.9017	.0527	.9002
Autumn	.0569	.8945	.0527	.9022
Truk				
Winter	.0633	.9342	.0684	.8903
Spring	.0834	.9077	.0897	.8913
Summer	.0956	.8112	.1085	.7857
Autumn	.0765	.8937	.0849	.8821
ERT SST	.0869	.8354	.0697	.8681
Azores Summer				
IN = 0.1	.0177	.9664	.0159	.9699
IN = 1.0	.0940	.8221	.0961	.8181
Average	.0607	.8832	.0613	.8794

Table 9

Frequency Combination Selection Study for LIQ (gm/cm^2)

Instrumental Noise = .5 (19.35, 22.235, 37 GHz) and .25 (85.5 GHz)

	Original RMS (gm/cm^2)	FC	First Choice RMS (gm/cm^2)	CF	FC	Second Choice RMS (gm/cm^2)	CF	FC	Third Choice RMS (gm/cm^2)	CF
Jan Mayen										
Winter	.0568	3	.0005	.9905	5	.0008	.9862	7,35	.0009	.9847
Spring	.0336	14	.0005	.9846	7	.0006	.9821	3	.0007	.9801
Summer	.0521	5	.0004	.9926	3	.0006	.9882	33	.0007	.9864
Autumn	.0735	5	.0008	.9887	6	.0011	.9844	18	.0013	.9826
Azores										
Winter	.0337	19	.0006	.9823	14	.0008	.9774	3	.0008	.9771
Spring	.0250	12	.0006	.9759	3	.0007	.9738	16	.0007	.9731
Summer	.0265	16	.0006	.9756	12	.0007	.9748	14	.0007	.9744
Autumn	.0409	12	.0006	.9850	20	.0008	.9807	14,16	.0009	.9771
Truk										
Winter	.0487	33	.0012	.9758	20	.0013	.9725	34	.0013	.9723
Spring	.0832	5	.0010	.9875	11	.0014	.9827	30	.0016	.9804
Summer	.0766	11	.0005	.9931	5	.0016	.9795	20	.0019	.9749
Autumn	.0372	17	.0013	.9642	20	.0014	.9629	8,14,18	.0014	.9617
ERT SST	.0265	16	.0007	.9729	3	.0007	.9720	14	.0008	.9699
Azores Summer										
IN = 0.1	.0265	23	.0003	.9901	3	.0004	.9857	22	.0004	.9855
IN = 1.0	.0265	16	.0012	.9538	14	.0013	.9499	12	.0014	.9488

Table 10

The Best Two Frequency Combinations for LIQ (gm/cm^2)

Instrumental Noise = .5 (19.35, 22.235, 37 GHz) and .25 (85.5 GHz)

	FC 3		FC 14	
	RMS (gm/cm^2)	CF	RMS (gm/cm^2)	CF
Jan Mayen				
Winter	.0005	.9905	.0015	.9737
Spring	.0007	.9801	.0005	.9846
Summer	.0006	.9882	.0017	.9675
Autumn	.0027	.9638	.0040	.9688
Azores				
Winter	.0008	.9771	.0008	.9774
Spring	.0007	.9738	.0007	.9717
Summer	.0007	.9732	.0007	.9744
Autumn	.0010	.9757	.0009	.9807
Truk				
Winter	.0015	.9689	.0014	.9709
Spring	.0028	.9662	.0020	.9757
Summer	.0033	.9569	.0023	.9705
Autumn	.0017	.9531	.0014	.9617
ERT SST	.0007	.9720	.0008	.9699
Azores Summer				
IN = 0.1	.0004	.9857	.0007	.9721
IN = 1.0	.0014	.9481	.0013	.9499
Average	.0013	.9715	.0013	.9710

III. Conclusions and Discussions

In this study, a number of simulations were performed for the purpose of selecting four channel subsets from the seven SSM/I channels for the retrieval of sea surface temperature, wind speed, columnar water vapor density and columnar cloud liquid water density The geophysical model and climate statistics needed for the simulation were developed and assembled at NRL. The approach of applying the so-called 'D' matrix coefficients to satellite observed brightness temperatures for environmental parameter retrievals is similar to that used to develop the algorithm for the SSM/I by Hughes/ERT. The four channel subset recommended for the retrieval of each parameter is listed in Table 11.

The expected RMS estimation error for each of the parameters is within the specifications for the SSM/I project, indicating that the use of four channel subsets for retrieval purposes is reasonable.

The small estimation error does not imply accuracy in the case of sea surface temperature, since the confidence factor for sea surface temperature is extremely low. The small estimation error is mainly due to the fact that the natural variance of the sea surface temperature is small for properly defined climate types as can be deduced from Table 3. The confidence factor for wind speed estimation indicates it is much more reliably retrieved than the sea surface temperature. The SSM/I instrument is excellent for retrieving the distribution of moisture in the atmosphere, as indicated by the large confidence factors and the small residual RMS errors for the columnar densities of water vapor and cloud liquid water content.

Even though the geophysical model employed in this study is basically similar to the Hughes/ERT model, the performance of a channel subset still depends to an extent upon the model. NRL is presently acquiring the Hughes/ERT model and plans to do a similar study for the selection of optimum channel subsets for the marine environmental parameters with that model.

Table 11

The Recommended Frequency Subsets for the Retrieval of Marine Environmental Parameters

Parameter	Recommended Frequency Subset				Confidence Factor	Estimation Error
SST(^{o}C)	19.3 H	19.3 V	85.5 H	85.5 V	.1064	.6706
WS(m/sec)	19.3 H	19.3 V	22.2 V	37.0 V	.6516	.9720
VAP(gm/cm^2)	19.3 H	19.3 V	22.2 V	37.0 H	.8832	.0607
LIQ(gm/cm^2)	19.3 H	19.3 V	22.2 V	85.5 H	.9715	.0013

References

1. Wisler, M.M. and J.P. Hollinger, "Estimation of Marine Environmental Parameters Using Microwave Radiometric Remote Sensing Systems", Naval Research Laboratory Memorandum Report 3661, November 1977.

2. Poe, G., "Retrieval Accuracy of Sea Surface Temperature (SST) from Satellite Microwave Radiometer Data", Hughes 816318-61 A, December 1981.

3. Hollinger, J.P., **et al.**, "Joint Services 5D-2 Microwave Scanner Definition Study", Naval Research Laboratory Memorandum Report 3807, August 1978.

4. Hardy, K.R., et al., "A Study of Sea Surface Temperature Estimates Using the SSM/I", Environmental Research and Technology, Inc., ERT Document No. P-B088-F, October 1981.

5. "Special Sensor Microwave/Imager (SSM/I) Critical Design Review, Vol. II, Ground Segment", Contract No. F04701-79-C-0061, Hughes, p. 117, March 1980.

6. "Proposal for Microwave Environmental Sensor System (SSM/I), Volume 1. Technical Proposal", Hughes RFP No. F04701-78-R-0094, January 1979.

Appendix C

A Simulation Study of the Sensitivity of Environmental Parameter Retrievals Based on the Special Sensor Microwave Imager (SSM/I)

May 1982

Robert C. Lo and James P. Hollinger
Space Sensing Applications Branch
Naval Research Laboratory
Washington, D. C. 20375

A SIMULATION STUDY OF THE SENSITIVITY OF ENVIRONMENTAL PARAMETER RETRIEVALS BASED ON THE SPECIAL SENSOR MICROWAVE IMAGER (SSM/I)

Prepared by

Robert C. Lo and James P. Hollinger
Space Sensing Applications Branch
Aerospace Systems Division
Naval Research Laboratory
Washington, D.C. 20375

Prepared for

Navy Space Systems Activity
Los Angeles, CA

May 1982

A Simulation Study of the Sensitivity of Environmental Parameter Retrievals Based on the Special Sensor Microwave Imager (SSM/I)

Robert C. Lo and James P. Hollinger
Space Sensing Applications Branch
Aerospace Systems Division
Naval Research Laboratory
Washington, DC 20375

I. Introduction

During the qualification tests of the Special Sensor Microwave Imager (SSM/I) partial failure of the structure resulted in debris from the hot calibration load lodging in the feed horn blocking the 85.5V port and rendering the channel inoperative. Since then the problem has been corrected but, as a consequence of the event, a number of questions were raised. How good would the retrieval of environmental parameters be if the 85.5V channel is lost? What if any one channel is lost? Which channel is the retrieval of each parameter most sensitive to? Would the loss of that channel cause significant loss of confidence in that retrieval?

The purpose of this study is to provide insight into these questions through simulations using a geophysical model and retrieval scheme developed at the Naval Research Laboratory (NRL) (1), and a set of environmental statistics representing high, middle, and low latitude ocean conditions for all four seasons, produced by Wentz and Associates for the definition study the of SSM/I performed at NRL (2).

II. Simulations and Discussions

The geophysical model employed in this study (1) is basically a set of general equations describing the physical relationship among a number of environmental parameters and their microwave radiative characteristics. A retrieval scheme based on the geophysical model, climate statistics and the instrumental noise characteristics produces a matrix of linear regression coefficients, or the so-called "D-matrix" for a given set of frequencies and polarizations such as the SSM/I channels. The coefficients provide estimates of the environmental parameters when they are appropriately combined with brightness temperature observations. The geophysical model and retrieval scheme are applicable to a subset of SSM/I channels or any combinations of frequencies within the microwave and millimeter wave spectrum.

In addition to estimates of environmental parameters, the retrieval scheme produces certain other quantities which are indicative of the retrieval accuracy and the performance of a given channel combination. Two of these quantities are the residual root-mean-square (RMS) error, which is the total error associated with the retrieved parameter, and the confidence factor (CF) associated with the retrieval. They are defined as follows:

$$RMS = \sqrt{\sigma_o^2 - \sigma_m^2}\ , \qquad \text{(II.1)}$$

where σ_o^2 is the original variance associated with a parameter as part of the climate statistics, and σ_m^2 is the amount of variance explanable by the model and

$$CF = 1 - \sqrt{\frac{\sigma_o^2 - \sigma_m^2}{\sigma_o}}\ . \qquad \text{(II.2)}$$

These two quantities are the main criteria for the evaluations made in this study.

The climate statistics utilized in this study include twelve subsets representing the four season for three different locations: Jan Mayen, Azores and Truk. They are taken to represent high, middle, and low latitude ocean conditions (2).

The operational marine parameters to be retrieved by the SSM/I system include ocean surface wind speed, ice concentration, age and edge location, rain rate, and the columnar densities of water vapor and cloud liquid water (3). The sea surface temperature was included later on an experiment basis. The NRL geophysical model presently does not contain a submodel for rain rate and the climatology for ice is not yet complete. The marine parameters examined in this study are restricted to the columnar densities of water vapor and cloud liquid water, the surface wind speed, and the sea surface temperature.

The most accurate retrieval of the parameters is expected when all seven channels are used. However, limitations of the computational facilities at Air Force Global Weather Central dictated a maximum of four channels for the retrieval of each parameter. The channels adopted for wind speed and the columnar densities of water vapor and cloud liquid water are 19.35H, 22.235V, 37.0H and V (3). The combination of 19.35H, 22.235V, 85.5H and V is assessed to be the best four channel subset for sea surface temperature retrieval by the Environmental Research Technology, Inc. (ERT) (4) in a study conducted under contract to Hughes Aircraft Company. The residual RMS error in the sea surface temperature from the four channel retrieval is only minutely greater than the case when all seven channels are used according to this study (4).

The instrumental noise temperatures measured at Hughes (5) during the final qualification test are used for the present simulations. They are 0.48, 0.51, 0.64, 0.40, 0.39, 0.64 and 0.81K for 19.35H and V, 22.235V, 37.0H and V, and 85.5H and V.

II.A. Sea Surface Temperatures

Simulations for the 12 climates were performed using the 19.35H, 22.235V, 85.5H and V channel combination and all 3-channel subsets. The results are shown in Table 1. The same conclusion reached in a previous study (6) is apparent here; the SSM/I is not well-suited for the retrieval

of sea surface temperature. Even the highest confidence factor listed in Table 1 is less than 0.03. This is particularly true in the tropical cases, represented by Truk, where the combination of low surface emissivity and high atmospheric water content diminishes the little sensitivity the SSM/I has to sea surface temperature. The last two columns in Table 1 represents the retrievals with the 85.5V channel missing. The confidence factors in this case are significantly less than those for the other cases.

II.B. Wind Speed

Simulation of retrievals for wind speed and columnar densities of water vapor and cloud liquid water based on (19.35H, 22.235V, 37.0H and V) channel combination and the three-channel subsets are listed in Tables 2 through 4. The SSM/I RMS error specification for surface wind speed retrieval is 2 m/sec (3). Wind speed retrieval results for all the 12 climates in Table 2 indicate that the results are good not only when all four channels are used but also for all the subsets of three channels. The only exception is the case for tropical summer if the 37.0V channel is lost. The RMS error for this case is approximately 2.1 m/sec. The confidence factor values indicate that the most significant channels for wind speed retrievals are 19.35H and 22.235V, especially for the polar and the mid-latitude climates. For tropical ocean the most significant channel is 37V. The loss of it could cause an increase in RMS error of $\sim$ 0.8 m/sec.

II.C. Columnar Density of Water Vapor

The most significant channel for water vapor retrieval is the 22.235V GHz as is apparent from Table 3. However, for cases when the atmospheric water content is very high as represented by spring, summer and autumn of the tropical ocean, 19.35H becomes the most significant channel. This is probably due to the fact that the 22.235 GHz tends to approach saturation and becomes less sensitive when the water vapor content reaches a high level. It is observed, however, that even for these tropical cases, the retrieval performance for all channel combinations is significantly better than the SSM/I requirement which specifies the RMS error to be within $\pm$0.2 gm/cm^2.

II.D. Columnar Density of Liquid Water

Among the four marine parameters examined in this study, SSM/I has the greatest sensitivity to cloud liquid water. The SSM/I specification requirement of liquid water retrieval RMS error is $\pm$ 0.07 gm/cm^2 (3). From Table 4, the RMS error for the worst case is 0.0055 which is more than an order of magnitude less than the requirement specification. This implies that the loss of any single channel will not significantly affect the accuracy of liquid water content retrieval. The liquid water retrieval is most sensitive to the 19.35H channel as indicated by the RMS error and confidence factor values in Table 4.

III. Conclusion

A number of simulations were performed in this study to assess the effect on SSM/I parameter retrieval accuracy when one of the channels used in the retrieval was lost. Particular attention was given to the 85.5V channel which was rendered inoperative during a qualification vibration test. Results from this study indicate that the 85.5V channel is the most significant one only for sea surface temperature retrieval. Although it's loss could eliminate the ability of SSM/I to retrieve sea surface temperature, it would have little impact since the simulations also indicate that SSM/I has very little ability to assess the sea surface temperature even when all channels are intact. This is not surprising since the sea surface temperature was not a required parameter, and its retrieval was not a consideration during the design of the SSM/I.

The loss of 19.4H channel would deteriorate somewhat the wind speed retrieval for polar and moderate climates, and the water vapor density retrieval for the tropics. However, the simulation results indicate that the deterioration is not significant enough to cause the retrieval results to be below specification. The 19.4H channel is also the most significant channel for liquid water density retrieval. But the loss of this or any other channel does not affect the excellent retrieval ability of SSM/I for liquid water. The loss of the 22.235V channel would result in a loss of accuracy in the wind speed and water vapor density retrievals for high and middle latitudes. However, the increased error would still be within the SSM/I specification.

The loss of 37.0V channel can cause the wind speed retrieval performance to be below specification for tropical conditions.

The 19.35V channel is not used in the retrieval of the parameters examined here, and the loss of either the 37.0H or 85.5H channel does not result in deterioration in the retrieval of any of the four environmental parameters.

Table 1

SIMULATION RESULTS FOR SEA SURFACE TEMPERATURE

	19H, 22V, 85H&V		22V, 85H & V		19H, 85H & V		19H, 22V, 85V		19H, 22V, 85H	
	RMS	CF	RMS	CF	RMS	CF	RMS	CF	RMS	CF
Jan Mayen										
Winter	.2023	.0007	.2023	.0007	.2023	.0007	.2024	.0005	.2025	.0000
Spring	.7690	.0121	.7707	.0100	.7690	.0121	.7772	.0017	.7784	.0001
Summer	.5921	.0048	.5921	.0048	.5924	.0043	.5937	.0022	.5947	.0004
Autumn	1.2437	.0183	1.2503	.0131	1.2488	.0143	1.2458	.0167	1.2605	.0050
Azores										
Winter	.3402	.0012	.3402	.0012	.3402	.0011	.3404	.0004	.3406	.0001
Spring	1.4930	.0252	1.4554	.0245	1.4564	.0218	1.4604	.0114	1.4760	.0036
Summer	.7558	.0076	.7561	.0072	.7571	.0059	.7587	.0038	.7603	.0017
Autumn	1.3583	.0193	1.3594	.0185	1.3643	.0149	1.3700	.0108	1.3803	.0030
Truk										
Winter	.2120	.0007	.2120	.0004	.2121	.0003	.2120	.0007	.2121	.0004
Spring	.2623	.0013	.2626	.0005	.2626	.0002	.2624	.0012	.2625	.0008
Summer	.0837	.0001	.0837	.0001	.0837	.0000	.0837	.0001	.0837	.0001
Autumn	.2566	.0013	.2567	.0007	.2568	.0004	.2566	.0012	.2567	.0007

Table 2
Simulation Results for Wind Speed

	19H, 22V, 37H&V		22V, 37H & V		19H, 37H & V		19H, 22V, 37V		19H, 22V, 37H	
	RMS	CF	RMS	CF	RMS	CF	RMS	CF	RMS	CF
Jan Mayen										
Winter	.9980	.7552	1.6690	.5907	1.5788	.6128	1.0133	.7515	1.2592	.6912
Spring	.9021	.8034	1.3748	.7004	1.3777	.6998	.9574	.7914	1.2220	.7337
Summer	.8637	.7196	1.3066	.5758	1.3321	.5675	.9055	.7060	1.1370	.6309
Autumn	1.0495	.6975	1.9425	.4401	1.8192	.4756	1.0508	.6971	1.2311	.6451
Azores										
Winter	.8386	.7541	1.2674	.6283	1.2678	.6282	.9040	.7349	1.1193	.6718
Spring	.8248	.6187	1.1159	.4841	1.1227	.4810	.9134	.5777	1.0946	.4940
Summer	.8411	.6000	1.0918	.4808	1.0996	.4771	.9639	.5416	1.1473	.4544
Autumn	.9185	.6994	1.3322	.5640	1.3407	.5613	.9894	.6762	1.2058	.6054
Truk										
Winter	.9190	.4709	1.1187	.3559	1.1334	.3475	1.0606	.3894	1.2045	.3066
Spring	1.1831	.5081	1.4117	.4131	1.4394	.4016	1.4212	.4091	1.6191	.3268
Summer	1.3653	.6855	1.6491	.6201	1.6569	.6183	1.7726	.5916	2.1143	.5129
Autumn	1.0703	.5091	1.2564	.4237	1.2787	.4135	1.3128	.3978	1.4924	.3155

Table 3
Simulation Results For Columnar Density Of Water Vapor

	19H, 22V, 37H&V		22V, 37H & V		19H, 37H & V		19H, 22V, 37V		19H, 22V, 37H	
	RMS	CF	RMS	CF	RMS	CF	RMS	CF	RMS	CF
Jan Mayen										
Winter	.0586	.7929	.0686	.7576	.1397	.5061	.0712	.7483	.0587	.7926
Spring	.0520	.8658	.0611	.8422	.1237	.6806	.0627	.8381	.0523	.8649
Summer	.0518	.9055	.0609	.8888	.1228	.7757	.0623	.8863	.0521	.9049
Autumn	.0630	.8102	.0724	.7818	.1661	.4992	.0769	.7683	.0630	.8102
Azores										
Winter	.0522	.8802	.0620	.8578	.1147	.7369	.0637	.8538	.0530	.8784
Spring	.0590	.8940	.0698	.8747	.1052	.8111	.0691	.8759	.0595	.8931
Summer	.0613	.8841	.0760	.8564	.1045	.8026	.0743	.8596	.0627	.8815
Autumn	.0654	.8785	.0754	.8601	.1256	.7668	.0759	.8591	.0660	.8774
Truk										
Winter	.0785	.9182	.1081	.8873	.1185	.8765	.0992	.8965	.0815	.9151
Spring	.1050	.8840	.1563	.8274	.1451	.8398	.1409	.8444	.1126	.8757
Summer	.1233	.7582	.1851	.6370	.1641	.6783	.1794	.6481	.1455	.7147
Autumn	.0952	.8680	.1417	.8035	.1303	.8193	.1269	.8241	.1023	.8581

Table 4
Simulation Results for Columnar Density of Cloud Liquid Water

	19H, 22V, 37H&V		22V, 37H & V		19H, 37H & V		19H, 22V, 37V		19H, 22V, 37H	
	RMS	CF	RMS	CF	RMS	CF	RMS	CF	RMS	CF
Jan Mayen										
Winter	.0021	.9615	.0028	.9482	.0018	.9663	.0027	.9508	.0024	.9554
Spring	.0015	.9536	.0022	.9320	.0014	.9542	.0020	.9368	.0020	.9354
Summer	.0017	.9697	.0022	.9603	.0015	.9727	.0021	.9622	.0020	.9628
Autumn	.0028	.9599	.0035	.9510	.0021	.9697	.0035	.9510	.0029	.9596
Azores										
Winter	.0017	.9473	.0025	.9196	.0017	.9465	.0024	.9251	.0023	.9261
Spring	.0018	.9427	.0025	.9197	.0018	.9416	.0025	.9212	.0025	.9222
Summer	.0019	.9403	.0027	.9132	.0019	.9385	.0027	.9149	.0026	.9169
Autumn	.0020	.9561	.0029	.9354	.0020	.9561	.0027	.9388	.0027	.9390
Truk										
Winter	.0024	.9453	.0036	.9188	.0024	.9456	.0036	.9193	.0031	.9296
Spring	.0033	.9602	.0047	.9436	.0026	.9685	.0044	.9469	.0038	.9545
Summer	.0029	.9624	.0055	.9294	.0030	.9617	.0048	.9386	.0045	.9420
Autumn	.0025	.9211	.0042	.8676	.0026	.9192	.0039	.8756	.0034	.8914

References

1. Wisler, M. M. and J. P. Hollinger, "Estimation of Marine Environmental Parameters Using Microwave Radiometric Remote Sensing Systems", Naval Research Laboratory Memorandum Report 3661, November 1977.

2. Hollinger, J. P., **et al.**, "Joint Services 5D-2 Microwave Scanner Definition Study", Naval Research Laboratory Memorandum Report 3807, August 1978.

3. "Proposal for Microwave Environmental Sensor System (SSM/I) Volume I. Technical Proposal", Hughes RFP No. F04701-78-R-0094, January 1979.

4. Hardy, K. R., et. al., "A Study of Sea Surface Temperature Estimates Using the SSM/I", ERT Document No. P-B088-F, October 1981.

5. "SSM/I Sensor Qualification Test Report", HS256-0006-0733; April, 1982.

6. Lo, R. C., and J. P. Hollinger, "Selection of Optimal Combinations of Frequencies for the Special Sensor Microwave Imager (SSM/I) Environmental Retrievals", NRL letter to NSSA and PME, 1982.

Appendix D

A Comparison Study of the Sensitivity and Retrieval Performance of 21.0 and 22.235 GHz Channels

September 1982

Robert C. Lo and James P. Hollinger
Space Sensing Applications Branch
Naval Research Laboratory
Washington, D. C. 20375

NRL LETTER REPORT
7910-152:JPH:ms

A COMPARISON STUDY OF THE SENSITIVITY AND RETRIEVAL PERFORMANCE OF 21.0 AND 22.234 GHz CHANNELS

Prepared by

Robert C. Lo and James P. Hollinger

Aerospace Systems Division
Naval Research LAboratory
Washington, D.C. 20375

For

Navy Space Systems Activity
Los Angeles, CA 90009

September 1982

A Comparison Study of the Sensitivity and Retrieval Performance of 21.0 and 22.235 GHz Channels

Robert C. Lo and James P. Hollinger

Space Sensing Applications Branch
Aerospace Systems Division
Naval Research Laboratory
Washington, DC 20375

I. Introduction

The Special Sensor Microwave Imager (SSM/I) contains horizontally and vertically polarized channels at 19.35, 37.0 and 85.5 GHz and a single vertically polarized channel at 22.235 GHz. The 22.235 GHz channel is centered on a water vapor absorption line and was selected primarily to determine the columnar density of atmospheric water vapor and to provide corrections for its absorption and emission effects at the other channels. Two arguments have been raised against the use of 22.235 GHz frequency for these purposes. One is that the 22.235 GHz channel could saturate under tropical conditions. The other argument is that the absorption coefficient per unit mass of water vapor at 22.235 GHz increases with height, whereas, at 21.0 GHz it varies only slightly with height and actually decreases above about 7 km. Thus, moisture in the upper troposhere will be unduly weighted and cause a significant bias in the total water vapor content estimation based on the 22.235 GHz frequency. An alternative frequency, 21.0 GHz on the wing of the absorption band, has been suggested in place of 22.235 GHz. It is speculated that at this frequency, there is enough sensitivity for accurate estimation of water vapor but not enough to cause saturation. Further, the absorption coefficient at 21.0 GHz is practically constant with height over the lower atmospheric layers which contain most of the atmosphere water vapor.

The purpose of this study is to assess the validity of the above two arguments through the use of sensitivity studies and retrieval result comparisons.

II. Saturation Under Tropical Conditions

A. Comparison of Sensitivity

Wisler and Hollinger (2) designed a geophysical model and environmental parameter retrieval scheme which provides a measure of the sensitivity of the microwave signal to the environmental parameter and the uncertainty in the retrieval for any given combination of microwave frequencies. This model was used for an SSM/I definition study (3) and other SSM/I related studies (4, 5, 6).

Climate statistics representing the most humid atmospheric conditions generally encountered, i.e. tropical summer ocean (3), are used in the

geophysical model for the examination of the sensitivity of 21.0 and 22.235 GHz channels to water vapor content in the atmosphere. First, all clouds are removed from the climate statistics while the vertical temperature structure as well as surface statistics remain. A range from 0 to 7 gm/cm^2 is assigned to the water vapor parameter, that is, the columnar density of water vapor. The upper end of this range is very high even for tropical conditions (7, 8). Brightness temperatures at 21.0 and 22.235 GHz are calculated and are presented in Figure 1. The slope of the curve representing 22.235 GHz is greater than that of 21.0 GHz for water vapor density values up to 5.5 gm/cm^2. Then it becomes slightly less than at 21.0 GHz. The slope of both curves remains significantly high over the entire range. This implies that the 22.235 GHz channel is a better predictor of water vapor content than the 21.0 GHz channel in the absence of clouds for most conditions found in the atmosphere. And even in the extremely humid case, the sensitivity of 22.235 GHz is still not significantly less than that of 21.0 GHz.

A similar set of simulations is performed with clouds restored, to evaluate the effect of clouds on the sensitivity of the two channels. The average cloud liquid water content is 0.0738 gm/cm^2 corresponding to a cloud thickness of approximately 1.4 kms. The range used for water vapor density is again from 0 to 7 gm/cm^2. The brightness temperature curves for the 21.0 and 22.235 GHz channels under these conditions are presented in Figure 2. The slopes of both curves are less than those in Figure 1. That is to say, the presence of the cloud deck decreases the sensitivity of both frequencies to water vapor density. The slope of the 22.235 GHz curve is greater than that of 21.0 GHz for water vapor density values up to 4.5 gm/cm^2. It then becomes slightly less than that of 21.0 GHz but not significantly so. From this set of simulations, it appears that both frequencies would have adequate sensitivity for the evaluation of water vapor density even with a moderately thick cloud. The 22.235 GHz has an advantage over the 21.0 GHz for the majority of the cases. The opposite is true for the extremely humid cases.

The third set of simulations is designed to compare the sensitivity of the two frequencies under various cloud conditions. The water vapor density is held constant at 5.558 gm/cm^2 representing a very humid atmosphere, while cloud liquid water content varies from 0 to 0.2 gm/cm^2. Simulation results are presented in Figure 3. The curves in Figure 3 indicate that 21.0 GHz is more sensitive to the variations in columnar density of cloud liquid water than 22.235 GHz. Both channels start to lose their sensitivity when the liquid water density approaches 0.2 gm/cm^2. The 22.235 GHz curve levels off faster than the 21.0 GHz.

From the above sensitivity studies, it appears that 22.235 GHz is a better frequency than the 21.0 GHz for the retrieval of water vapor density over most of the atmospheric conditions. In the more humid conditions, it tends to lose some of the sensitivity but should still be adequate.

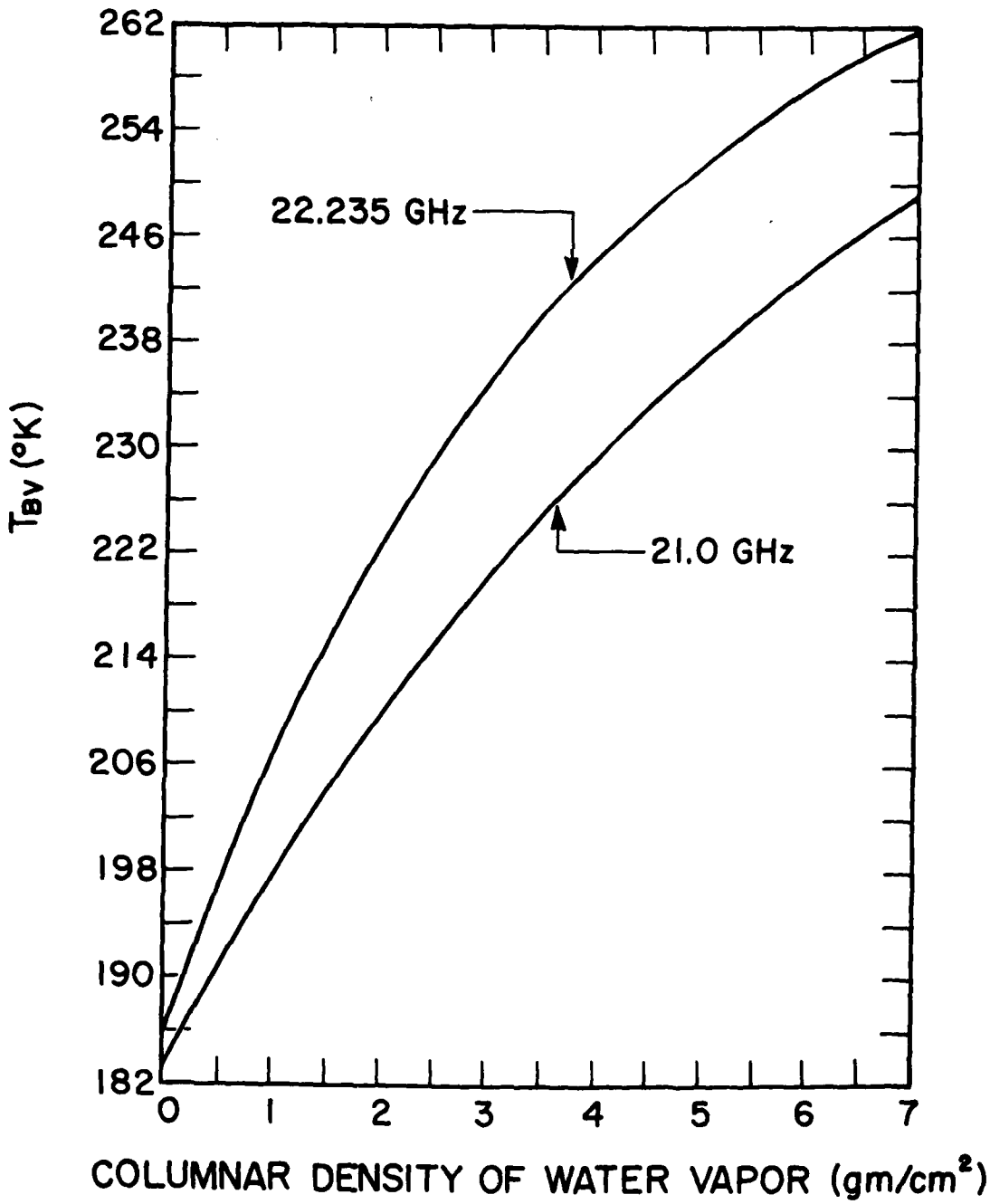

Figure 1 Sensitivity of the water vapor absorption bands under cloudless conditions.

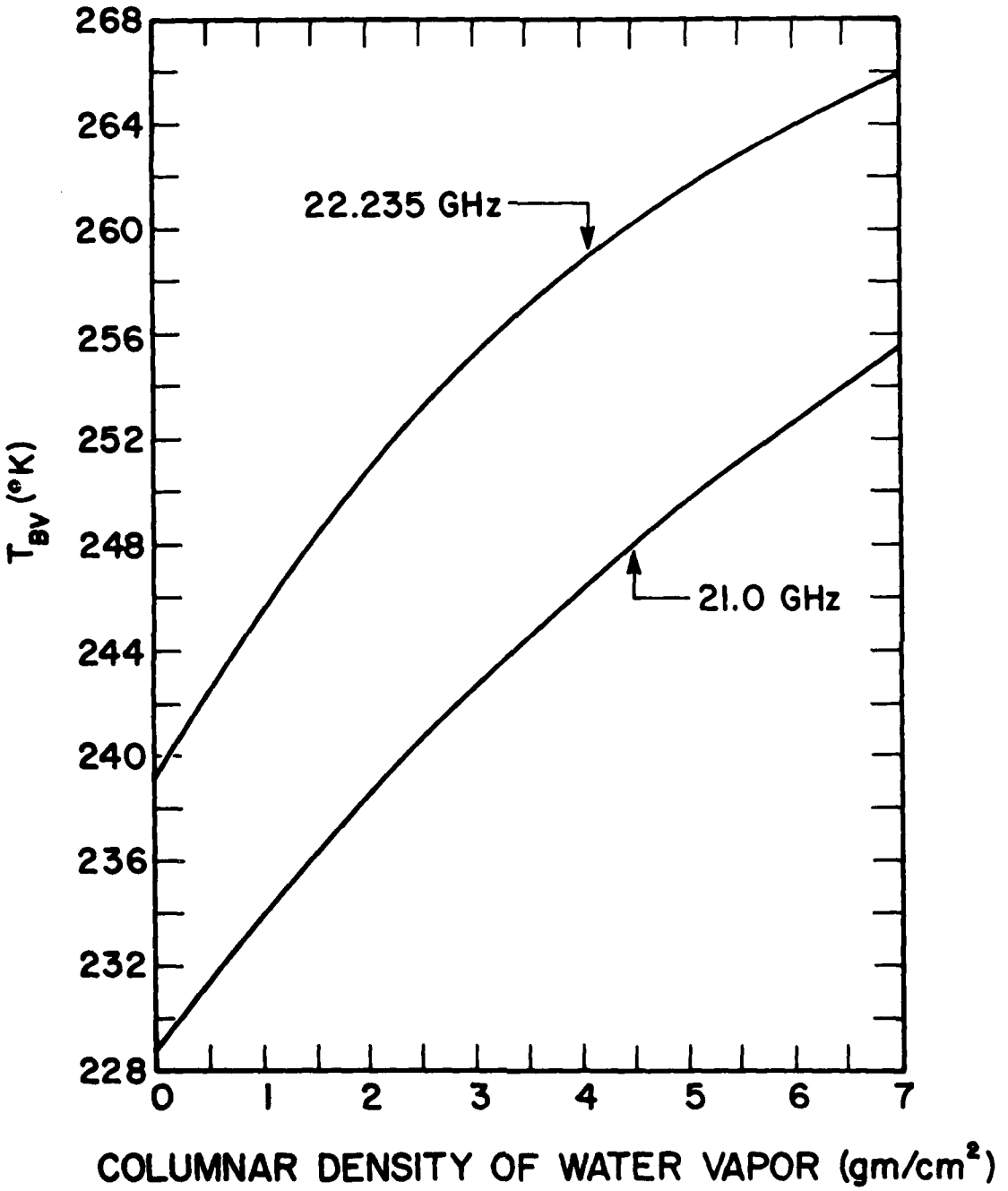

Figure 2 Sensitivity of the water vapor absorption bands under cloudy conditions

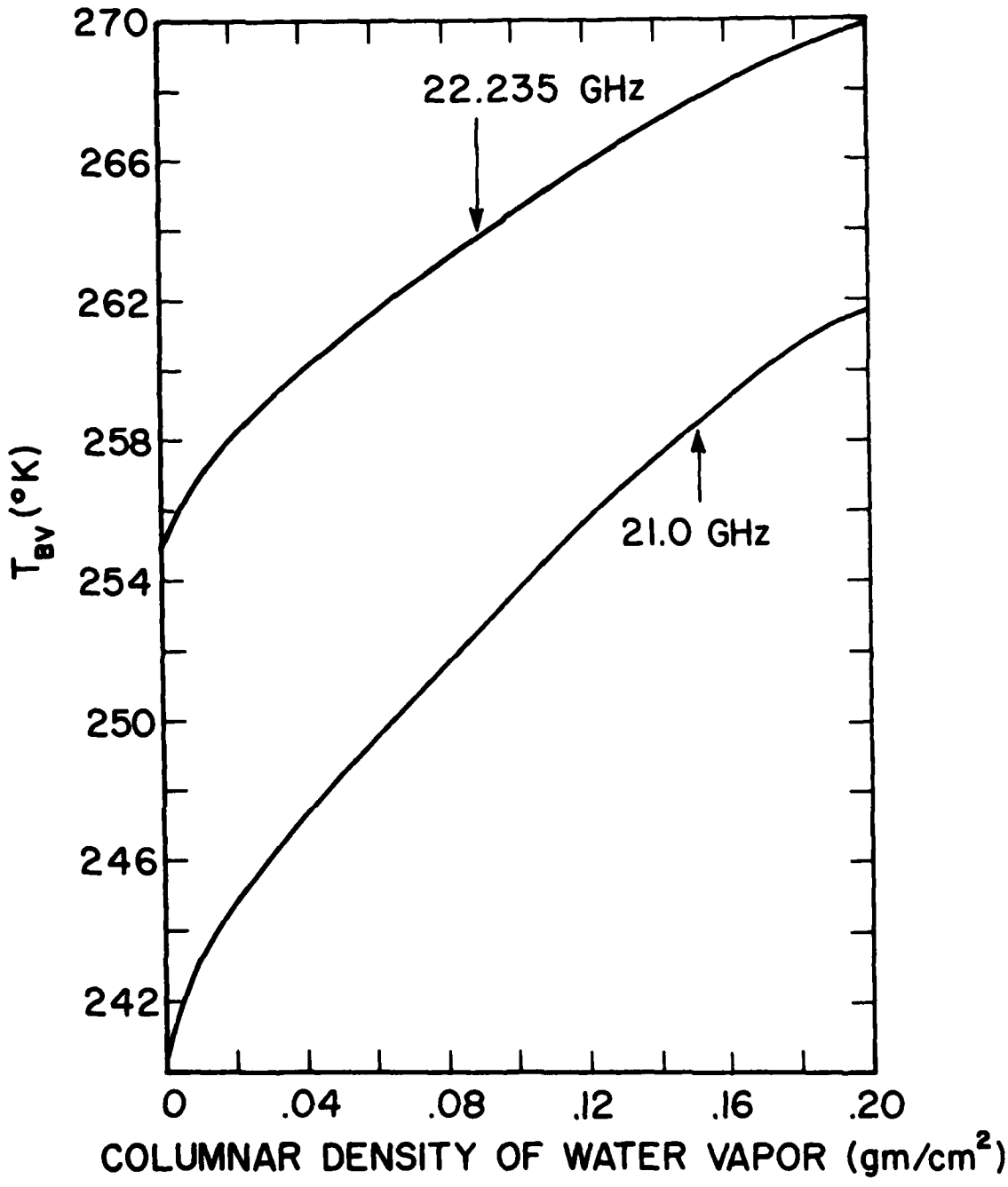

Figure 3 Sensitivity of the water vapor absorption bands as function of cloud liquid water content

B. Comparison of Retrievals

The relative advantage of using the 21.0 GHz versus 22.235 GHz frequency is further examined through simulated retrievals. The (19.35 H, 22.235 V, 37.0 H and V) channels are the specified frequency combination for SSM/I retrieval of wind speed, columnar densities for water vapor and cloud liquid water (1). For comparison, another frequency combination, with 21.0 V replacing the 22.235 V channel, is used for the retrievals. The twelve sets of climate statistics (3) describing the four seasons for arctic, moderate and tropical oceans are used in conjunction with the Wisler and Hollinger (2) geophysical model and retrieval scheme. The residual root-mean-square (RMS) error and the confidence factor (CF) are included as part of the retrieval products. They are defined as follows:

$$RMS = \sqrt{\sigma^2 - \sigma_r^2}$$

and

$$CF = 1 - \sqrt{\frac{\sigma^2 - \sigma_r^2}{\sigma^2}}$$

where σ^2 is the natural variance of the environmental parameter being retrieved and σ_r^2 is the variance of the parameter after retrieval. The confidence factor ranges between 0 and 1. A large confidence factor value implies a good retrieval ability.

The RMS errors and confidence factors of wind speed, columnar density of water vapor and cloud liquid water retrievals for all 12 climates are listed in Table 1. Results from both frequency combinations are included in the table. The performance of the frequency combination with 22.235 V channel is consistently better in the retrievals of wind speed and water vapor density for 9 of the 12 climates. Only for the three warmest and most humid climates, i.e., the spring, summer and autumn seasons for the tropical ocean does the 21.0 V channel combination result in lower retrieval errors. The difference in RMS error for wind speed retrieval of the tropical summer case, where this phenomenon is most pronounced, is approximately 0.02 m/sec. And the difference for water vapor density is about .013 gm/cm^2. Both are extremely small. The SSM/I requirement specification is 2 m/sec RMS error for wind speed and 0.2 gm/cm^2 for water vapor density (1). The performance of both frequency combinations for all the 12 climates meets the SSM/I specifications. It is concluded, therefore, that the 22.235 GHz is preferred to 21.0 GHz for overall performance in the wind speed and water vapor density retrievals.

Both of the frequency combinations yield excellent retrieval results for the cloud liquid water density. The SSM/I specifications for the RMS error of this parameter is 0.07 gm/cm^2 (1), which is more than an order of magnitude greater than that from the retrieval results. The relative performance between the two frequency combinations does not follow the pattern for wind speed and water vapor density. Retrievals with 22.235 GHz are better in 8 out of the 12 climates, judging by the confidence factor

Table 1

Retrieval Result of Wind Speed and Moisture Terms
from the Two Frequency Combinations

21.0 V
19.35 H, or , 37.0 H, 37.0 V
22.235 V

	Wind Speed (m/sec)					Columnar Water Vapor Density (gm/cm^2)				
	Original RMS	Residual RMS (21)	CF (21)	Residual RMS (22)	CF (22)	Original RMS	Residual RMS (21)	CF (21)	Residual RMS (22)	CF (22)
Jan Mayen										
Winter	4.0773	1.0656	.7387	.9980	.7552	.2828	.0738	.7391	.0586	.7929
Spring	4.5889	.9606	.7907	.9021	.8034	.3873	.0660	.8295	.0520	.8658
Summer	3.0801	.9163	.7025	.8637	.7196	.5477	.0648	.8816	.0518	.9055
Autumn	3.4693	1.1234	.6762	1.0495	.6975	.3317	.0801	.7585	.0630	.8102
Azores										
Winter	3.4100	.8867	.7400	.8386	.7541	.4359	.0627	.8562	.0522	.8802
Spring	2.1631	.8682	.5986	.8248	.6187	.5568	.0688	.8765	.0590	.8940
Summer	2.1029	.8702	.5862	.8411	.6000	.5292	.0685	.8706	.0613	.8841
Autumn	3.0558	.9738	.6813	.9185	.6994	.5385	.0768	.8574	.0654	.8785
Truk										
Winter	1.7370	.9242	.4679	.9190	.4709	.9592	.0809	.9157	.0785	.8182
Spring	2.4052	1.1463	.5234	1.1831	.5081	.9055	.0996	.8900	.1050	.8840
Summer	4.3407	1.2746	.7064	1.3653	.6855	.5099	.1101	.7840	.1233	.7582
Autumn	2.1801	1.0463	.5201	1.0703	.5091	.7211	.0916	.8730	.0952	.8680

Columnar Cloud Liquid Water Density (gm/cm^2)

Jan Mayen					
Winter	.0548	.0021	.9611	.0021	.9615
Spring	.0316	.0014	.9542	.0015	.9536
Summer	.0548	.0019	.9649	.0017	.9697
Autumn	.0707	.0025	.9649	.0028	.9599
Azores					
Winter	.0316	.0017	.9470	.0017	.9473
Spring	.0316	.0018	.9420	.0018	.9427
Summer	.0316	.0019	.9396	.0019	.9403
Autumn	.0447	.0020	.9545	.0020	.9561
Truk					
Winter	.0447	.0024	.9461	.0024	.9453
Spring	.0837	.0032	.9623	.0033	.9602
Summer	.0775	.0034	.9565	.0029	.9624
Autumn	.0316	.0025	.9208	.0025	.9211

Table 2

Retrieval Results of Sea Surface Temperature
from the Two Frequency Combinations

Sea Surface Temperature(K) 19.35 H, 21.0 V or 22.235 V, 85.5 H, 85.5 V

	Original RMS	Residual RMS (21)	CF (21)	Residual RMS (22)	CF (22)
Jan Mayen					
Winter	.2025	.2023	.0007	.2023	.0007
Spring	.7785	.7690	.0121	.7690	.0121
Summer	.5950	.5922	.0047	.5921	.0048
Autumn	1.2669	1.2455	.0168	1.2437	.0183
Azores					
Winter	.3406	.3401	.0013	.3402	.0012
Spring	1.4930	1.4501	.0287	1.4554	.0252
Summer	.7616	.7544	.0094	.7558	.0076
Autumn	1.3849	1.3542	.0222	1.3583	.0193
Truk					
Winter	.2121	.2119	.0010	.2120	.0007
Spring	.2627	.2623	.0015	.2623	.0013
Summer	.0837	.0837	.0001	.0837	.0001
Autumn	.2569	.2565	.0015	.2566	.0013

values. The residual RMS error, however, shows no detectable difference in several of the cases. The conclusion is that the use of 21.0 GHz channel by no means improves the retrieval performance for the columnar density of cloud liquid water.

The frequency combination suggested for the retrieval of sea surface temperature by a study performed at the Environmental Research and Technology, Inc. (9) is 19.35 H, 22.235 V, 85.5 H and V. Retrieval results for the 12 climates using this frequency combination and the alternate combination (19.35 H, 21.0 V, 85.5 H and V) for sea surface temperature are listed in Table 2. The performance of the combination with 21.0 GHz is better in most of the cases. An examination of the confidence factor values reveals, however, that the ability to retrieve sea surface temperature is dismal for both combinations. The minimal improvement in sea surface temperature retrieval alone is not sufficient to justify the substitution of the 22.235 GHz channel.

III. Upper Tropospheric Water Vapor

The vertical profiles of the absorption coefficient per unit mass of water vapor are calculated using the climatology of Azores, Summer (3) at 22.235 GHz, 21.0 GHz and 23.470 GHz. The absorption coefficient integrated over the SSM/I passband of ± 10 to 250 MHz centered on the L.O. frequency of 22.235 GHz (1) is also shown to display the effects of bandwidth smoothing. The equation used for the calculation is

$$A_{H_2O} = \alpha_{H_2O}/\rho = \left[3.24 \times 10^{-4} \exp\left(\frac{-644}{T}\right)\frac{\nu^2 P}{T^{3.125}}\left(1 + 0.0147\ \frac{\rho T}{P}\right)\right.$$

$$\left.\left(\frac{1}{(\nu-\nu_0)^2+\Delta\nu^2} + \frac{1}{(\nu+\nu_0)^2+\Delta\nu^2}\right) + 2.55 \times 10^{-8}\ \frac{\nu^2\Delta\nu}{T^{1.5}}\right] \times 10^5 \quad \text{(III.1)}$$

where

$$\Delta\nu = 2.58 \times 10^{-3}\left(P + 0.147\ \rho T\right)\left(\frac{T}{318}\right)^{-0.625} \quad \text{(III.2)}$$

A_{H_2O} is the absorption of water vapor per unit mass; T is the temperature(K); P is atmospheric pressure (mb); ν is frequency (GHz); ν_0 is 22.235 GHz and ρ is water vapor density (gm/m3). A_{H_2O} has only a very weak dependence on ρ. The four profiles are shown in Figure 4. A_{H_2O} increases steadily with height at 22.235 GHz while only slightly at 21.0 GHz for the first few kilometers where most of the atmospheric moisture resides.

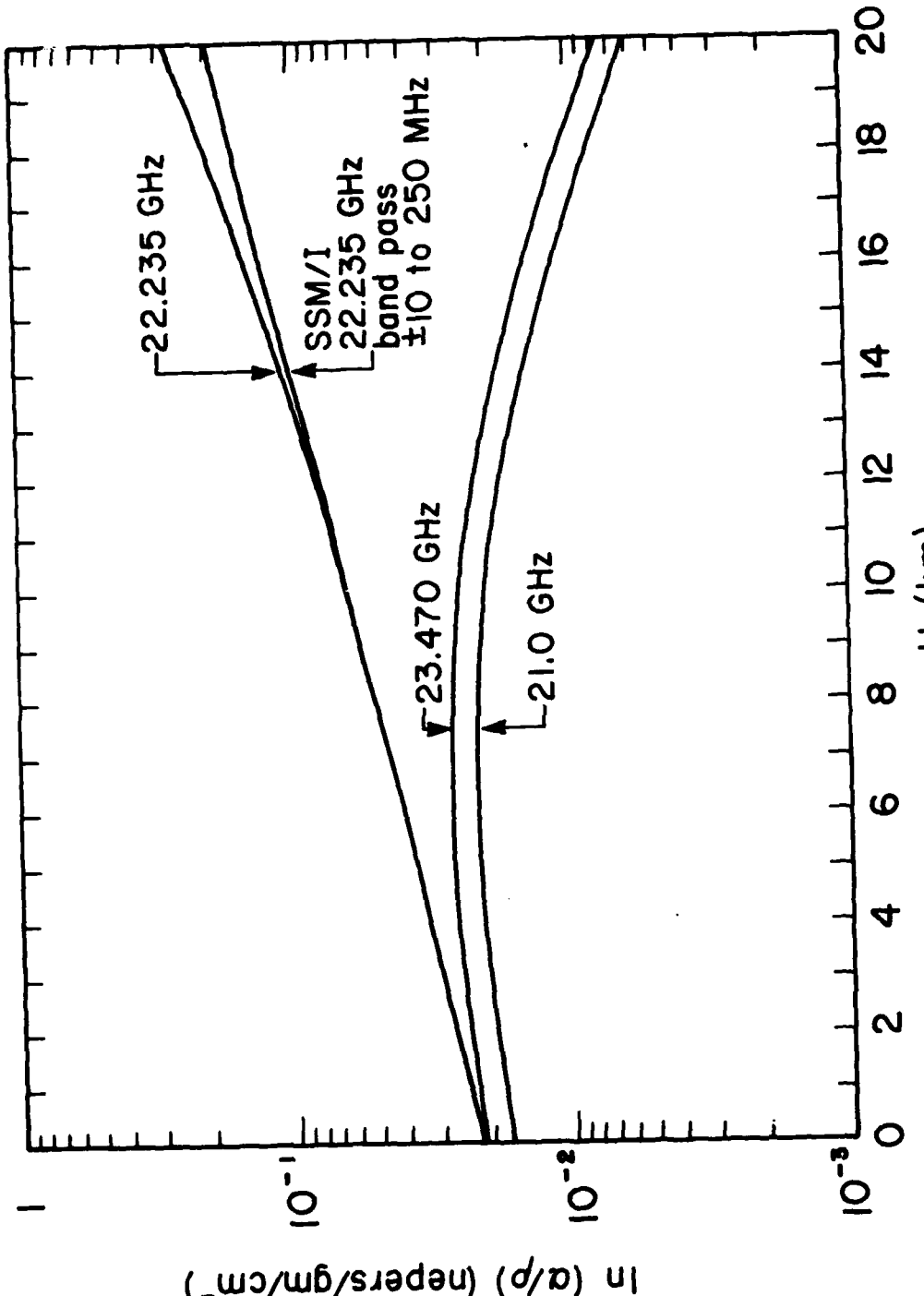

Figure 4 Absorption coefficient as function of height

Even though the profiles representing the two frequency regions are distinctly different, the advantage of using one rather than the other in the SSM/I system must still be evaluated through retrieval simulations. A modification is made to the climate statistics used for retrievals shown in Tables 1 and 2, in order to keep the columnar water vapor density constant while allowing more moisture at the higher levels. An exponentially decreasing absolute humidity profile is assumed in the geophysical model (1). The profile is a function only of the surface absolute humidity and the water vapor scale height. By changing the scale height to 1.5 times the normal climate mean while decreasing the surface absolute humidity so as to hold the total water vapor constant, some moisture is artificially moved from the lower to higher layers. A change of scale height by 50% is a very significant change for the real atmosphere as it represents quite an extreme variation in the vertical distribution of moisture. The retrieval results for the new moisture profiles are shown in Tables 3 and 4. The comparison between 21.0 and 22.235 GHz retrieval is very similar to those obtained earlier and shown in Tables 1 and 2. The 22.235 GHz channel combination does better for wind speed and water vapor in all except the tropical climates and there is no difference for cloud water retrievals for any of the climates. Although the 22.235 GHz channel is to be slightly preferred the overall performance, including all climates and parameters, is very similar for both the 22.235 GHz and 21.0 GHz combinations. The RMS from the retrievals in all cases are within the SSM/I specifications (1).

IV. Summary and Conclusions

This comparison is performed to evaluate the speculation that 22.235 GHz, included in the SSM/I, may become saturated and lose sensitivity for environmental parameter retrievals, particularly under tropical conditions, and that moisture present in higher leve may bias the estimation of total water vapor using 22.235 GHz.

The 21.0 and 22.235 GHz brightness temperatures as functions of the columnar density of water vapor with and without clouds, and as a function of columnar density of cloud liquid water for the tropical summer ocean are examined. The results indicate that the brightness temperature at 22.235 GHz is more sensitve to changes in water vapor content then that of 21.0 GHz in most cases except when the humidity is very high. And even under such condition, the 22.235 GHz channel does not lose its sensitivity significantly.

Retrieval simulations with normal climate and with modified moisture profiles are then performed comparing the performance of 22.235 GHz and 21.0 GHz. The wind speed and water vapor density retrievals indicate that 22.235 GHz is consistently better except for the more humid seasons in the tropics, for which case, 21.0 GHz offers a slight advantage. The retrieval results with either frequency are better than the SSM/I requirement specifications. The 21.0 GHz is somewhat better for the sea surface temperature retrieval. However, both frequency combinations yield extremely poor results for this parameter. A channel of much lower frequency than both 21.0 and 22.235 GHz is needed before significant improvement in sea surface temperature retrieval can be expected.

Table 3

Retrieval Results of Wind Speed and Moisture Terms
from the Two Frequency Combinations

19.35 H, 21.0 V or 22.235 V, 37.0H, 37.0 V

	Wind Speed (m/sec)					Columnar Water Vapor Density (gm/cm^2)				
	Original RMS	Residual RMS (21)	CF (21)	Residual RMS (22)	CF (22)	Original RMS	Residual RMS (21)	CF (21)	Residual RMS (22)	CF (22)
Jan Mayen										
Winter	4.0773	1.0619	.7396	.9910	.7569	.2828	.0754	.7333	.0580	.7950
Spring	4.5889	.9557	.7917	.8950	.8050	.3873	.0678	.8248	.0516	.8669
Summer	3.0801	.9120	.7039	.8568	.7218	.5477	.0669	.8779	.0519	.9052
Autumn	3.4693	1.1192	.6774	1.0419	.6997	.3317	.0823	.7518	.0624	.8118
Azores										
Winter	3.4100	.8855	.7403	.8337	.7555	.4359	.0651	.8506	.0527	.8791
Spring	2.1631	.8683	.5986	.8232	.6195	.5568	.0717	.8712	.0605	.8914
Summer	2.1029	.8732	.5848	.8465	.5975	.5292	.0722	.8636	.0648	.8774
Autumn	3.0558	.9743	.6812	.9184	.6995	.5385	.0809	.8498	.0683	.8731
Truk										
Winter	1.7370	.9331	.4628	.9513	.4523	.9592	.0877	.9086	.0907	.9054
Spring	2.4052	1.1709	.5132	1.3051	.4574	.9055	.1119	.8764	.1356	.8502
Summer	4.3407	1.3153	.6970	1.5833	.6352	.5099	.1261	.7527	.1684	.6698
Autumn	2.1801	1.0643	.5118	1.1557	.4699	.7211	.1020	.8585	.1192	.8347

	Columnar Cloud Liquid Water Density (gm/cm^2)				
Jan Mayen					
Winter	.0548	.0021	.9616	.0021	.9610
Spring	.0316	.0015	.9527	.0014	.9546
Summer	.0548	.0019	.9657	.0019	.9653
Autumn	.0707	.0026	.9638	.0026	.9628
Azores					
Winter	.0316	.0017	.9478	.0016	.9487
Spring	.0316	.0018	.9438	.0018	.9445
Summer	.0316	.0019	.9408	.0018	.9418
Autumn	.0447	.0019	.9569	.0019	.9574
Truk					
Winter	.0447	.0024	.9472	.0024	.9468
Spring	.0837	.0028	.9670	.0026	.9685
Summer	.0775	.0030	.9618	.0030	.9618
Autumn	.0316	.0024	.9226	.0025	.9224

Table 4

Retrieval Results of Sea Surface Temperature
from the Two Frequency Combinations

Sea Surface Temperature(K) 19.35 H, 21.0 V / 22.235 V, 85.5 H, 85.5 V

	Original RMS	Residual RMS (21)	CF (21)	Residual RMS (22)	CF (22)
Jan Mayen					
Winter	.2025	.2023	.0007	.2023	.0007
Spring	.7785	.7690	.0122	.7690	.0122
Summer	.5950	.5922	.0047	.5921	.0049
Autumn	1.2669	1.2475	.0153	1.2447	.0175
Azores					
Winter	.3406	.3401	.0014	.3402	.0013
Spring	1.4930	1.4474	.0305	1.4535	.0265
Summer	.7616	.7539	.0101	.7554	.0082
Autumn	1.3849	1.3516	.0241	1.3563	.0206
Truk					
Winter	.2121	.2119	.0011	.2119	.0009
Spring	.2627	.2622	.0017	.2622	.0017
Summer	.0837	.0837	.0001	.0837	.0002
Autumn	.2569	.2565	.0017	.2565	.0017

It is concluded, therefore, that the arguments concerning these two frequencies may be more academic and speculative than real. The minimal advantage of using 21.0 GHz, for some of the tropical cases does not justify the replacement of the 22.235 GHz.

References

1. "Proposal for Microwave Environmental Sensor System (SSM/I), Volume 1. Technical Proposal", Hughes RFP No. F04701-78R-0094, January 1979.

2. Wisler, M. M., and J. P. Hollinger, "Estimation of Marine Environmental Parameters Using Microwave Radiometric Remote Sensing Systems", NRL Memorandum Report 3661, November 1977.

3. Hollinger, J. P., R. M. Lerner, B. E. Troy and M. M. Wisler, "Joint Services 5D-2 Microwave Scanner Definition Study", NRL Memorandum Report 3807, August 1978.

4. Lo, R. C., and J. P. Hollinger, "NRL Comments on the ERT SST Study for the SSM/I" NRL Letter Memo to NSSA and PME, December 1981.

5. Lo, R. C., and J. P. Hollinger, "Selection of Optimal Combinations of Frequencies for the Special Sensor Microwave Imager (SSM/I) Environmental Retrievals" NRL, Letter Memo to NSSA and PME, April 1982.

6. Lo, R. C., and J. P. Hollinger, "A Simulation Study of the Sensitivity of Environmental Parameter Retrievals Based on the Special Sensor Microwave Imager (SSM/I)" NRL Letter Memo to NSSA and PME, May 1982.

7. Grody, N. C., A. Gruber and W. C. Shen, "Atmospheric Water Content Over the Tropical Pacific Derived from the Nimbus-6 Scanning Microwave Spectrometer", Journal of Applied Meteorology, Vol. 19, No. 8, August 1980, p. 986.

8. Prabhakara, C., G. Dalu, R. C. Lo and N. R. Nath, "Remote-Sensing of Seasonal Distribution of Precipitable Water-Vapor Over the Oceans and the Inference of Boundary-Layer Structure", Monthly Weather Review, Vol. 107, pp. 1388-1401, 1979.

9. Hardy, K. R., H. K. Burke, J. Ho and N. K. Tripp, "A Study of Sea Surface Temperature Estimates Using the SSM/I", ERT Document No. P-B088-F, October 1981.

Appendix E

A Study of the Cross Polarization Effects on the Special Sensor Microwave Imager (SSM/I) Environmental Parameter Retrievals

September 1982

Robert C. Lo and James P. Hollinger
Space Sensing Applications Branch
Naval Research Laboratory
Washington, D. C. 20375

NRL LETTER REPORT
7910-271:JPH:ms

A STUDY OF THE CROSS POLARIZATION EFFECTS ON THE SPECIAL SENSOR MICROWAVE IMAGER (SSM/I) ENVIRONMENTAL PARAMETER RETRIEVALS

Prepared by

Robert C. Lo and James P. Hollinger

Aerospace Systems Division
Naval Research Laboratory
Washington, D.C. 20375

For

Navy Space Systems Activity
Los Angeles, CA 90009

September 1982

A Study of the Cross Polarization Effects on the Special Sensor Microwave Imager (SSM/I) Environmental Parameter Retrievals

Robert C. Lo and James P. Hollinger

Aerospace Systems Division
Naval Research Laboratory
Washington, D. C. 20375

I. Introduction

The original development specification required cross polarization levels of less than one percent for all the seven SSM/I channels. This was relaxed later to two percent for the 19.35 GHz channels and the 22.235 GHz channel and five percent for the four higher frequency channels (1). The relaxation of the cross polarization specification could have a significant impact on the environmental retrieval accuracies. Although larger cross polarization will increase retrieval errors it is the uncertainty in the cross polarization which can have the most serious consequences. This uncertainty will degrade the performance of the SSM/I and may result in environmental parameter retrieval errors over specification.

The purpose of the present study is to examine the effects of cross polarization and its uncertainty on the retrieval accuracy of the environmental parameters.

II. The Effect of Cross Polarization Errors

Let T_H and T_V be the true horizontal and vertical polarization brightness temperatures and let T_{HM} and T_{VM} be the corresponding values measured in the presence of cross polarization. Assume that the leakage of the two polarizations are the same and denote it as α ($0 \leq \alpha < 1$). The relationship among these variables can be written as follows.

$$T_{HM} = (1-\alpha)\, T_H + \alpha\, T_V \tag{II.1}$$

$$T_{VM} = (1-\alpha)\, T_V + \alpha\, T_H \tag{II.2}$$

Solving for T_H and T_V

$$T_H = \frac{(1-\alpha)\, T_{HM} - \alpha\, T_{VM}}{1-2\alpha} \tag{II.3}$$

$$T_V = \frac{(1 - \alpha)\, T_{VM} - \alpha\, T_{HM}}{1 - 2\,\alpha} \qquad \text{(II.4)}$$

The error in α, T_{HM} and T_{VM} would cause estimation errors in the true brightness temperatures T_H and T_V, which are input to the retrieval schemes. Let σ_{HM}, σ_{VM} and σ_α be the standard errors of T_{HM}, T_{VM} and α. The relationship between these error terms and that of the true brightness temperature is:

$$\sigma^2_{H \text{ or } V} = \left(\frac{\partial T_{H \text{ or } V}}{\partial \alpha}\right)^2 \sigma^2_\alpha + \left(\frac{\partial T_{H \text{ or } V}}{\partial T_{VM}}\right)^2 \sigma^2_{VM} + \left(\frac{\partial T_{H \text{ or } V}}{\partial T_{HM}}\right)^2 \sigma^2_{HM} \qquad \text{(II.5)}$$

For the sake of simplicity, assume that the instrumental error, σ_R, is the same for both polarization, i.e., $\sigma_R = \sigma_{VM} = \sigma_{HM}$. Applying equation (II.4), it follows:

$$\sigma^2_T = \frac{(T_{VM}-T_{HM})^2}{(1-2\,\alpha)^4}\, \sigma^2_\alpha + \frac{(1-\alpha^2) + \alpha^2}{(1-2\,\alpha)^2}\, \sigma^2_R \qquad \text{(II.6)}$$

where σ_T is the standard deviation of the true brightness temperature, either of the vertical or of the horizontal component.

The instrumental noise, σ_R, is measured for each channel in the sensor tests as a function of the radiometer only, and independent of the antenna. But the error that affects the retrieval result is σ_T. Equation (II.6) shows that both the cross polarization α and the uncertainty in cross polarization, σ_α, increase σ_T and contribute to the degradation of the retrieval accuracy. A number of cases are simulated to examine the effect of α and σ_α.

Figures 1 through 4 are constructed from equation (II.6) assuming $T_{VM} - T_{HM} = 40$, which is typical for ocean observation from the SSM/I. The figures represent cases with cross polarization uncertainty, σ_α, of 0, 0.5, 1 and 2 percent, respectively. The instrument noise, σ_R, is allowed to vary between 0 and 1 degree contigrade and the cross polarization, α, varies between 0 to 5 percent for each figure. The magnification of instrumental error is not very strong when σ_α is zero, as indicated in Figure 1. Even for a five percent cross polarization, an instrument noise of 1.0 increases to only 1.06. However, when σ_α is no longer zero, the magnification of instrumental error becomes more significant as shown on Figures 2, 3 and 4. Even with a "perfect" radiometer, having no instrumental noise, i.e., $\sigma_R = 0$, the cross polarization uncertainty would still introduce an error in the

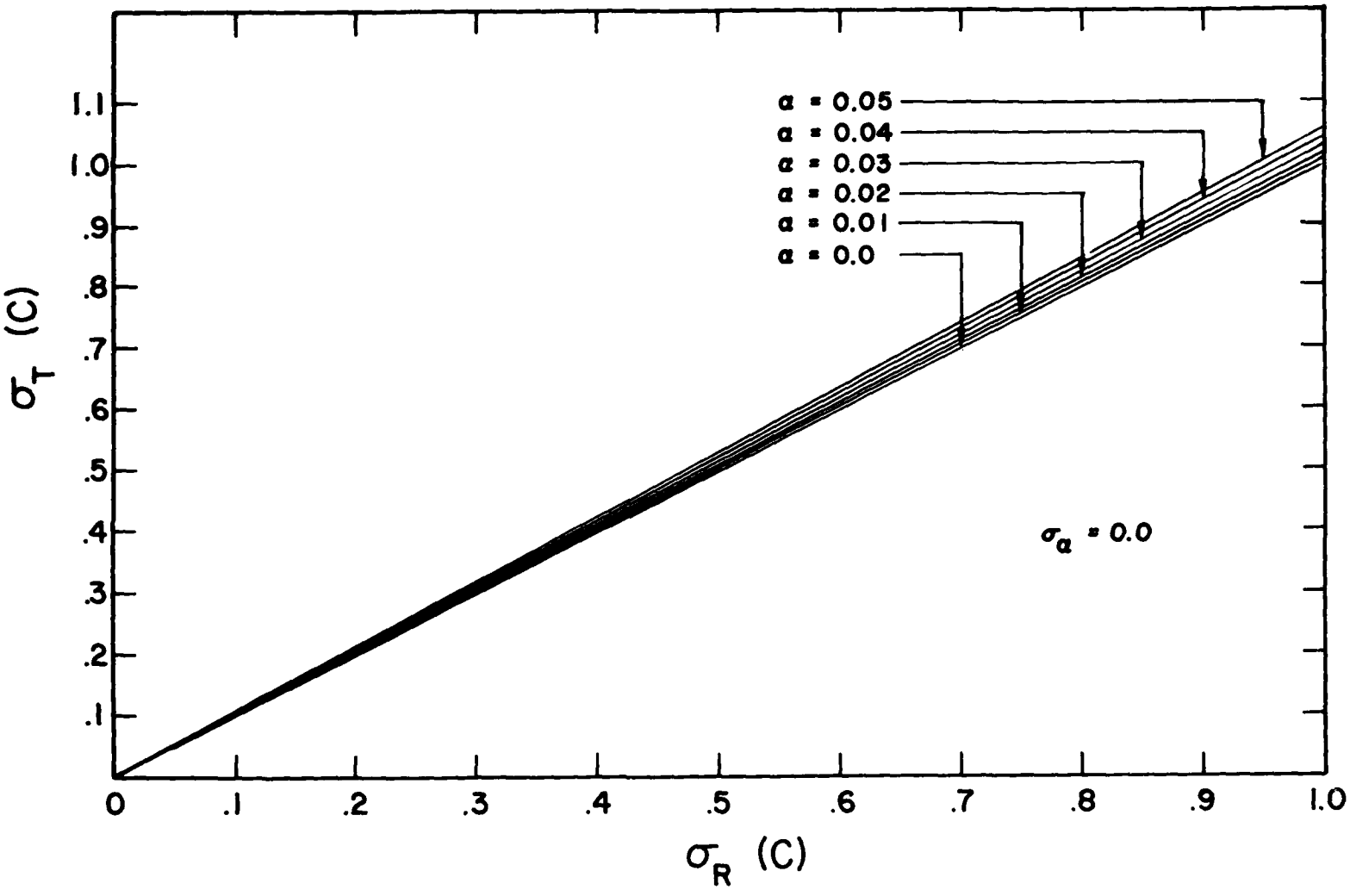

Figure 1 Retrieval Error as function of instrumental noise without cross-polarization uncertainty

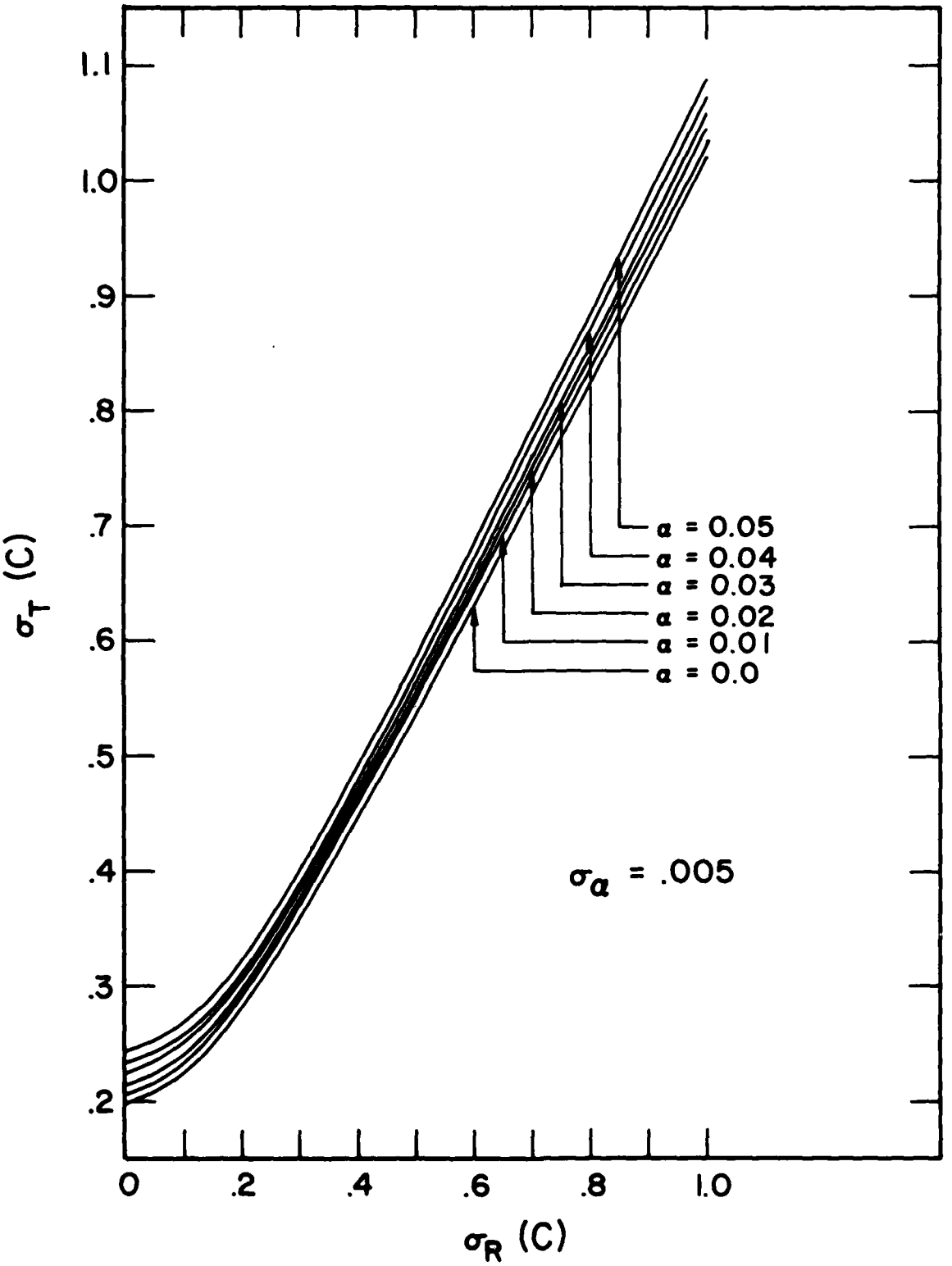

Figure 2 Retrieval Error as function of instrumental noise with 0.5% cross-polarization uncertainty

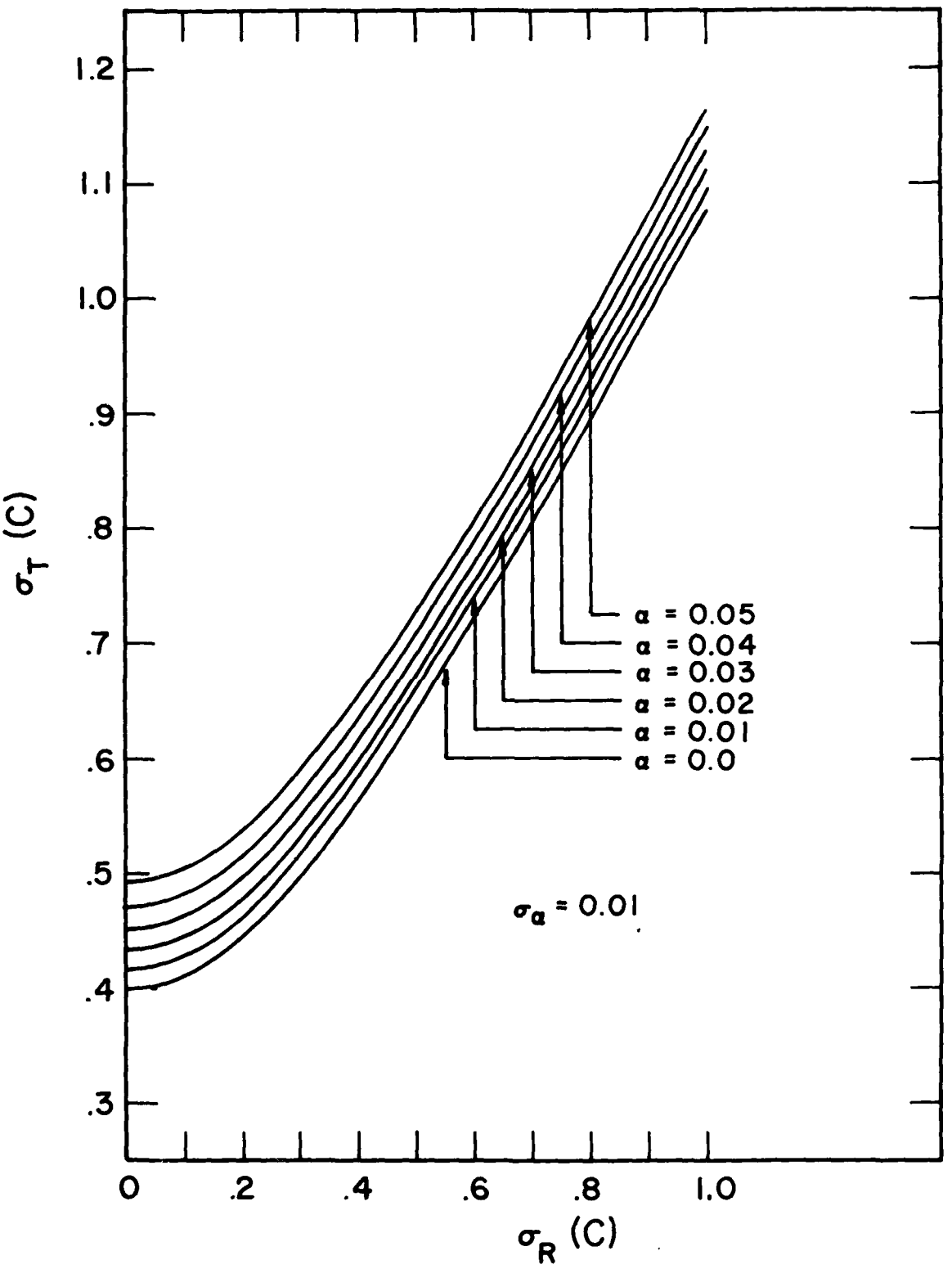

Figure 3 Retrieval Error as function of instrumental noise with 1% cross-polarization uncertainty

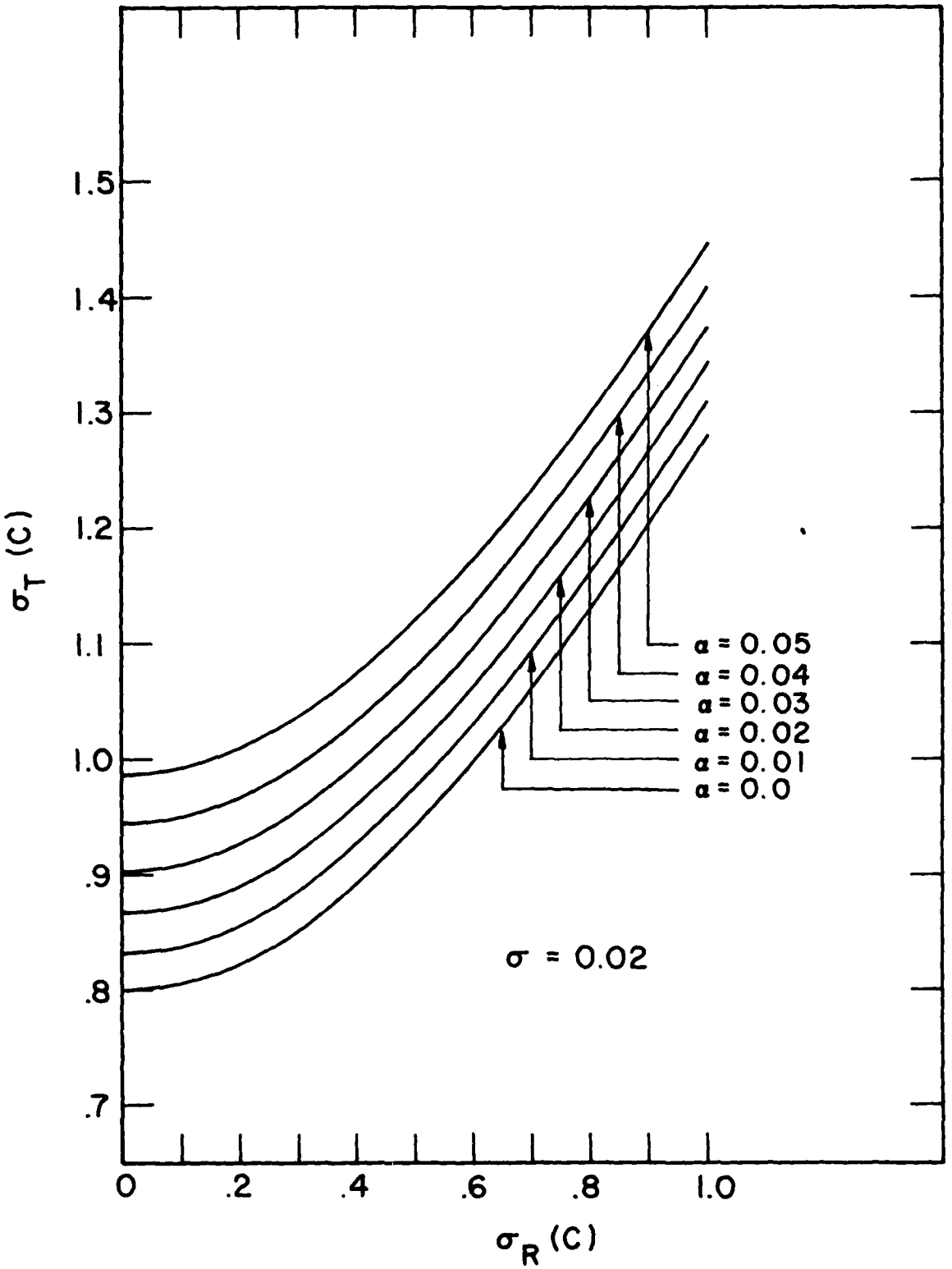

Figure 4 Retrieval Error as function of instrumental noise with 2% cross-polarization uncertainty

brightness temperature measurement. The error, σ_T, is 0.98 K when α is 5 percent and σ_α is 2 percent (see Figure 4), with no radiometric noise. The error is 0.8 K when α is zero. Two sets of cross polarization measurements (2, 3) made at the Hughes Aircraft Company facilities are listed in Table 1.

Table 1
Cross Polarization Measurements
α x 100 (%)

Channels		First Measurement	Second Measurement
19.35	V	.35	.10
	H	.30	.10
22.235	V	.65	.63
37.0	V	1.80	.45
	H	1.20	1.30
85.5	V	.60	1.40
	H	1.40	2.50

Note that the difference in α for 37.0 V and 85 H between the two measurements are 1.35 and 1.1 percent, respectively. This indicates that the α and σ_α values used for Figure 1 through 4 are by no means unrealistic.

The effect of cross polarization error on geophysical parameter estimations must be examined through a retrieval model. The retrieval results, of necessity, are model dependent. In the present study, the model employed is that originally designed by Wisler and Hollinger (5). Use of this model provided an understanding and useful evaluation in the application of the SSM/I system in several previous studies (6, 7, 8, 9, 10). The criterion chosen to examine the effect of cross polarization error is the percentage increase in the retrieval RMS error.

$$P\% = \frac{\text{RMS}\ (\alpha,\ \sigma_\alpha) - \text{RMS}\ (\alpha=0,\ \sigma_\alpha=0)}{\text{RMS}\ (\alpha=0,\ \sigma_\alpha=0)} \times 100\% \qquad \text{(II.7)}$$

Where P is the percentage increase, the parameters retrieved are the surface wind speed, sea surface temperature, and the columnar densities of water vapor and cloud liquid water. The climate statistics (10) employed in the model are those of Azores, Summer. The input data for the retrieval simulations are presented in Table 2 in the form of noise vectors. The value of σ_R is taken from the most recent Hughes measurement (4) made on 2/16/82. The cross polarization values are taken from the first measurement in Table 1. The error vectors of σ_α = 0.0, .005, .010 and .020 are then derived from Figures 1 through 4. Results of the retrieval simulations are shown in Figure 5.

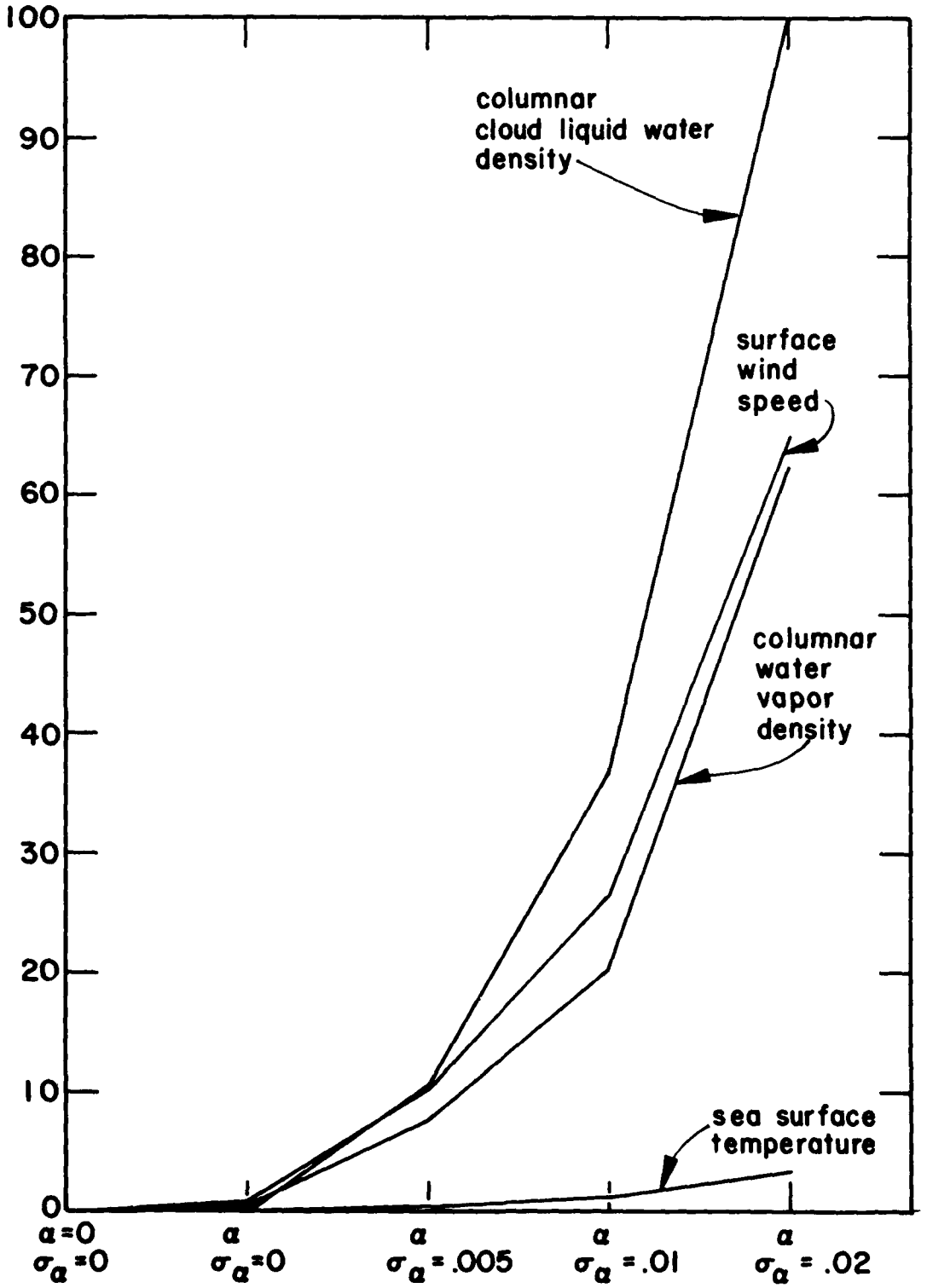

Figure 5 Percentage Increase in Retrieval Error as function of cross-polarization uncertainty

Table 2

		Instrumentation	Cross Polarization	σ_T (measurement error in T_B) at cross polarization level of			
		σ_R (measured)	α (measured)	0.0	.005 (inferred)	.010	.020
19.25	H	.48	.0030	.481	.548	.630	.942
	V	.51	.0035	.512	.552	.655	.960
22.235	V	.64	.0065	.643	.687	.765	1.042
37.0	H	.40	.0120	.406	.459	.583	.933
	V	.39	.0180	.398	.452	.585	.947
85.5	H	.64	.0140	.650	.685	.775	1.068
	V	.81	.0059	.816	.841	.912	1.151

From the results, it is apparent that the effects of cross polarization errors can be very significant. The curve for sea surface temperature in Figure 5 is misleading. It does not imply stability in sea surface temperature retrieval because of the low confidence of its estimation (7, 8).

Results shown in this section are derived under the assumptions of identical coupling between the two polarizations and the same instrumental noise. This assumption was made for simplicity. However, an exact formulation to take into account non symmetric leakage and instrumental error is straightforward if precise measurements of these quantities become available. Such a treatment is not likely to produce significantly different results than the present one. More important is the fact that the cross polarization, though uncertain, is some fixed value and will remain constant over the life of the SSM/I. Thus the cross polarization uncertainty should not merely be treated as a random error and simply squared and summed with the radiometer noise to obtain the overall measurement error. Rather the uncertainty in cross polarization will result in an unknown bias in the derived brightness temperatures input into the environmental parameter retrieval algorithms. This can be assessed by comparing the values retrieved with and without cross polarization imposed biases as the biases are varied over the expected range in uncertainty of the cross polarization in all possible channel combinations. A separate study has been planned to examine the effects due to the biases.

III. Conclusions and Recommendations

The present study has demonstrated that the cross polarization and its uncertainty can cause serious degradation of retrieved geophysical parameters, even when the SSM/I cross polarization measurements are within the relaxed specification values.

Proper correction of the cross polarization effects, however, can be made, as demonstrated in this study, if the cross polarization between ports at each frequency (i.e., H to V, and V to H) is accurately measured along with the VSWR of the feed horn for each channel. The uncertainty of these measurements must also be accurately assessed, ε it may be the most important error source for the environmental retrievals.

The effect of cross polarization measurement uncertainty has been evaluated as a factor which magnifies the noise in brightness temperature measurements. Results of the study indicate that it can be very significant. However, the uncertainty, just like the true cross polarization value is more likely a fixed value and should remain constant over the life of the SSM/I. Its greatest effect is probably in the form of bias rather than noise in brightness temperatures. A separate study has been planned to examine this aspect.

REFERENCES

1. "Specification Change Notice, Development Specification" (Part I, Type B1), Code ID 82577, Spec. No. DS 32268-040, January 20, 1982.

2. "SSM/I Formal Qualification Review, Part I," Hughes, December 18, 1981.

3. "Acceptance Test Report, Option 1, SSM/I Antenna Subsystem," Hughes, CDRL Item No. 034A3.

4. "SSM/I Sensor Qualification Test Report," CDRL Item No. 054A2.

5. Wisler, M. M. and J. P. Hollinger, "Estimation of Marine Environmental Parameters Using Microwave Radiometric Remote Sensing Systems," NRL Memorandum Report 3661, Naval Research Laboratory, November 1977.

6. Lo, R. C. and J. P. Hollinger, "NRL Comments on the ERT SST Study for the SSM/I," Letter Report to NSSA, Naval Research Laboratory, December 1981.

7. Lo, R. C. and J. P. Hollinger, "Selection of Optimal Combinations of Frequencies for the Special Sensor Microwave Imager (SSM/I) Environmental Retrievals," Letter Report to NSSA, Naval Research Laboratory, April 1981.

8. Lo, R. C. and J. P. Hollinger, "A Simulation Study of the Sensitivity of Environmental Parameter Retrievals Based on the Special Sensor Microwave Imager (SSM/I)," Letter Report to NSSA, Naval Research Laboratory, May 1982.

9. Lo, R. C. and J. P. Hollinger, "A Comparison Study of the Sensitivity and Retrieval Performance at 21.0 and 22.235 Ghz Channels," Letter Report to NSSA, Naval Research Laboratory, August 1982.

10. Hollinger, J. P., R. M. Lerner, B. E. Troy, and M. M. Wisler, "Joint Services 5D-2 Microwave Scanner Definition Study," NRL Memorandum Report 3807, Naval Research Laboratory, August 1978.

* U.S. GOVERNMENT PRINTING OFFICE: 1983-381-334:001